NASA TECHNICAL NOTE

NASA TN D-8222

NASA TN D-8222

CHARACTERISTICS OF WAKE VORTEX GENERATED BY A BOEING 727 JET TRANSPORT DURING TWO-SEGMENT AND NORMAL ILS APPROACH FLIGHT PATHS

R. L. Kurkowski, M. R. Barber, and L. J. Garodz

Ames Research Center
Moffett Field, Calif. 94035

NATIONAL AERONAUTICS AND SPACE ADMINISTRATION • WASHINGTON, D. C. • APRIL 1976

1. Report No.	2. Government Accession No.	3
NASA TN D-8222		

4. Title and Subtitle	5. Report Date
CHARACTERISTICS OF WAKE VORTEX GENERATED BY A BOEING 727 JET TRANSPORT DURING TWO-SEGMENT AND NORMAL ILS APPROACH FLIGHT PATHS	April 1976
	6. Performing Organization Code
7. Author(s)	8. Performing Organization Report No.
R. L. Kurkowski, M. R. Barber, and L. J. Garodz	A-6208
	10. Work Unit No.
9. Performing Organization Name and Address	513-51-01
NASA Ames Research Center, Moffett Field, Calif. 94035 NASA Flight Research Center, Edwards, Calif. Federal Aviation Administration, NAFEC, Atlantic City, N. J.	11. Contract or Grant No.
	13. Type of Report and Period Covered
12. Sponsoring Agency Name and Address	Technical Note
National Aeronautics and Space Administration, Washington, D. C. and Federal Aviation Administration, Washington, D. C.	14. Sponsoring Agency Code

15. Supplementary Notes

16. Abstract

A series of flight tests was conducted to evaluate the vortex wake characteristics of a Boeing 727 (B727-200) aircraft during conventional and two-segment ILS approaches. Twelve flights of the B727, which was equipped with smoke generators for vortex marking, were flown and its vortex wake was intentionally encountered by a Lear Jet model 23 (LR-23) and a Piper Twin Comanche (PA-30). Location of the B727 vortex during landing approach was measured using a system of photo-theodolites.

The tests showed that at a given separation distance there were no readily apparent differences in the upsets resulting from deliberate vortex encounters during the two types of approaches. Timed mappings of the position of the landing configuration vortices showed that they tended to descend approximately 91 m (300 ft) below the flight path of the B727. The flaps of the B727 have a dominant effect on the character of the trailed wake vortex. The clean wing produces a strong, concentrated vortex but as the flaps are lowered, the vortex system becomes more diffuse. Pilot opinion and roll acceleration data indicate that 4.5 n.mi. would be a minimum separation distance at which roll control of light aircraft (less than 5,670 kg (12,500 lb)) could be maintained during parallel encounters of the B727's landing configuration wake. This minimum separation distance is generally in scale with results determined from previous tests of other aircraft using the same roll control criteria.

17. Key Words (Suggested by Author(s))	18. Distribution Statement
Trailing vortices Wake turbulence Aircraft wakes Vortex wake effects Airway spacing Two-segment approach	Unlimited STAR Category – 03

19. Security Classif. (of this report)	20. Security Classif. (of this page)	21. No. of Pages	22. Price*
Unclassified	Unclassified	107	$5.25

For sale by the National Technical Information Service, Springfield, Virginia 22161

TABLE OF CONTENTS

SYMBOLS

A_n	normal acceleration, g units
A_x	longitudinal acceleration, g units
A_y	lateral acceleration, g units
C_l	rolling moment coefficient
$C_{l_{\delta_a}}$	lateral control effectiveness derivative, per degree
P	roll rate, rad/sec or deg/sec
$\dot{P}_{\delta_{a_{max}}}$	maximum roll control acceleration, rad/sec^2
$\dot{P}_{vortex}$	roll acceleration induced by vortex, rad/sec^2
q	pitch rate, rad/sec
r	yaw rate, rad/sec
α	angle of attack, deg
β	angle of sideslip, deg
γ	glide slope angle, deg
$\Delta( )$	change in value of the parameter
δ_a	aileron deflection, deg
δ_e	elevator deflection, deg
δ_f	flap deflection, deg
θ	airplane pitch angle, deg
ϕ	airplane roll angle, deg
ψ	airplane yaw angle, deg

A dot over a quantity denotes the time derivative of that quantity.

CHARACTERISTICS OF WAKE VORTEX GENERATED BY A BOEING 727 JET TRANSPORT DURING TWO-SEGMENT AND NORMAL ILS APPROACH FLIGHT PATHS

R. L. Kurkowski
Ames Research Center

M. R. Barber
Flight Research Center

and

L. J. Garodz
Federal Aviation Administration

SUMMARY

A series of flight tests was conducted to evaluate the vortex wake characteristics of a Boeing 727 (B727-200) aircraft during conventional and two-segment ILS approaches. Twelve flights of the B727, which was equipped with smoke generators for vortex marking, were flown and its vortex wake was intentionally encountered by a Lear Jet model 23 (LR-23) and a Piper Twin Comanche (PA-30). Location of the B727 vortex during landing approach was measured using a system of phototheodolites.

The tests showed that at a given separation distance there were no readily apparent differences in the upsets resulting from deliberate vortex encounters during the two types of approaches. Timed mappings of the position of the landing configuration vortices showed that they tended to descend approximately 91 m (300 ft) below the flight path of the B727. The flaps of the B727 have a dominant effect on the character of the trailed wake vortex. The clean wing produces a strong, concentrated vortex but as the flaps are lowered, the vortex system becomes more diffuse. Pilot opinion and roll acceleration data indicate that 4.5 n.mi. would be a minimum separation distance at which roll control of light aircraft (less than 5,670 kg (12,500 lb)) could be maintained during parallel encounters of the B727's landing configuration wake. This minimum separation distance is generally in scale with results determined from previous tests of other aircraft using the same roll control criteria.

INTRODUCTION

Results of NASA, FAA, and airline flight tests and of on-line evaluations of two-segment approaches indicate such approaches to be an operationally effective means of noise abatement (refs. 1 and 2). However, because of the terminal area mixture of two-segment traffic with normal ILS traffic, concern has been expressed that the wake vortex resulting from a two-segment approach

may present a problem to other aircraft, especially light general aviation aircraft making a standard ILS approach. The purpose of this program was to assess the severity of vortices trailing a typical narrow-body jet with aft-mounted engines on a two-segment approach and to assess the effect, if any, on existing or proposed IFR separation standards.

A joint NASA/FAA test team was organized to investigate wake turbulence characteristics associated with operation of a Boeing 727 (B727) aircraft during conventional and two-segment ILS approaches. A series of flight tests was conducted at the NASA Flight Research Center from 31 October 1973 through 5 November 1973.

The objectives of these flight tests were as follows: (1) to obtain qualitative and quantitative evaluations of the upset responses of two general aviation aircraft, the Lear Jet LR-23 and Piper PA-30, during *deliberate encounters* of the vortex wake of a B727 (landing configuration) during two-segment and conventional approaches, (2) to measure the drift and persistence of the B727's wake during two-segment and conventional ILS approaches, (3) to measure the effect of different flap deflections, thrust settings, etc., on the wake characteristics, and (4) to compare the vortex shed by the B727 with those shed by other aircraft. It should be noted that the bulk of the encounter data was obtained during simulated approaches at high altitude in order to provide adequate safety margins for this type of exploratory flight testing.

This flight test investigation was conducted as a joint effort by NASA Ames Research Center, NASA Flight Research Center, and FAA NAFEC. The authors wish to acknowledge the valuable contributions of the following: flight research pilots Glen W. Stinnett (Ames), Thomas C. McMurtry (Flight), and Joseph J. Tymczyszyn (FAA Western Region); flight test engineers Robert A. Jacobsen (Ames), Glenn H. Robinson (Ames), Harriet J. Smith (Flight), Lawrence C. Montoya (Flight), Terry Putnam (Flight), and Hermilio R. Gloria (Ames); observer pilots R. L. Devereaux and A. J. Bolster (FAA Flight Standards); chase plane pilots Einar Enevoldson (Flight), John J. Ryan (NAFEC), Fred Daniloff (USAASTA), and Gary Bradburn (Ames contract pilot); chase plane photographer Robert M. Rhine (Flight); and avionics engineers William R. Wehrend Jr., Kent Bourquin, and Fred H. Shigemoto (all Ames). This report describes the flight tests and test equipment, and presents the results of the study.

TEST AIRCRAFT AND EQUIPMENT

Wake Vortex Generator Aircraft

The B727 was selected as the wake vortex generator aircraft because it constitutes a large portion of the current air carrier service fleet, is expected to continue in airline service in significant numbers well into the 1980s, and because its vortex wake characteristics were not well documented. The aircraft was equipped with corvus oil smoke generators for vortex marking. Figure 1 is a photograph of the generating aircraft and figure 2 is a closeup photograph of the vortex markers. The aircraft's pertinent physical characteristics are contained in table 1.

The B727-200 aircraft used in this program was leased from United Airlines. It had just been used in a six-month operational flight evaluation of a two-segment approach guidance system. The evaluation included 65 approaches in actual IFR weather. The aircraft was equipped with both a

two-segment approach avionics system and a digital data recording system. Detailed descriptions of the avionics and data systems are contained in reference 2. A DME transmitter/antenna was co-located with the glide slope antenna at Edwards AFB to provide information needed for the two-segment guidance.

Wake Vortex Probe Aircraft

A Lear Jet Model 23 (LR-23) and a Piper Twin Comanche (PA-30) were used to probe the B727's wake. Figures 3 and 4 present photographs of the two aircraft, respectively; pertinent physical characteristics of the LR-23 and PA-30 are given in table 1. Both aircraft were instrumented to measure vortex-induced upset characteristics. Both aircraft were also equipped with air-to-air ranging DME using a beacon system that was mounted in the B727. The DME range was displayed to the probe aircraft pilots and recorded on the data systems. The LR-23 was equipped with a three-component hot-wire anemometer that was mounted on a nose boom in proximity to the airspeed and angles-of-attack and sideslip sensors. The anemometer was used for measuring the velocities in the vortex flow field. The data from these measurements will be contained in a subsequent NASA report.

It should be noted that the LR-23 control system is equipped at the factory with autopilot, yaw damper, stick shaker, and stick pusher. For the purposes of this program, the autopilot and yaw damper were deactivated. For stall protection, the stick shaker and pusher remained active and were activated on occasion during the penetration probes.

Supporting Aircraft

A Lockheed F-104 fighter aircraft was utilized to probe the B727's vortex prior to probes by the LR-23 and PA-30. These probes were performed as a safety precaution because calculations had indicated that the LR-23 and PA-30 might experience severe loads during the probes. The F-104 probes showed that the calculations were too conservative and the tests were continued as planned.

A Cessna 402-B (C-402) aircraft was used for airborne meteorological surveys. The instrument package for meteorological determinations consisted of an ambient air temperature sensor, a dew point hygrometer, a barometer, altimeter, airspeed indicators, and an inertial navigation system used to provide geographical location and to derive local horizontal wind fields. An inertial subrange turbulence meter (epsilon meter) was used to establish the levels of atmospheric turbulence. Altitude surveys were made for every flight condition. The survey aircraft flew in the vicinity during all vortex probes and vortex mapping runs, in order to document the atmospheric conditions.

A North American T-28 and a Grumman Gulfstream were used as photo chase aircraft.

Wake Vortex Mapping System

A phototheodolite vortex mapping system was used to track the vortex marking smoke. Figure 5 presents the conventional and two-segment approach geometries and points out the

location of the phototheodolites. By placing the phototheodolites on both sides of the runway, the horizontal and vertical drift of the vortex could be determined.

TEST DESCRIPTION

The test program is outlined in table 2; it consisted of 12 flights of the B727. During these flights the probe aircraft were used to evaluate (1) vortex-upset characteristics by in-trail probes and (2) wake-vortex velocity by cross-track probes. The crew of the LR-23 was comprised of a NASA pilot, an FAA pilot, and a NASA flight test engineer; the crew of the PA-30 consisted of two NASA pilots for initial flights. During later flights the PA-30 was crewed by a NASA pilot and an FAA pilot. The B727 was flown by a United Airlines crew with NASA and FAA pilot observers on board. The phototheodolite system was used to measure the vortex position relative to the two-segment and conventional approach paths during landing approach. Meteorological information (winds, turbulence, humidity, and temperature gradients) was documented for each test flight condition, using the instrumented C-402.

A summary of the separation distances at which data were obtained during in-trail penetrations of the vortex wake of the B727's landing configuration is shown in table 3. Deliberate in-trail wake encounters were attempted for a larger range of distances; however, these attempts were not always successful due to the inherent difficulty in locating the vortex core precisely in the diffused smoke trail. The information is grouped for probes (1) in level flight at altitude (3658 m (12,000 ft) m.s.l.), (2) for simulated 3° and 6° approach descents at altitude, and (3) for a limited sequence of low altitude approach runs.

RESULTS AND DISCUSSION

In the following section, the flight test results are summarized. The vortex wake characteristics during two-segment and conventional approaches are compared on the basis of upset responses for deliberate wake encounters by the probe aircraft, and vortex wake drift. The effect of flap configuration on the vortex wake is discussed. Finally, a comparison is made of the results of this investigation with those from previous tests of other transport aircraft.

Comparison of Vortex Wake Characteristics Generated During Two-Segment and Conventional Approaches

The vortex wake behind the B727 in a landing configuration with 30° flaps was evaluated. Evaluations were made first in level flight, and then for both 3° and 6° descending flight paths. The descending flight paths correspond to the conventional and the upper segment of a two-segment approach, respectively. A time history of the probe aircraft response is presented for a typical encounter and the maximum disturbances from all encounters are summarized. This is followed by a discussion of separation distances based on roll control criteria and pilot comments.

Typical response dynamics.– Figures 6(a and b) present a representative time history of the LR-23 response to an encounter with the B727 wake at an altitude of 2743 m (9000 ft) during a simulated 6° landing approach flight path. Separation distance between the two aircraft was 2.7 n.mi. at the time of encounter. The initial encounter occurred at 1.2 sec as indicated principally by large transient responses of the α and β sensor vanes, plus rapid generation of pitch and roll angular accelerations with no change in the corresponding controls. Additional manifestations of the vortex flow on this run were an abrupt 20 knot increase in indicated airspeed coincident with an abrupt 0.1 g change in longitudinal acceleration. A second encounter occurred about 3.0 sec later, disturbing the airplane primarily in pitch. Recovery from these two encounters was achieved after the airplane had pitched down approximately 17° from its initial pitch attitude and rolled to a 90° left bank, using full opposite aileron control to return to wings-level attitude. Protection from stall for the LR-23 is provided by a stick shaker and pusher system. Stick pusher actuation was initiated at 0.8 sec and again at 3.8 sec, contributing to the nose down pitch attitude change.

A summary observation from all the encounters is that, in general, the LR-23 excursions were primarily about the roll and pitch axes, with minor dutch-roll disturbances.

Maximum disturbance summary.– Maximum responses of the LR-23 from deliberate encounters with the B727 wake are summarized in figures 7(a and b). They cover a separation range between the aircraft varying from 2.1 to 3.3 n.mi. These data were obtained during flight along 3° and 6° descending flight paths from either 3658 m (12,000 ft) or 1524 m (5000 ft) initial altitude levels. The B727 flew a steady descending flight path (either 3° or 6°) while the LR-23 probed the vortex wake of the B727. Therefore, the flight path of the probe aircraft varied about the nominal 3° or 6° descending flight path. Both aircraft (probe and generator) were in the landing configuration. Figures 8(a and b) present the same data as a function of vortex age rather than separation distance. This is done to facilitate analysis because vortex breakdown depends on its age rather than a separation distance; furthermore, separation distance varies with aircraft true airspeed.

The vortex wake encounters produced maximum roll angular accelerations of the LR-23 as high as 3.0 rad/sec^2. Angular accelerations in pitch and yaw reached maximums of about one-half and one-tenth the roll acceleration, respectively. Peak-to-peak linear acceleration oscillations up to a maximum of about 0.3 g laterally were measured and peak-to-peak normal acceleration oscillations reached about 1.5 g. Maximum bank angles exceeded 45° in only one instance. Pitch attitude excursions, generally nose down, reached a maximum of 12°. The scatter in the data merely indicates that not all encounters result in large upsets or accelerations and the dynamics vary depending on entry angle, position, pilot control inputs, stability augmentation system inputs, and stick pusher inputs.

Any possible effect of altitude on the severity-of-encounter was obscured because at the time of these flight test measurements, atmospheric turbulence, as shown in figure 9, varied from negligible to light at altitude, but approached heavy turbulence at the lower altitude. Presuming that increased turbulence would cause earlier attenuation of the wake (ref. 3), less severe encounter excursions of the probing aircraft would be expected at lower altitudes for a given separation distance.

Comparison of the 3° and 6° data measured at high altitude with that obtained at low altitudes indicates that there are no obvious differences in encounter dynamics due to the glide path angle of the generator aircraft.

LR-23 roll control criteria for separation distance.– Reference 4 proposed a criterion for determining minimum safe separation behind larger aircraft using a rolling moment control ratio for the probe aircraft and the gross weight of the generating aircraft. The rolling moment control ratio is the measured vortex-induced roll acceleration divided by the maximum available roll acceleration control. When this ratio exceeds one, roll control is lost. The roll ratio data for the encounters by the LR-23 were calculated and are presented in figures 10 and 11 as a function of separation distance and vortex age, respectively, over the separation range covered. The B727 flaps were deflected to the landing configuration $\delta_f = 30°$.

To obtain the maximum roll acceleration induced by the vortex the measured values were adjusted for roll acceleration produced by any initial aileron deflection which may have existed at the time of encounter. Maximum roll control power was derived from data measured during a series of aileron pulses. An average value of $C_{l_{\delta_a}} = 0.00114$ per degree was obtained from the pulse maneuvers and this was used to determine $P_{\delta_{a_{max}}}$ for each encounter.

Using maximum encounter roll acceleration equal to maximum control power as the criterion for minimum separation, the limited data presented in figure 10 suggest that 4 n.mi. would be required for IFR[1] separation, for this aircraft combination. However, the test data covered a very small range of separation distances, compared with previous flight tests using this criterion and any judgments should be tempered by the additional factors influencing minimum separation distance as enumerated in reference 3 and as discussed in the following pilot comments.

LR-23 probe pilot comments.– Observations made by NASA and FAA pilots who flew the LR-23 probe airplane, and ground observations by the LR-23 pilot of low altitude over-flights by the generating aircraft, prompted the pilot comments that are quoted below.

1. Calm air and a "flaps-up" configuration of the generating airplane presented the worst case to the trailing airplane. With the passage of time, even in calm air, wake vortices dissipate. The characteristic breakup occurs as a longitudinal gathering of the vortex, followed by a radial expansion appearing as a large doughnut, and within approximately five or so seconds after that, dissipation is complete.

From the pilot point of view, safe separation must be based on this worst case until other effects can be adequately measured and taken into account. The above described break-up and dissipation consistently happens between a minute, and a minute and a half, in the case of the B727. A separation of two minutes should therefore provide safety as well as an adequate margin. With a typical approach speed of 130 knots for the generating airplane, a separation distance of 4.5 n.mi. would assure vortex dissipation even in the worst case for the trailing airplane.

2. Generating airplane flap-deflection was observed very clearly to provide secondary vortices which tended to mingle with and speed the destruction of the primary wing tip vortices in proportion to the amount of flap deflection. Penetration of the trailing vortices produced

[1] Radar controlled.

significantly less disturbance at 30° or more flap deflection compared to the flaps-up configuration at equal vortex ages.

3. Generating-airplane thrust was observed to have a significant effect on vortex destruction. Encounters behind the B727 with 15° flaps extended, first with approach power during a 3° descent and then with climb power at the same speed and flap setting, showed a marked reduction in vortex strength for the high-thrust condition. Thus, safe separation during climbout could be somewhat less than during approach. This same observation was made while penetrating the wake of a C-5A in a CV-990 in similar tests conducted in 1970.

4. Atmospheric turbulence was observed (as is well known) to speed the break-up of the tip vortices significantly, leading to the conclusion that safe separation could also be reduced during periods of gusty wind or similar atmospheric instability.

5. The wake vortex of the generator aircraft was probed while the generator aircraft flew the 6° and 3° descending flight paths. No significant difference in aircraft upset or vortex wake dissipation characteristics, due to flight path angle, could be determined. Therefore, a separation distance which provides adequate margin when following another aircraft on a conventional approach should also be acceptable when following that aircraft on a two-segment approach.

Piper Twin Comanche Vortex Encounters

PA-30 maximum disturbance summary.– Figures 12 (a and b) present the maximum absolute excursions of the pertinent parameters for the PA-30 encounters with the B727 wake. Figures 13 (a and b) present the same upset information in terms of vortex age rather than separation distances. In general, the PA-30 excursions are similar in character to those of the LR-23. The attitude deviations of the PA-30 are larger, which would be expected as a result of its lower velocity and lighter wing loading. Deviations in yaw were on the order of seven times greater and pitch about two times greater for the PA-30. The PA-30 data cover a somewhat larger range of separation distances than the LR-23 data. No consistent differences can be observed for the encounter upsets resulting from the different flight paths.

PA-30 roll control criteria for separation distance.– The ratio of the maximum vortex induced rolling accelerations to roll control power for the PA-30 flying at 100 KIAS, during several encounters, is plotted as a function of separation distance and vortex age in figures 14 and 15, respectively. The B727 was in the landing configuration (30° flaps, gear down) for all these encounters. The induced accelerations have been adjusted for control input in the same manner as for the LR-23 data. Maximum available roll control power was determined by measuring the roll accelerations resulting from sharp aileron pulses and was found to be approximately $Cl_{\delta_a} = 0.00088$ per degree. These data show that the ratio of vortex induced roll acceleration to roll control power is still greater than one at separation distances in excess of 4 n.mi.

PA-30 probe pilot comments.– The following quoted comments were made by a NASA pilot as a result of observations made while flying the PA-30 during deliberate wake vortex encounters at varying distances behind the B727.

"During all probes made by the PA-30, the B727 was in a landing configuration with 30° of flap and gear down. The vortex wake appeared to descend below the B727 about 76.2 meters (250 feet). All probes of the wake by the PA-30 were made from an in-trail position. Attempts were made to probe from above and below the wake. The majority of the probes of the wake were made from below the wake. Successful probes were made from between two and five nautical miles.

"To evaluate the upset of the PA-30 by the wake, I used the following criteria:

1. If the type of upset encountered could cause a break off of an ILS approach, it was considered severe.

2. If the bank angle exceeded 30° before the airplane roll could be controlled, this was considered a severe upset.

3. If normal accelerations excursions of ±1.0 g's were encountered, this was considered a severe upset.

"On the first two flights with the PA-30 I let the airplane respond to the wake by neutralizing controls. On the last two flights I tried to control the airplane at all times. During these last two flights, on several occasions, full aileron and rudder control were used in attempts to control the airplane during upsets.

"Severe upsets were occasionally encountered by the PA-30 at distances of up to four nautical miles behind the B727. However, most of the time only light to moderate turbulence was found in the vortex wake at distances greater than two miles behind the B727. It appeared as though there were patches of high energy wake behind the B727. If the PA-30 got into one of these, the upset was severe. If not, the upset was like flying in light to moderate atmospheric turbulence. It should be pointed out, however, that I never could be sure what part of the wake I encountered. When the PA-30 got a severe upset there was usually some very sharp normal acceleration changes followed by an uncontrollable rolling motion. Based on the results of these tests, I would not want to fly the PA-30 at separation distances closer than 4.5 nautical miles during approach to landing, behind a landing configured B727 type airplane."

Vortex Drift Characteristics

Figures 16(a through f) present the vertical position of the B727 vortex wake versus distance behind the aircraft for two conventional approaches (figs. 16(a and b)), two two-segment approaches (figs. 16(c and d)), and two take-off maneuvers (figs. 16(e and f)). A review of these data shows that the vortices tend to settle to something of the order of 91.4 m (300 ft) below the B727's flight path and that they then stop descending. Longer persistence of the smoke-marked vortex for the take-off configuration (15° flaps) allowed data to be taken for greater distances than during the landing approaches (30° flaps). It should not be concluded that the lack of vortex "track" indicates a lack of vortex existence. To the contrary, the PA-30 upsets shown in figure 14 verify that the vortex did exist behind the B727 to distances in excess of 4 n.mi. (note that the flagged symbols on fig. 14 are encounters at low altitude that were performed on an actual approach).

Given then that the vortex tends to settle and that it could exist for distances in excess of 4 n.mi. behind the generating aircraft, the simplified geometric analysis presented in figure 17can be performed. This analysis assumes a reasonable extrapolation of the wake settling data (for the vertical plane) presented in figure 16, and thereby indicates that the B727's vortex would be something of the order of 91.4 m (300 ft) below its flight path at a separation distance of 3 miles. Superimposing the vortex on the approach geometries would then indicate that an aircraft on a conventional approach that is following an aircraft on a two-segment approach might experience an encounter with the vortex somewhere prior to the "two-segment knee," at an altitude of the order of 243.8 m (800 ft). In evaluating the possibilities of a wake encounter when both aircraft are flying a conventional approach it can be seen that if a lead aircraft is "right on glidepath" or slightly high and an aircraft following at 3 miles is low on the glidepath beam, an encounter could occur. However, these encounters would likely occur at a higher altitude than the one predicted for the two-segment approach.

The question of the relative difference of the probability of encounter for the two types of approach profiles cannot be answered from this flight test. However, the data of this test should be of value for use in such a detailed analysis. The vortex location data for all 14 runs obtained during the tests are presented in the appendix. Figures 26(a through n) present the location as a function of distance behind the B727 generating aircraft. Figures 27(a through n) present the location data as a function of time after the B727 passage. In addition, many other variables must be considered in a probability analysis, including items such as statistical data on flight path control error, guidance system errors, wind shears, atmospheric turbulence, etc.

Effect of Generator Aircraft Flap Configuration

This section covers the effect of generator aircraft flap setting on the wake vortices. These effects are discussed in terms of (1) visual observations of the differences in the smoke-marked vortices, and (2) probe aircraft response as a function of flap setting.

Visual Observations

One significant observation of the program was that wing flap extension on the B727 aircraft had a pronounced effect on the characteristics and persistence of the trailing vortex system. With no flap extension ("clean configuration") the vortex, as visualized by the smoke, was small in diameter, approximately 0.61 m (2 ft), and retained a well defined structure to a distance of approximately 8 n.mi. behind the aircraft in smooth air at 3658 m (12,000 ft) altitude. This corresponded to a vortex age of approximately 120 sec. Probes of this clean configuration vortex system led to the qualitative assessment that these vortices produced large upsets of the probing aircraft (LR-23 and F-104) at separation distances of 6–7 n.mi. Figure 18 presents a photograph of the "clean configuration" B727 vortex.

Figures 19(a and b) present a photograph of the B727 with the flaps extended to the landing configuration (30°). In this configuration an interaction of the flap vortices with the wing-tip vortices creates a vortex system that is much larger in diameter than that of the vortex system associated with the clean configuration. This interaction appears to occur within a few span lengths behind the wing. One effect of this interaction was that it tended to diffuse the vortex-marking

smoke. With the smokers operating with peak performance, probe pilots could discern vortex-marking smoke at approximately 3–4 n.mi. behind the landing configured B727.

Figures 20 through 22 show the effect of aircraft flap configuration on vortex persistence. These photos were taken during low altitude fly-overs in smooth morning air. Figures 20(a through o) present photographs taken at 5-sec time intervals of the B727's vortex with the clean wing. A review of the figures shows that vortex bursting starts to occur at 55 sec of age, and that complete vortex breakdown has occurred by 70 sec.

Figures 21(a through p) present the same information for the take-off configuration (15° flaps) of the B727. The mode of breakdown appears to be viscous decay occurring at 75 sec. Data for this configuration illustrate the possible wake encounter hazard for a small aircraft during climbout after take-off.

Figures 22(a through h) present the landing configuration persistence. It is interesting to note that the vortex system 10 sec behind the aircraft has begun to take on a "ragged" appearance as compared to the previous configurations. However, at later times the vortex appears to have regained a smooth appearance until at 40 sec it became invisible to the photographer. This disappearance of the 30° flap configuration vortex before any onset of breakdown is obviously a result of the smoke becoming so diffuse that it can no longer mark the vortex. The diffusion is caused by the effect shown in figure 19 wherein the smoke entrained in the tip vortex appears to wrap around the flap vortex, thereby diffusing the smoke.

The fact that the landing configuration vortex smoke was diffusing prior to vortex breakdown created operational problems throughout the flight test. Lack of vortex visibility made the vortex encounters for this configuration difficult to achieve, limited the vortex drift measurements, and eliminated a visual measurement of vortex persistence.

Aircraft Response Data

Figures 23(a and b) present a summary of the Lear Jet's maximum response to an encounter with the B727 wake for two flap configurations during level flight tests near the nominal 3658 m (12,000 ft) altitude. Shown are comparisons between the wake generated from the landing-flaps configuration versus the clean-wing configuration. The upsets behind the clean configuration at about 7 n.mi. was roughly equivalent to the upsets behind the landing flaps configuration at about 3 n.mi. separation distance. Figures 24(a and b) present the same data versus vortex age. The upset response data indicate that the vortex wake for the clean configuration persisted for a longer time by a factor of 2.5 to 3.0, considering the difference in B727 speeds in the two configurations. In addition, these comparisons illustrate the effect of the vortex characteristics shown in figures 20 and 22 in terms of the upsets induced by the vortex.

Comparison With Previous Data

The wake vortex data for the landing-configured B727 obtained from these tests was compared with data from previous tests as reported in reference 3. As discussed earlier, the criteria used for this comparison was the measure of the ratio of roll disturbance to roll control capability. The

distances where this ratio becomes one are plotted in figure 25 for various average gross weights; pilot opinions of minimum separation distances are also plotted. Perhaps the most significant aspect of the pilot comments from the subject test is that pilots of both aircraft agree that 4.5 n.mi. would be the minimum separation distance that they would deem satisfactory for an operational encounter of the landing-configured B727's vortex. This agrees with the roll control criteria data of 4.5 n.mi. for the PA-30 and 4 n.mi. for the LR-23.

Figure 25 presents a relatively complete set of data for the determination of minimum separation distances for various generating and encountering aircraft combination. In general, the figure shows good correlation of the B727 results with those of other aircraft. The figure then would lead to the conclusion that the gross weight of the vortex generating aircraft is a dominant factor affecting separation distance.

CONCLUSIONS

1. Based on a limited number of *deliberate penetrations* of the B727 landing configuration (30° flaps) wake vortex, there were no readily apparent differences in the upsets resulting from two-segment and conventional approach paths.

2. The vortices from the B727 tend to settle to approximately 91.4 m (300 ft) below the flight path of the aircraft and then stop descending.

3. NASA and FAA pilot opinion and roll acceleration data indicate that 4.5 n.mi. would be a minimum separation distance at which roll control could be maintained during parallel encounters of the B727's landing configuration vortex wake by small aircraft. This minimum separation distance is generally in scale with results determined from previous tests of other aircraft using the same roll control criteria.

4. B727 flap configuration has a definite effect on the vortex shed by the aircraft. The clean wing results in a concentrated, well-defined vortex core. As the flaps are lowered the vortex tends to become more diffuse and creates less of an upset on an encountering aircraft.

Ames Research Center
National Aeronautics and Space Administration
Moffett Field, Calif. 94035, November 10, 1975

TABLE 1.– TEST AIRCRAFT CHARACTERISTICS

Characteristics	B727-200	LR-23	PA-30
Test weight, kg (lb)	68,038 (150,000)	5,443 (12,000)	1,587 (3,500)
Wing span, m (ft)	32.9 (108.0)	10.4 (34.1)	10.9 (36.0)
Wing area, m^2 (ft^2)	157.9 (1,700)	21.5 (231.8)	16.5 (178.0)
Test wing loading, kg/m^2 (lb/ft^2)	431 (88.2)	253 (51.8)	96 (19.7)
Test flap settings			
Take-off, deg	15	20	15
Landing, deg	30	40	27
Nominal test speeds			
Approach, indicated air speed, knots	145	150	90
Climb, indicated air speed, knots	150	150-170	90
Stall, indicated air speed, knots (landing configuration)	110	90-100	61

TABLE 2.– FLIGHT-TEST INVESTIGATION OF WAKE TURBULENCE BEHIND B727

Test objectives	Flight no.	Test time	Aircraft status: B727	F-104	Lear Jet	PA-30	C-402	T-28	Gulf-stream	Telemetered data	Radar	Lakebed	Noise	Echo 2
Date: Oct. 31, 1973														
A. Take-off runway 04 for noise measurements	1	0615	Gen.[a]				Meteorological measurement				X	X	X	
B. Two-segment approach vortex mapping (2)			LDG								X	X	X	
C. Flyovers (6) (TO, CLN, LDG, TO, CLN, LDG)[b]											X			
D. Conventional approach vortex mapping (2)			LDG								X	X	X	
		0745												
In-trail probes (B727 landing config.), 3658 m (12,000 ft)	2	1045	Gen.					Photo chase						
A. F-104 probes (2 runs)[c]				Probe	Provide separation distance					X	X			
B. Lear probes (3 runs)					Probe						X			
		1200												
In-trail probes (B727 CLN and LDG config.) 3658 m (12,000 ft)	3	1430	Gen.											
A. F-104 probes			CLN	Probe	Separation distance					X	X			
B. Lear probes			CLN		Probe						X			
C. PA-30 probes (6)			LDG			Probe				X	X			
		1600												
Date: Nov. 1, 1973														
Approach vortex mapping and noise measurement	4	0615	Gen.						Photo chase					
A. Take-off runway 04 for noise measurement (2)			TO								X	X	X	
B. Two-segment approaches (2)			LDG								X	X	X	
C. Conventional approaches (2)			LDG								X	X	X	
		0745												
Two-segment approach probes at altitude 3658 m (12,000 ft)	5	1300	Gen. (LDG)											
A. F-104 probe (1 run)				Probe	Provide separation distance					X	X			X
B. Lear probes (3 runs)					Probe						X			X
C. PA-30 probes (3 runs)						Probe				X	X			X
		1430												
Date: Nov. 2, 1973														
Smoke observation and in-trail probes level flt, 3658 m (12,000 ft), B727 all configs.	6	1030	Gen.											
A. Smoke observations				Observe	Observe						X			X
B. Lear probes in-trail					Probe						X			X
		1215												
Cross-track probes – level flight, 3658 m (12,000 ft), B727 all configs.	7	1430							Separation distance and photo					
Cross-track probes				Probe						X	X			X
		1600												

[a]Gen. = wake vortex generator

[b]TO = take off configuration
CLN = clean configuration
LDG = landing configuration

[c]Each run is 7 min with several probes

TABLE 2.– FLIGHT-TEST INVESTIGATION OF WAKE TUBULENCE BEHIND B727 – Concluded.

Test objectives	Flight no.	Test time	Aircraft status: B727	F-104	Lear Jet	PA-30	C-402	T-28	Gulf-stream	Telemetered data	Radar	Lakebed	Noise	Echo 2
Date: Nov. 3, 1973														
Cross-track probes Level flt, 3658 m (12,000 ft), B727 all configs.	8	1030	Gen. (improve smoker on left)				Meteorological measurement		Photo chase					
Run Flaps Gear 1 Up Up Observe only 2 Up Up Probe 3 15° Dn 4 15° Up 5 25° Dn 6 25° Up 7 30° Dn 8 30° Dn 9 30° Up					Probe									X X X X X X X X
		1200												
Cross-track and in-trail probes Descents and climbs, 3658 m (12,000 ft)	9	1430	Gen. (further improve left smoker)											
A. 3° descent and climb (2) B. Level flight (2) C. 3° descent (1) D. Smoke observations					Probe									X X X
		1600												
Date: Nov. 5, 1973														
Take-off with climbing turns (2) A. Clean config. B. Take-off config.	10	0700	Gen. (TO) and (LDG)								X X	X X	X X	
In-trail probes at altitude A. 3° descent B. Transition C. 6° descent						Probe				X X X	X X X		X X X	X X X
Photos of clean config. vortex			CLN								X		X	X
		0815												
Take-off with climbing turn	11	1100	Gen. (TO)								X	X	X	X
Two-segment approach "demonstration flight" A. Two-segment approach B. Conventional approach			(LDG) (LDG)			Probe				X X	X X	X X	X X	X X
Photos of vortex at various flap settings			(Various)								X			
		1230												
Take-off with climbing turn	12	1400	Gen. (TO)								X	X	X	X
In-trail probe of two-segment approach at 3658 m (12,000 ft)			(LDG)		Probe						X			
Two-segment approach "demonstration flight" A. Two-segment approach B. Conventional approach			(LDG) (LDG)								X X	X X	X X	X X
Cross-track probes at 3658 m (12,000 ft) A. Level flight, clean			(CLN)											
		1530												

TABLE 3.– SEPARATION DISTANCES AT WHICH UPSET RESPONSE DATA WERE OBTAINED – B727 CONFIGURATION: LANDING FLAPS (30°)

Probe aircraft	Separation distances, km (n.mi.)				
	High altitude			Low altitude[a]	
	Level	Three degree	Two segment	Three degree	Two segment
Lear Jet LR-23	2.96 – 6.48[b] (1.6 – 3.5)	4.26 – 6.11 (2.3 – 3.3)	3.89 – 5.18 (2.1 – 2.8)	5.18 – 5.56 (2.8 – 3.0)	5.37 – 5.93 (2.9 – 3.2)
Piper PA-30	4.63 – 5.55 (2.5 – 3.0)	6.57 – 8.06 (3.55 – 4.35)	6.94 – 7.04 (3.75 – 3.80)	6.17 – 7.63 (3.33 – 4.12)	No upset data obtained

[a]Only one pass was made for each of the two types of approaches for the low altitude flights.

[b]Additional LR-23 data were obtained behind the B727 clean configuration at distances of 5.6 to 7.5 n.mi.

Figure 1.– Boeing 727 wake vortex generating aircraft.

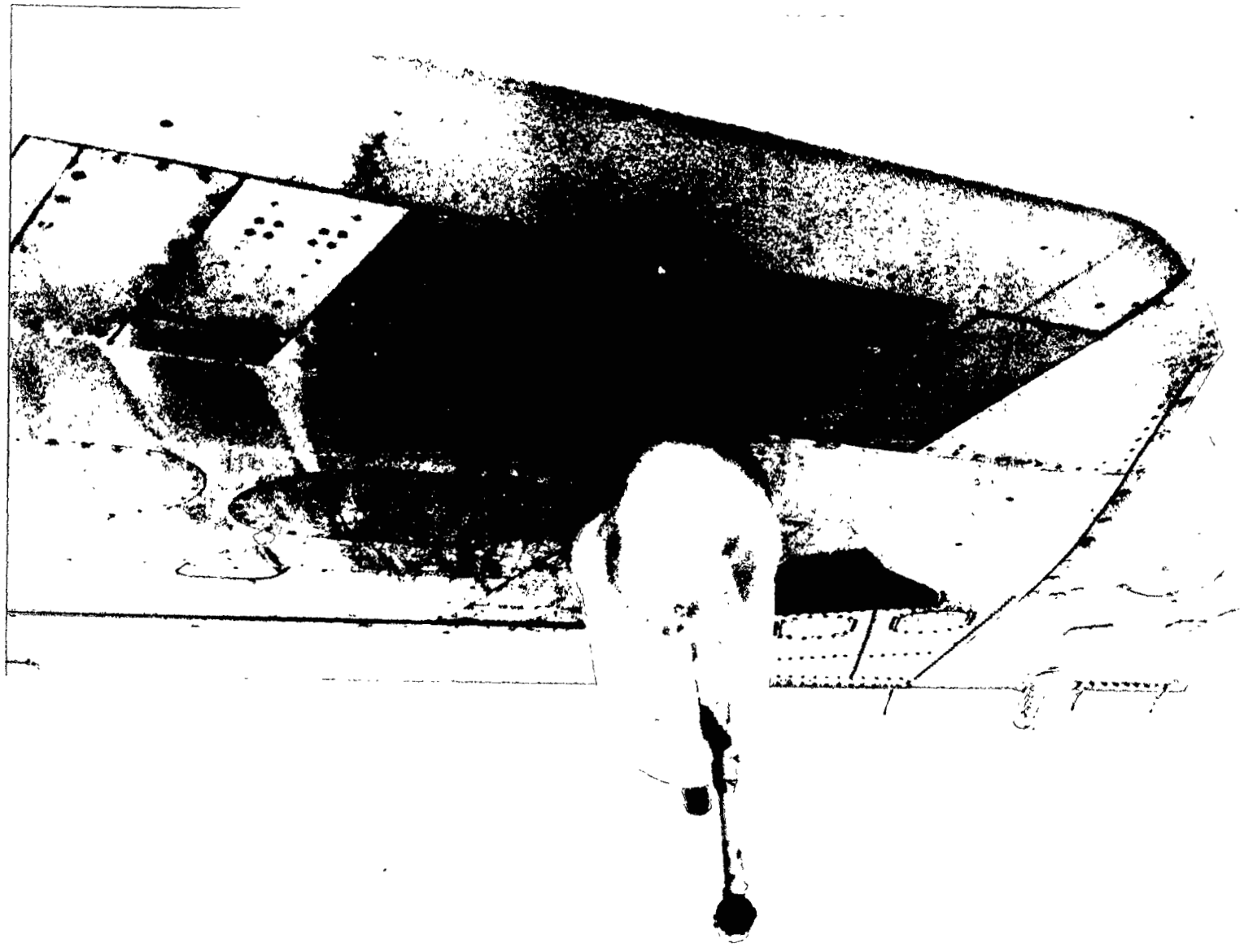

Figure 2.– Vortex marking smoke generators mounted on the B727 tip.

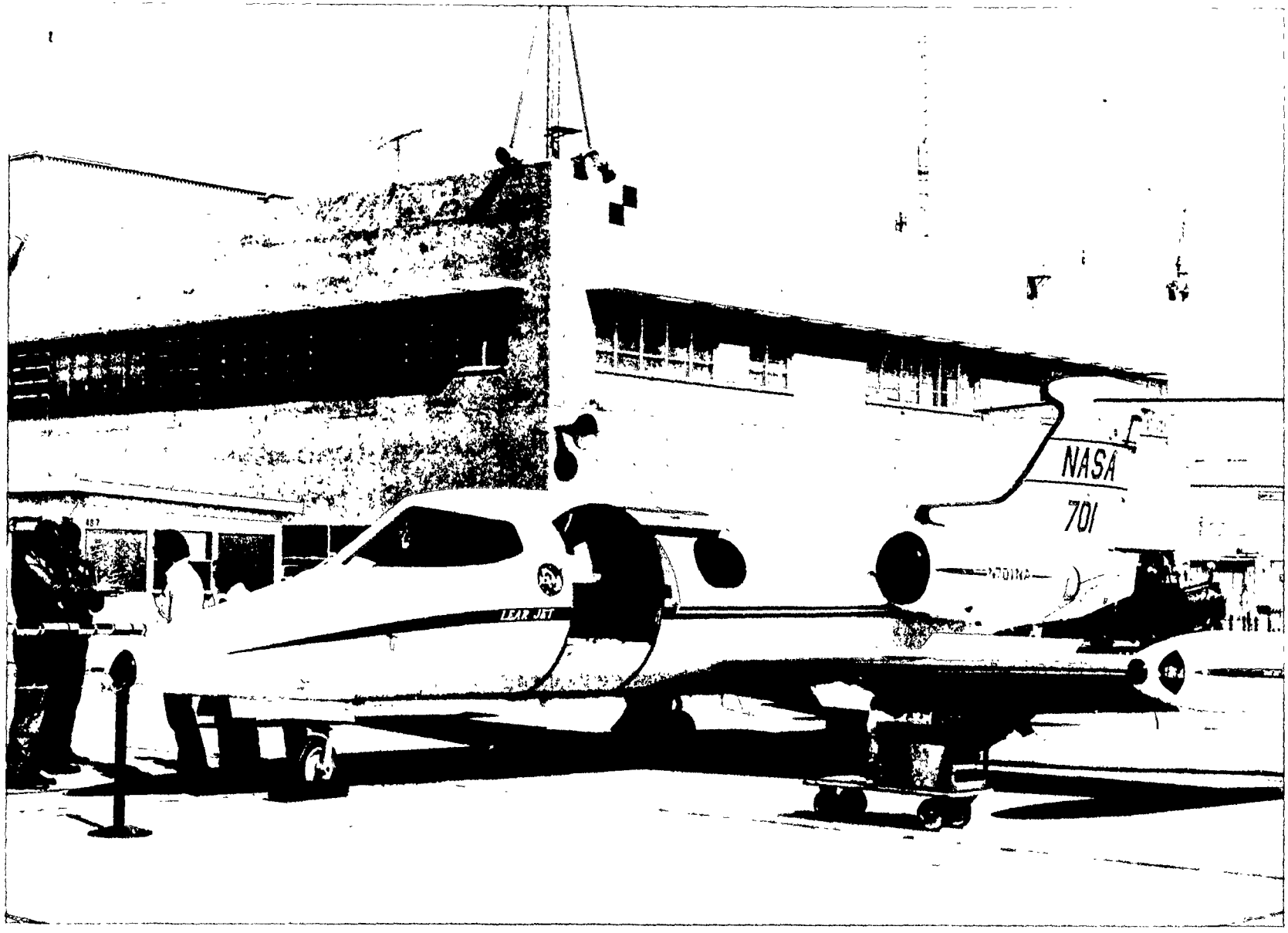

Figure 3.– Wake vortex probe aircraft; Lear Jet model 23.

Figure 4.– Wake vortex probe aircraft; Piper Twin Comanche.

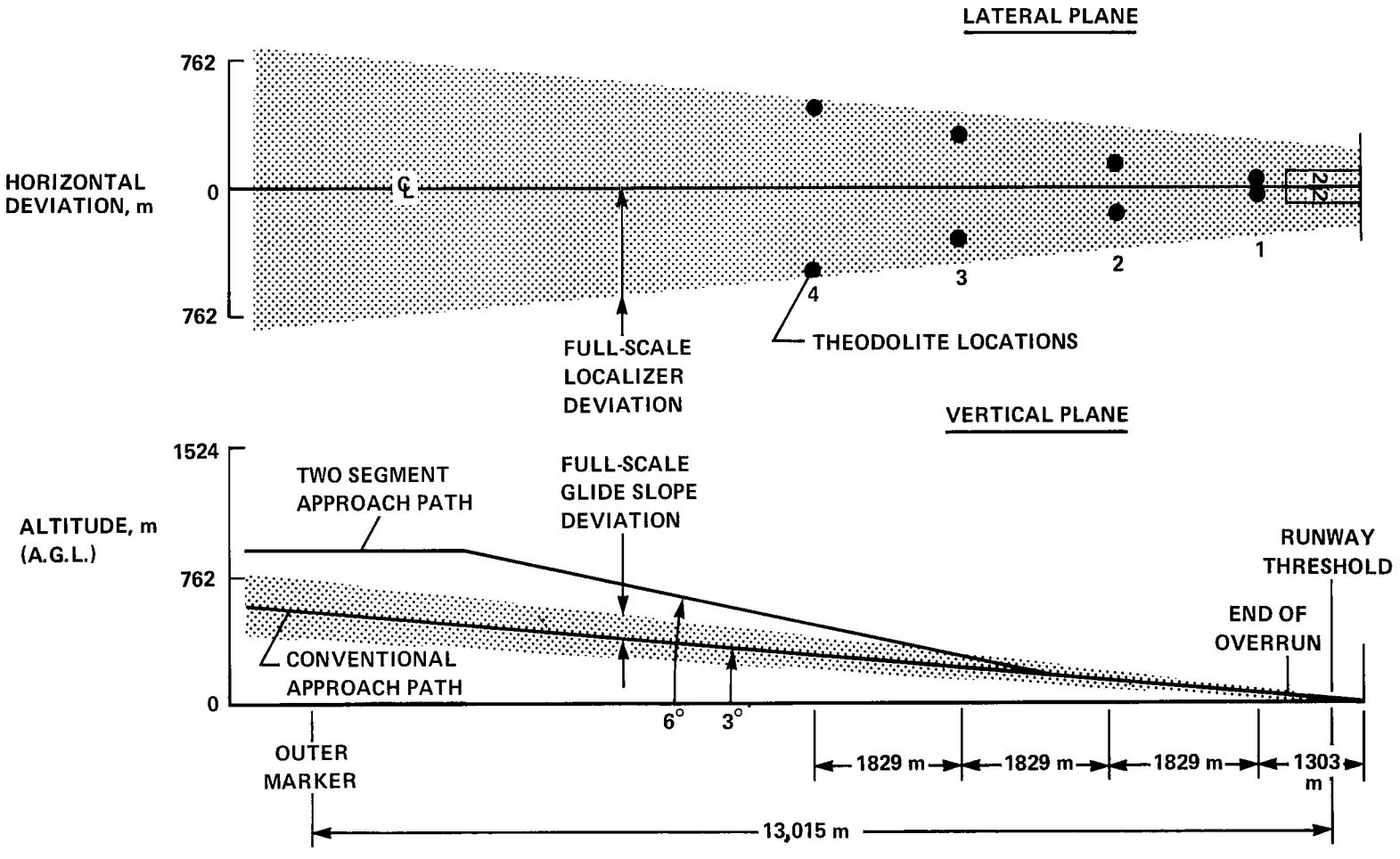

Figure 5.– Landing approach geometry; conventional and two-segment.

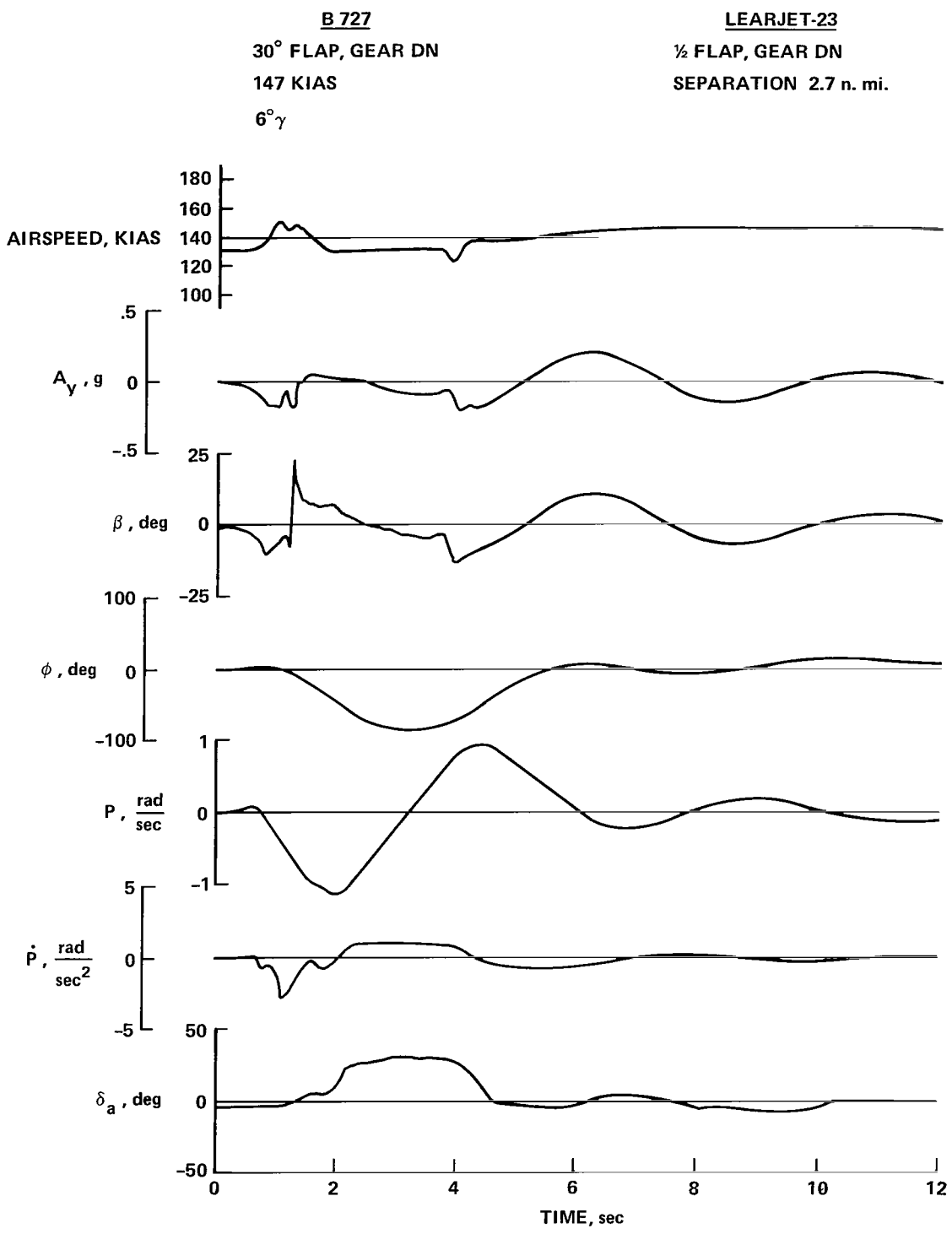

(a) Lateral-directional.

Figure 6.— Time histories of excursions experienced by the Lear Jet flying in the wake of the B727.

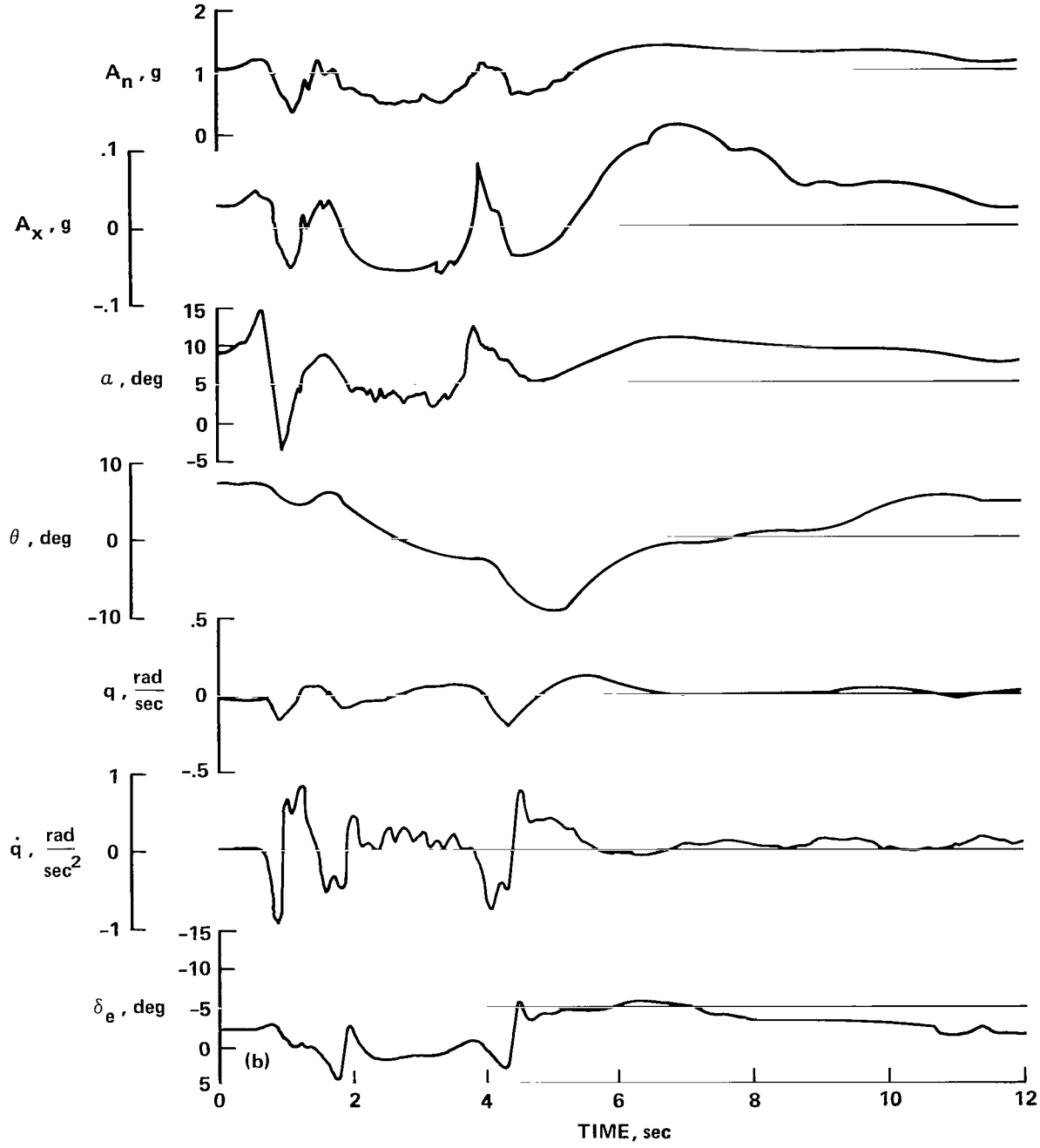

(b) Longitudinal.

Figure 6.– Concluded.

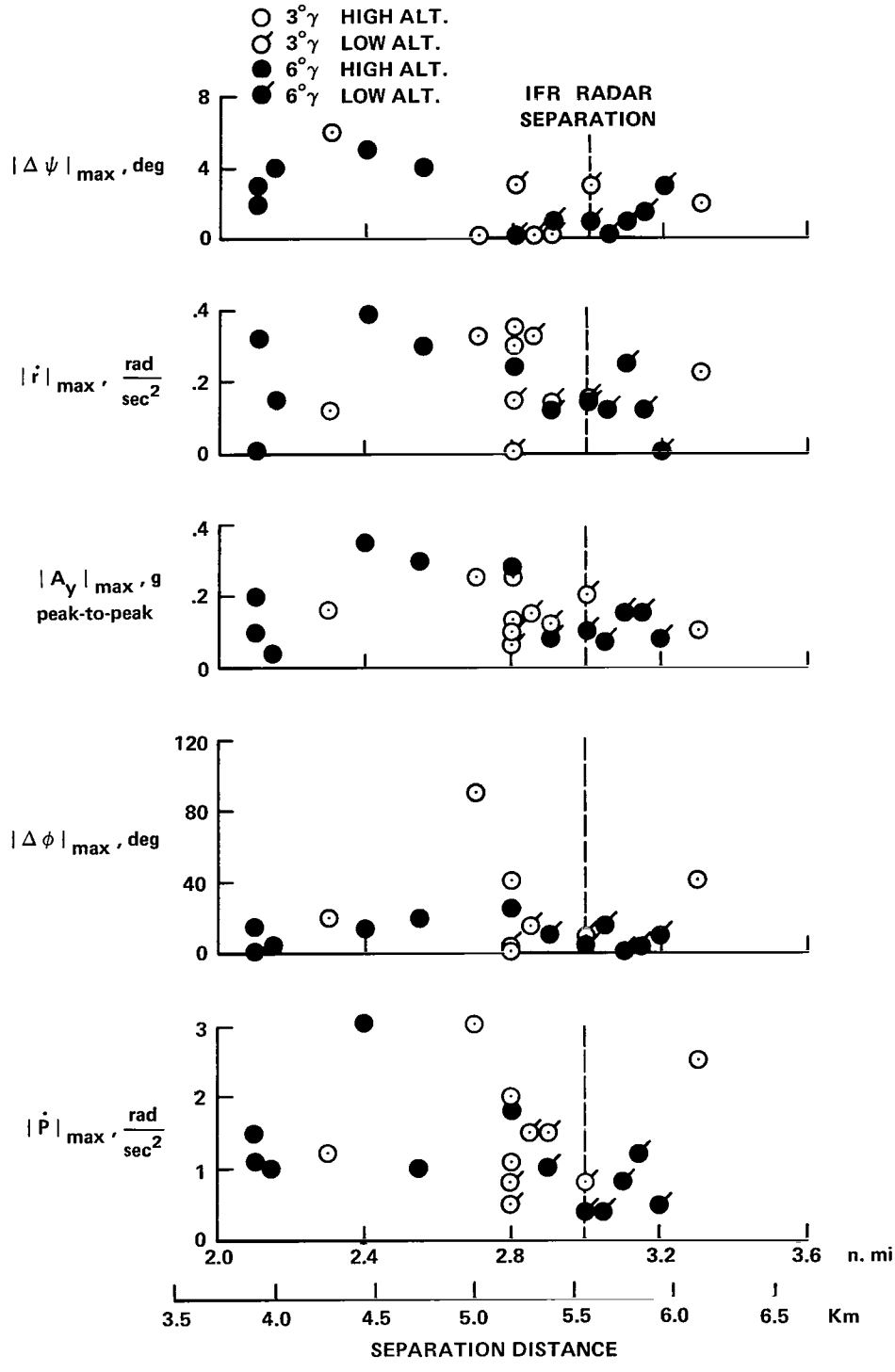

(a) Lateral-directional.

Figure 7.– Maximum excursions experienced by Lear Jet versus separation distance.

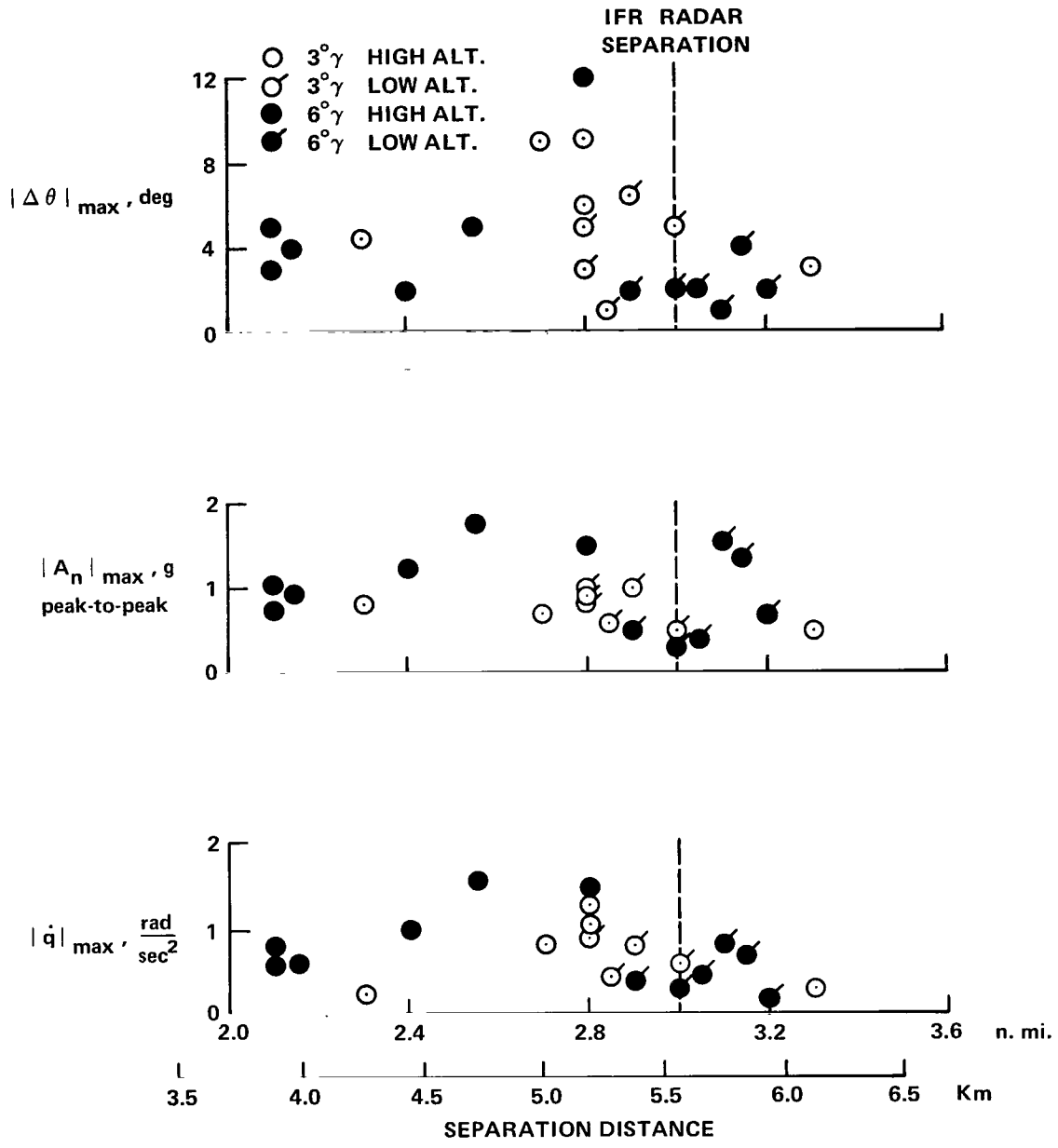

(b) Longitudinal.

Figure 7.– Concluded.

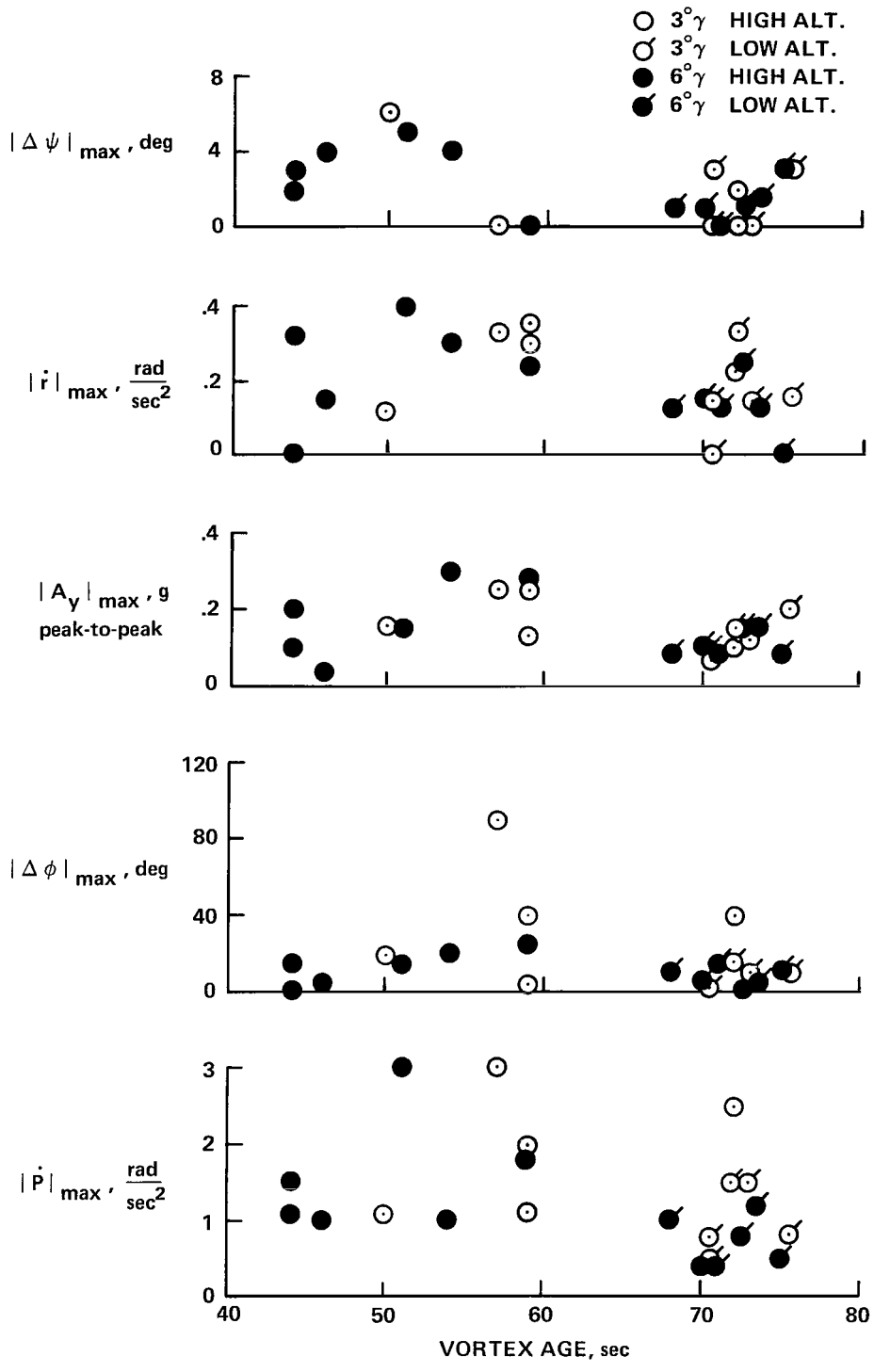

(a) Lateral-directional.

Figure 8.— Maximum excursions experienced by Lear Jet versus vortex age.

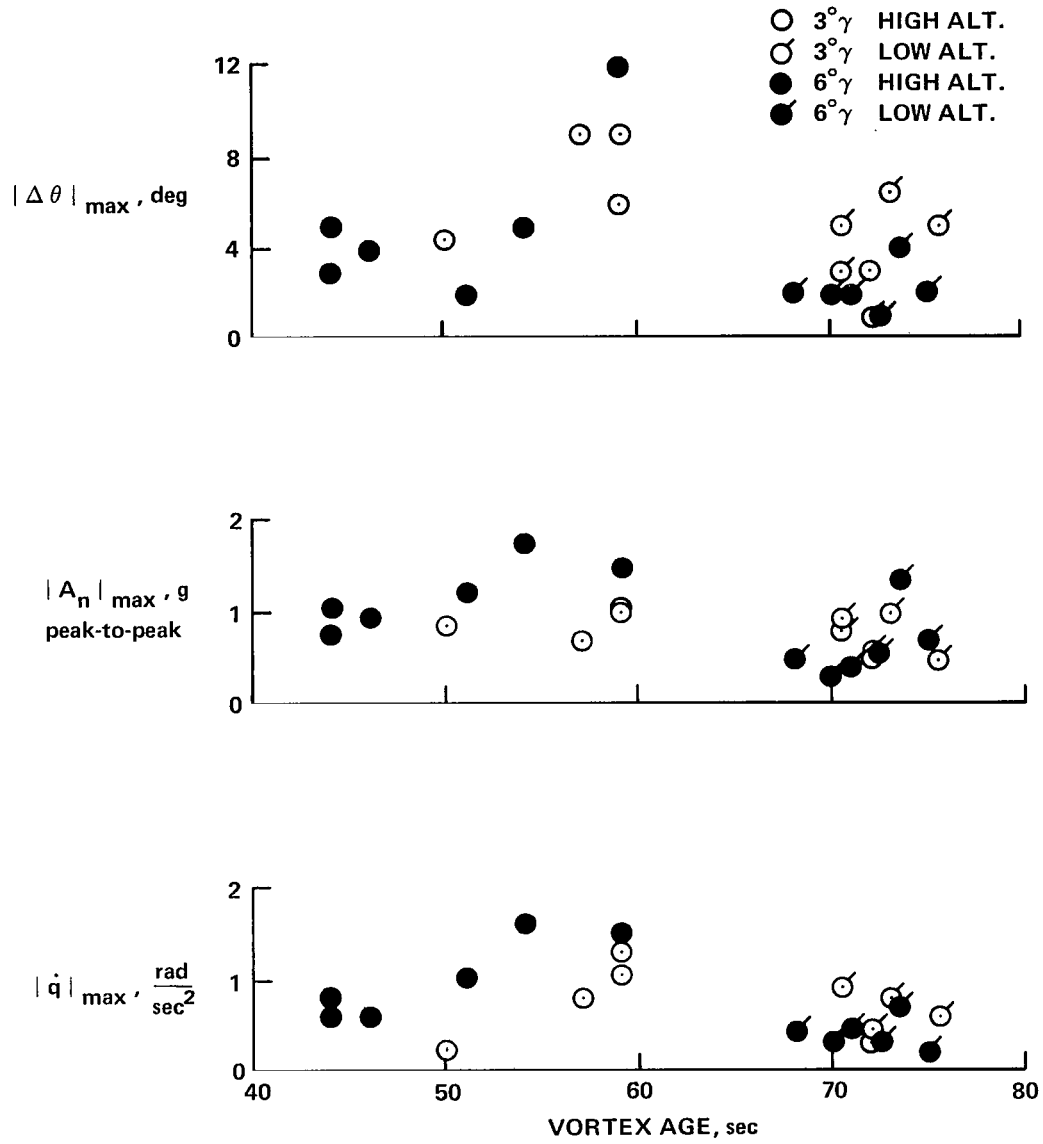

(b) Longitudinal.

Figure 8.– Concluded.

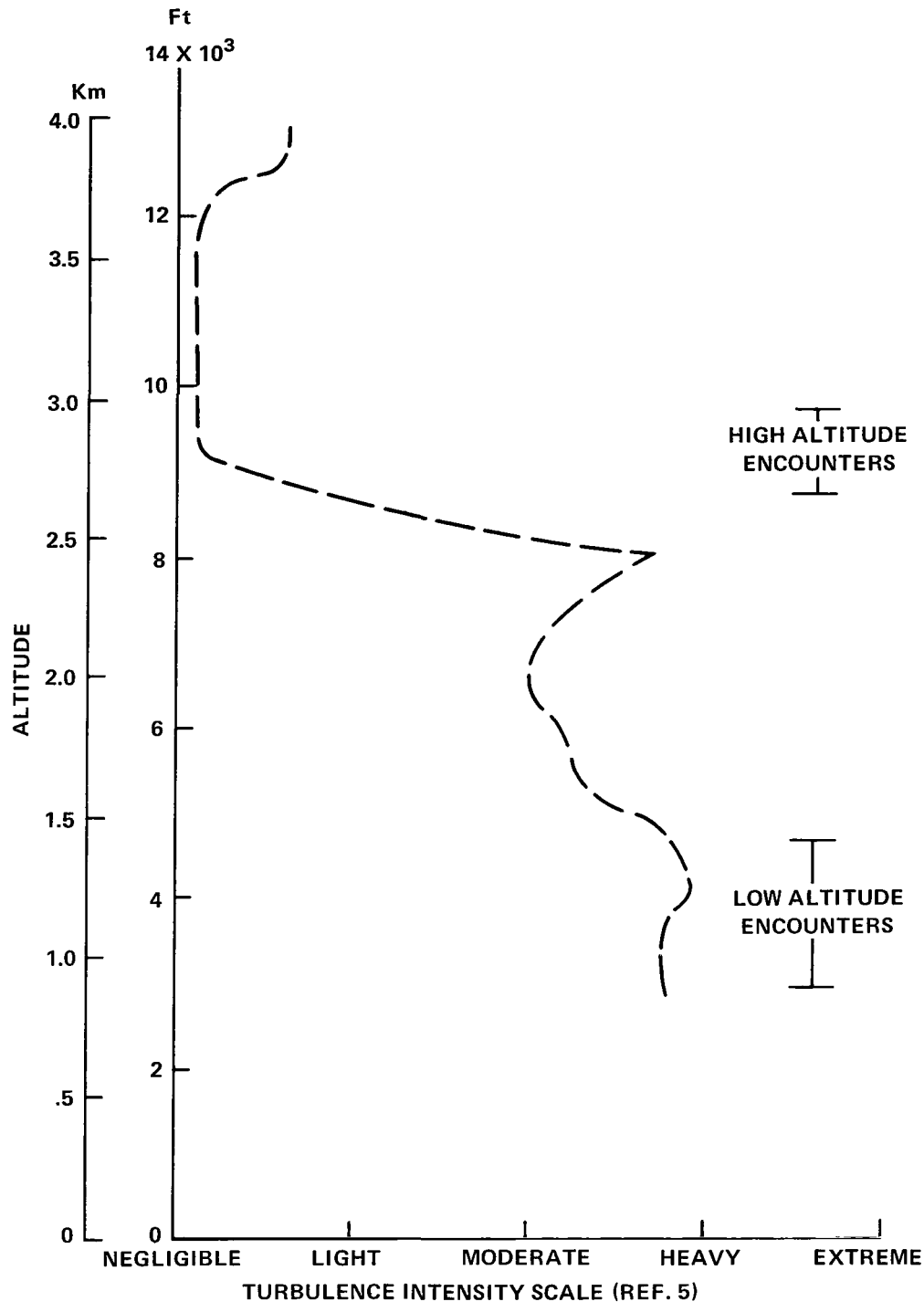

Figure 9.– Effect of altitude on turbulence environment for Lear Jet encounters during landing approaches.

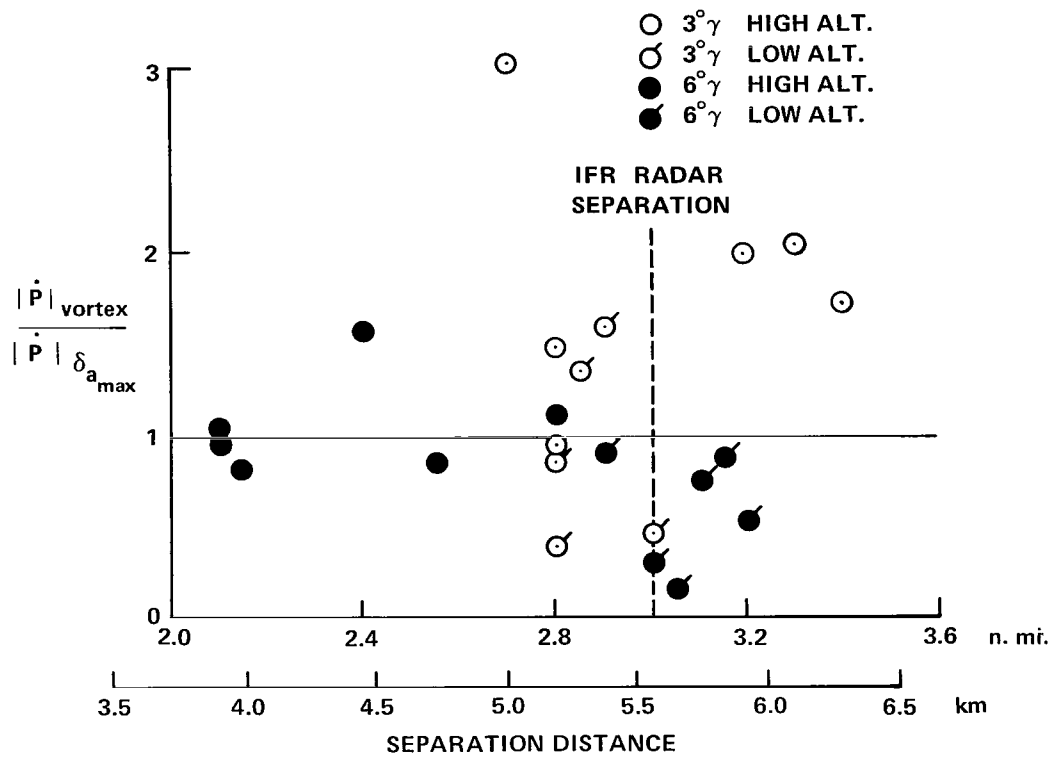

Figure 10.– Ratio of the vortex induced roll acceleration to maximum roll control power for the Lear Jet versus separation distance.

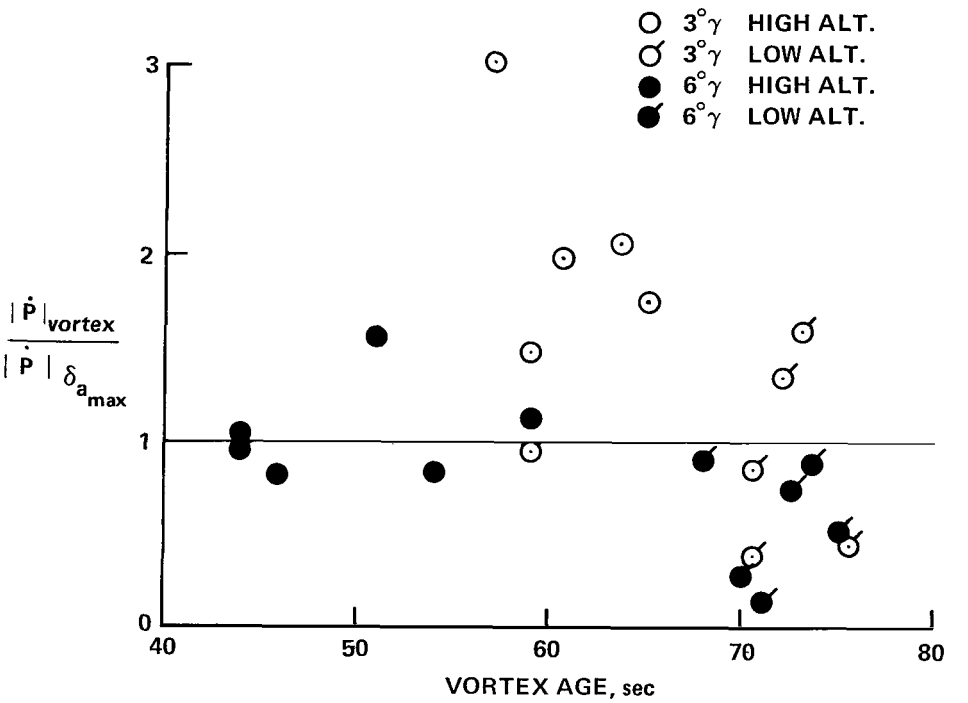

Figure 11.– Ratio of the vortex induced roll acceleration to maximum roll control power for the Lear Jet versus vortex age.

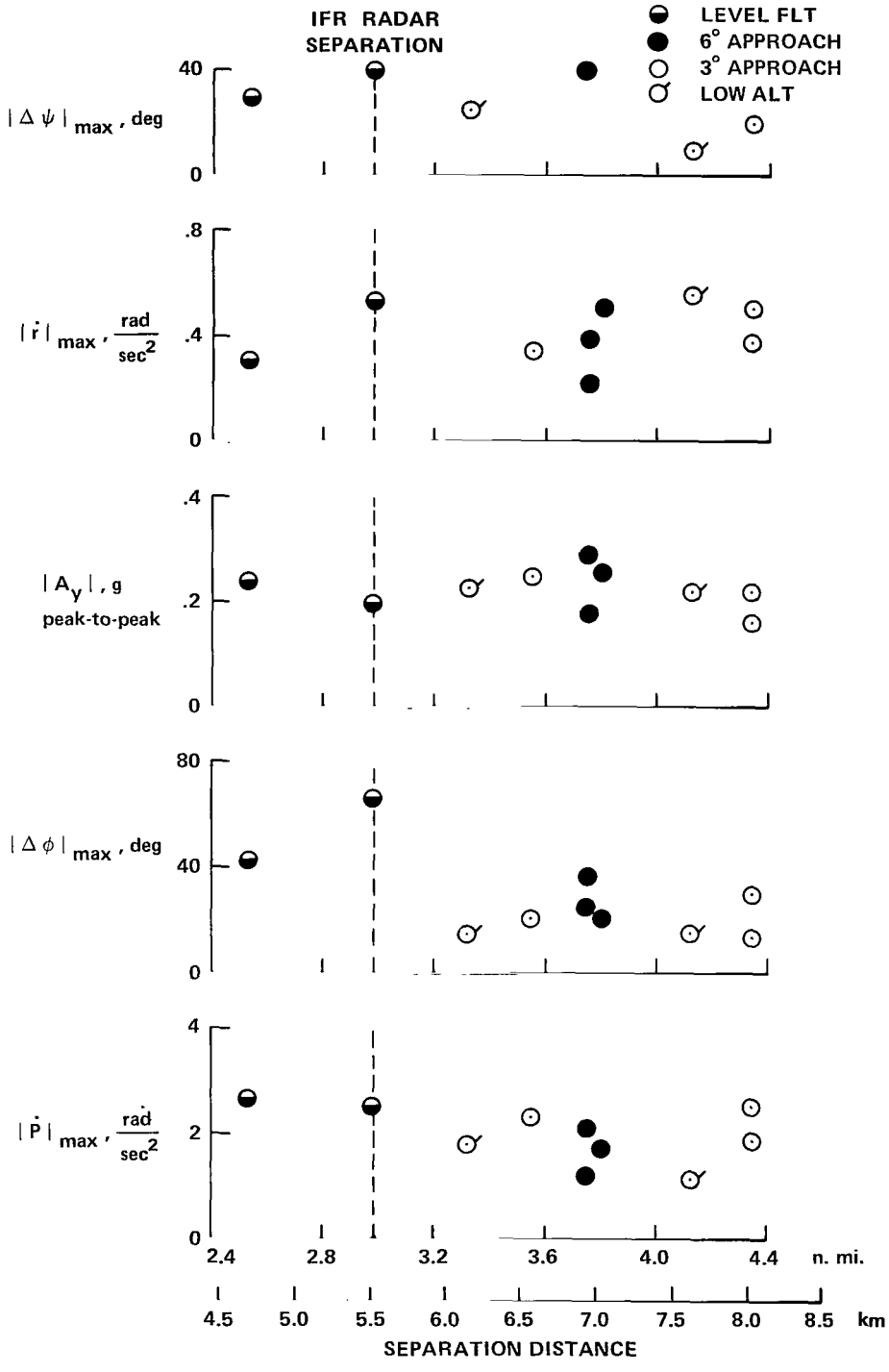

(a) Lateral-directional.

Figure 12.– Maximum excursions experienced by PA-30 versus separation distance.

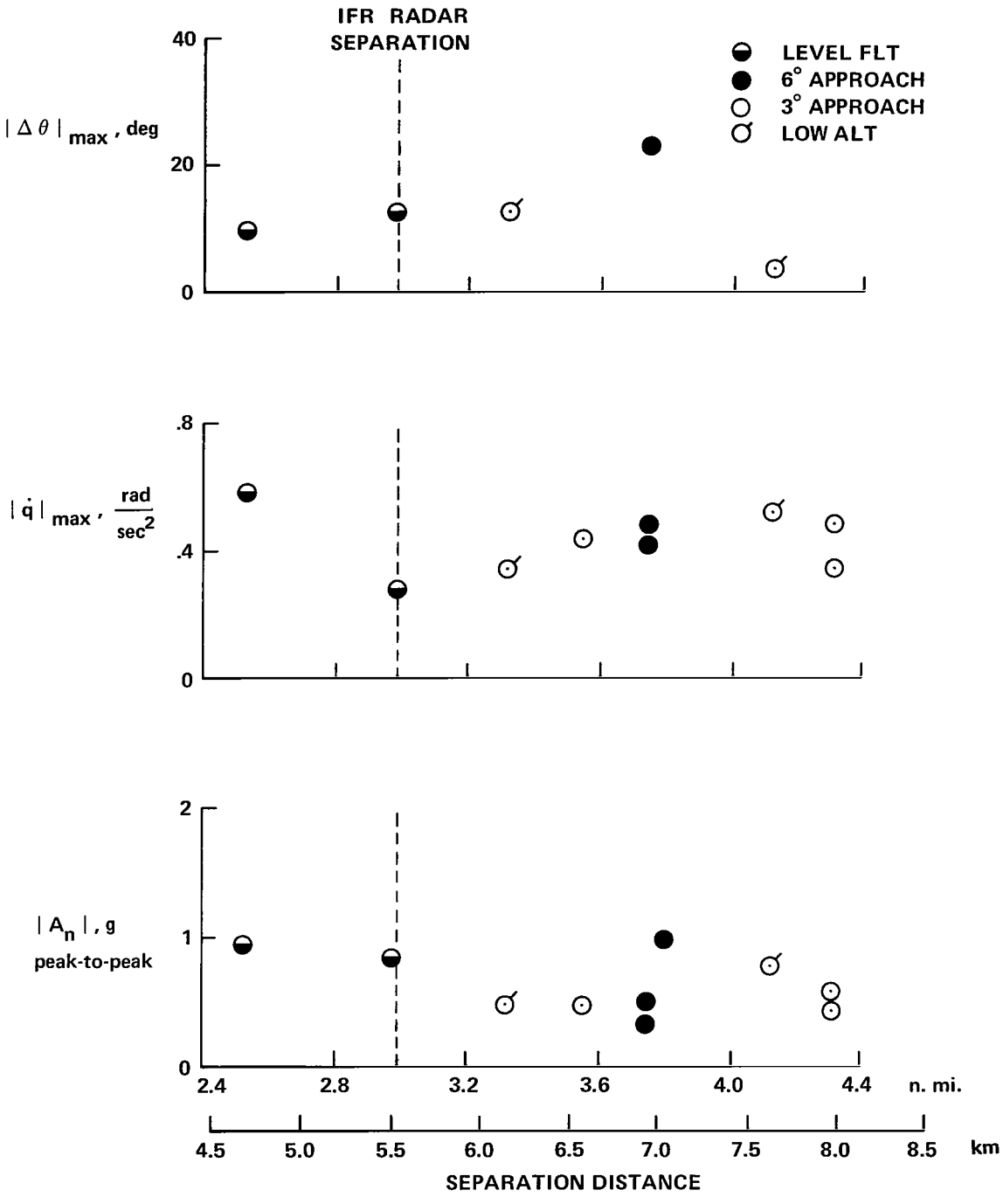

(b) Longitudinal.

Figure 12.– Concluded.

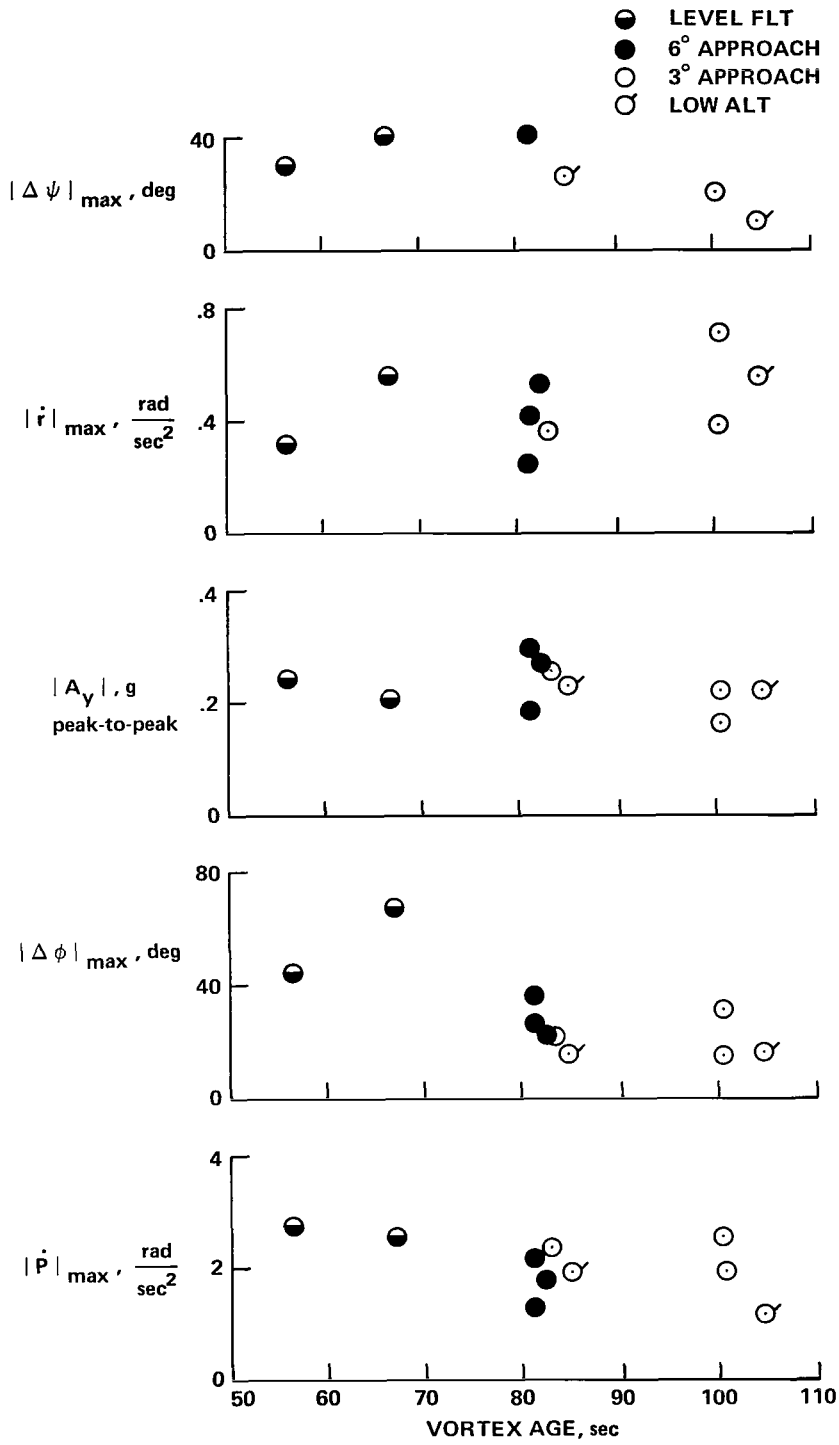

(a) Lateral-directional.

Figure 13.– Maximum excursions experienced by PA-30 versus vortex age.

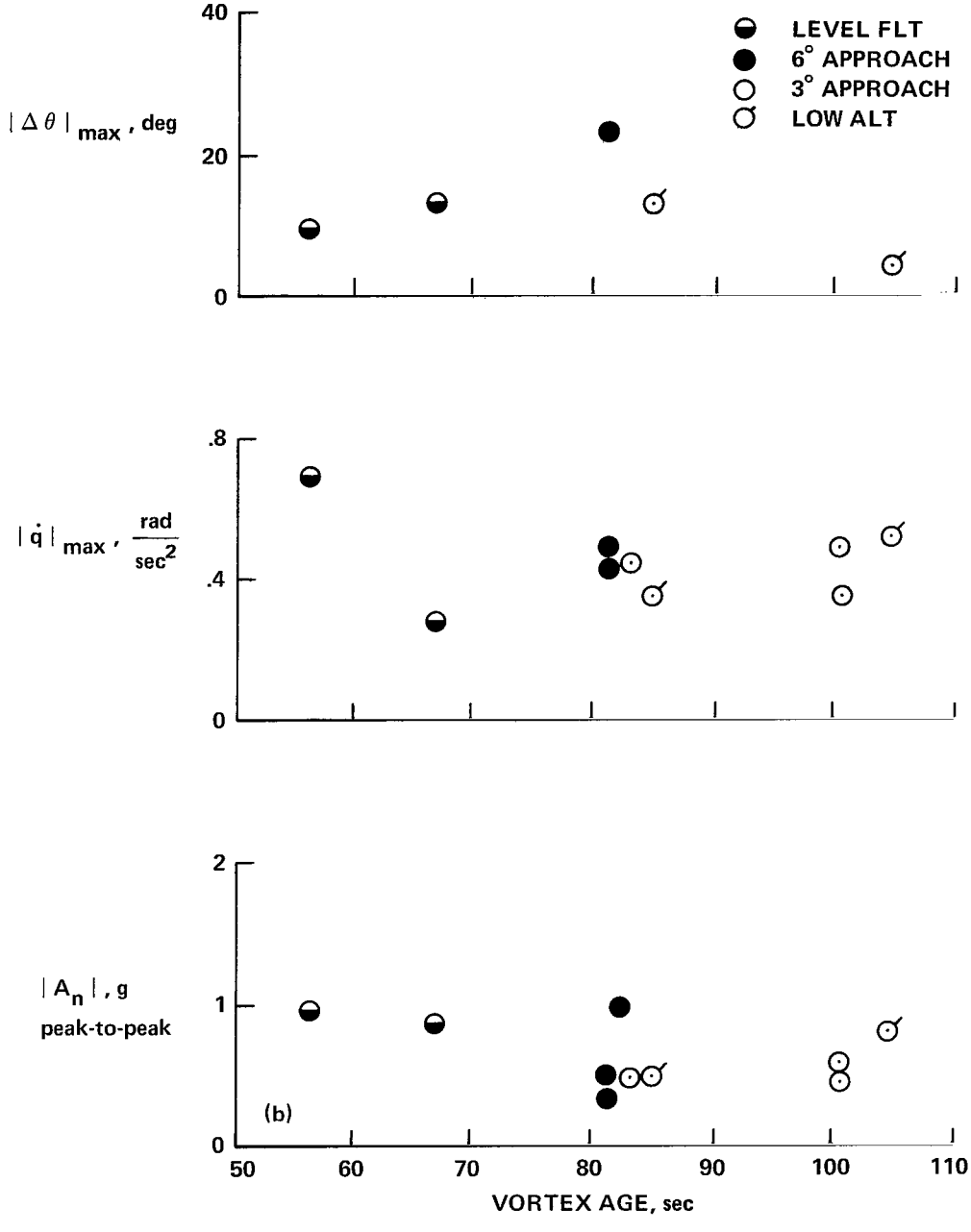

(b) Longitudinal.

Figure 13.– Concluded.

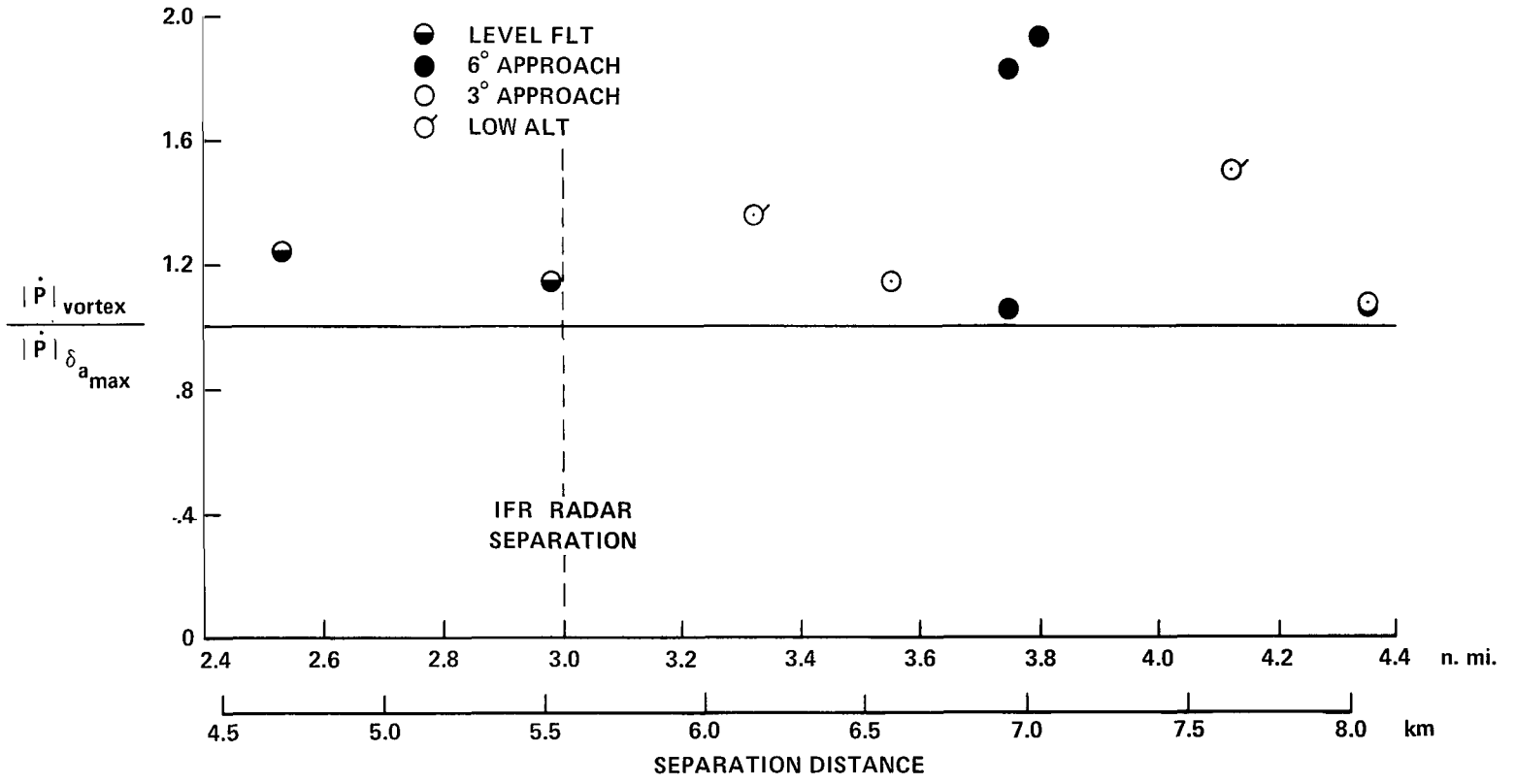

Figure 14.– Ratio of vortex induced roll acceleration to maximum roll control power for the PA-30 versus separation distance.

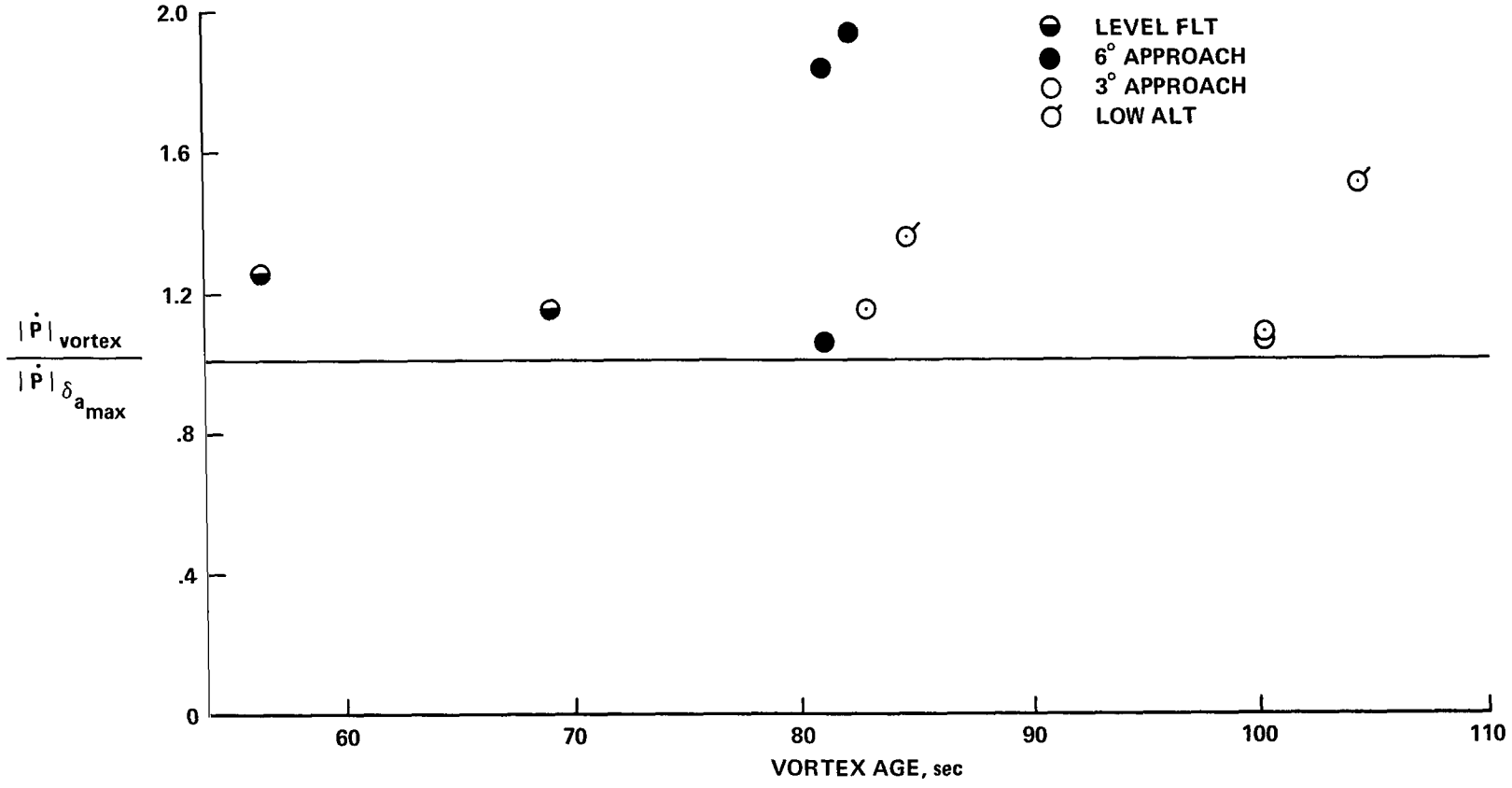

Figure 15.– Radio of vortex induced roll acceleration to maximum roll control power for the PA-30 versus vortex age.

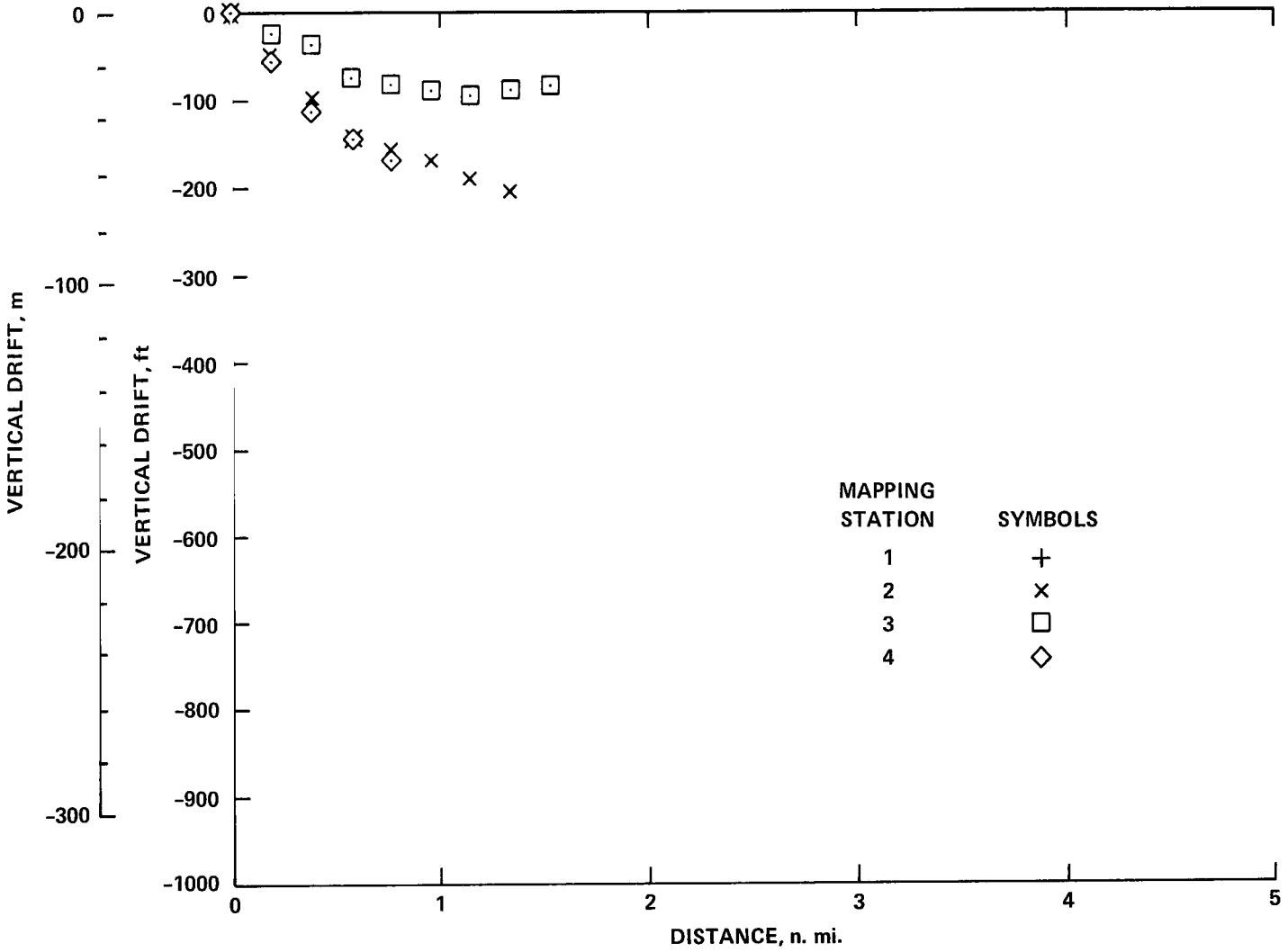

(a) Conventional approach; approach configuration, 132 knots.

Figure 16.– Trailed wake vortex position behind a B727 aircraft.

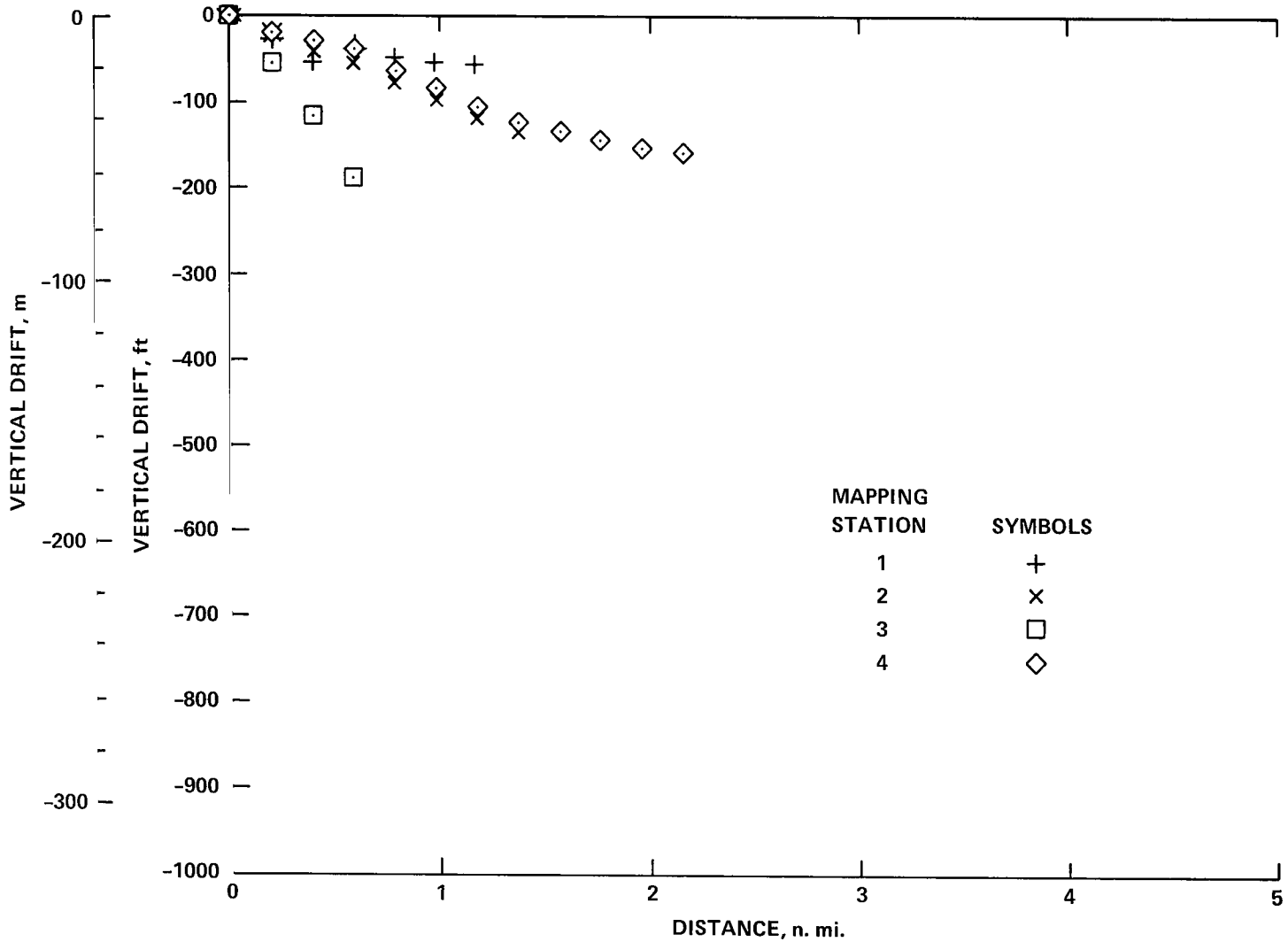

(b) Conventional approach; approach configuration, 135 knots.

Figure 16.– Continued.

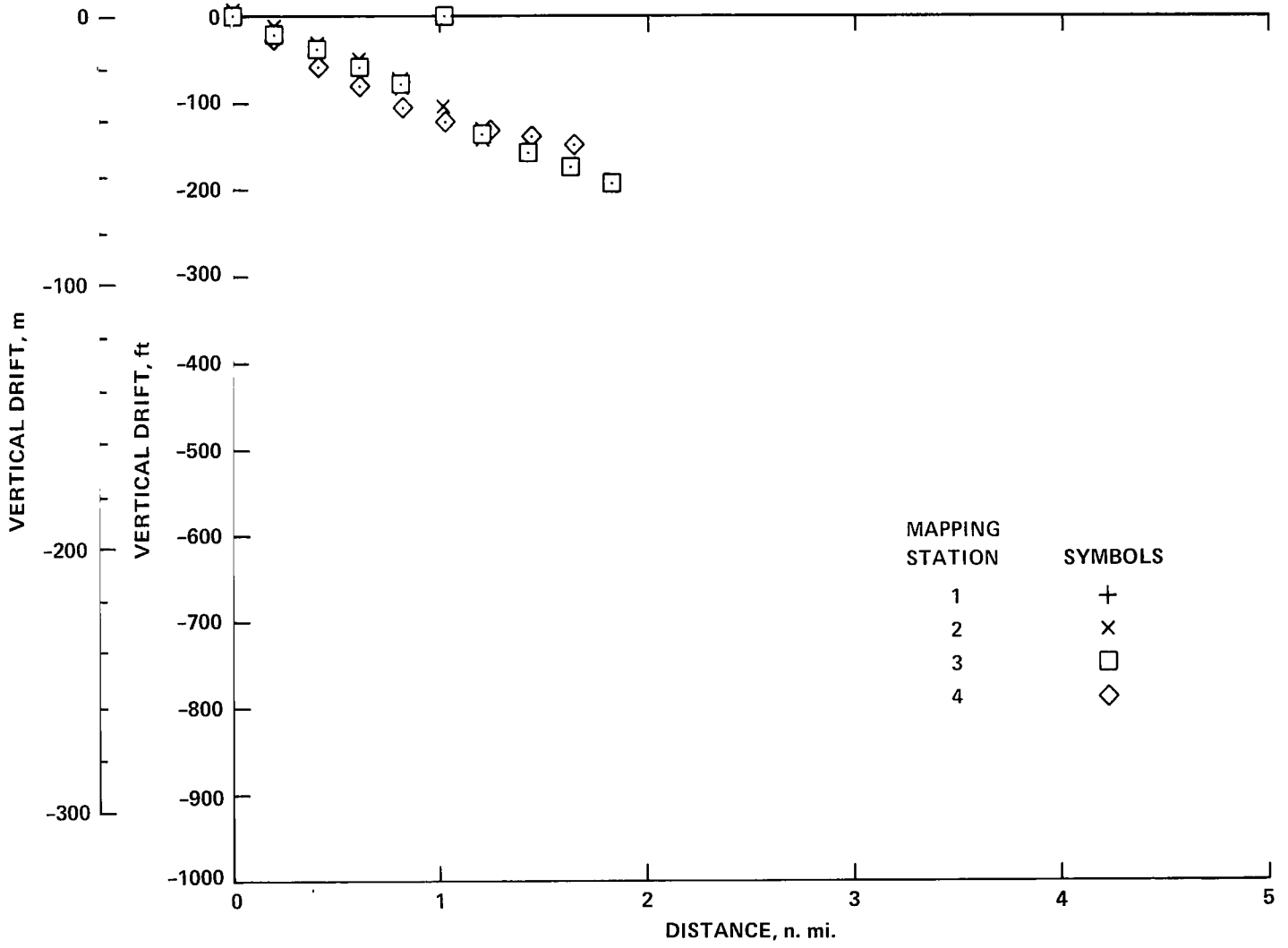

(c) Two-segment approach; approach configuration, 135 knots.

Figure 16.– Continued.

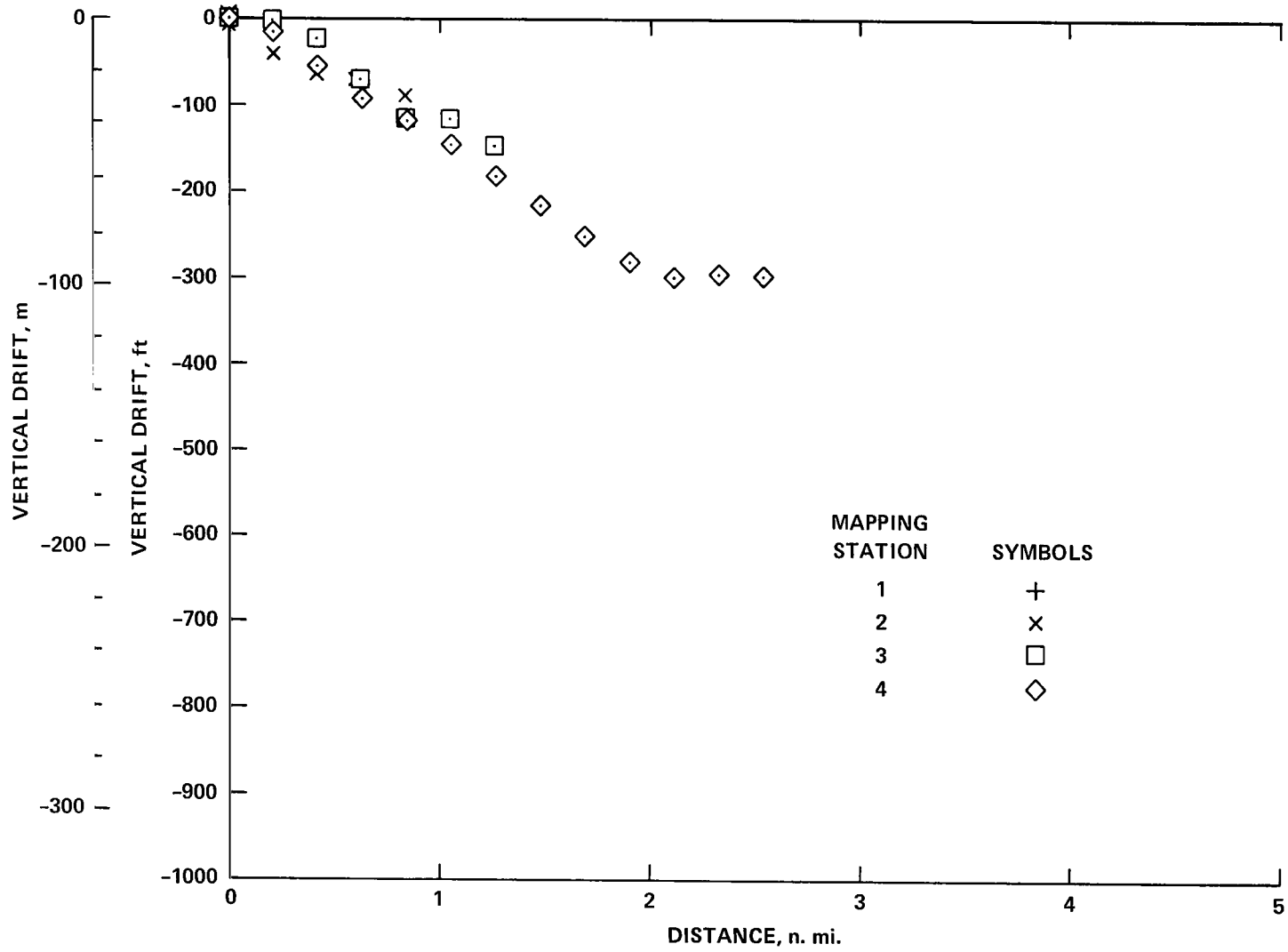

(d) Two-segment approach; approach configuration, 145 knots.

Figure 16.– Continued.

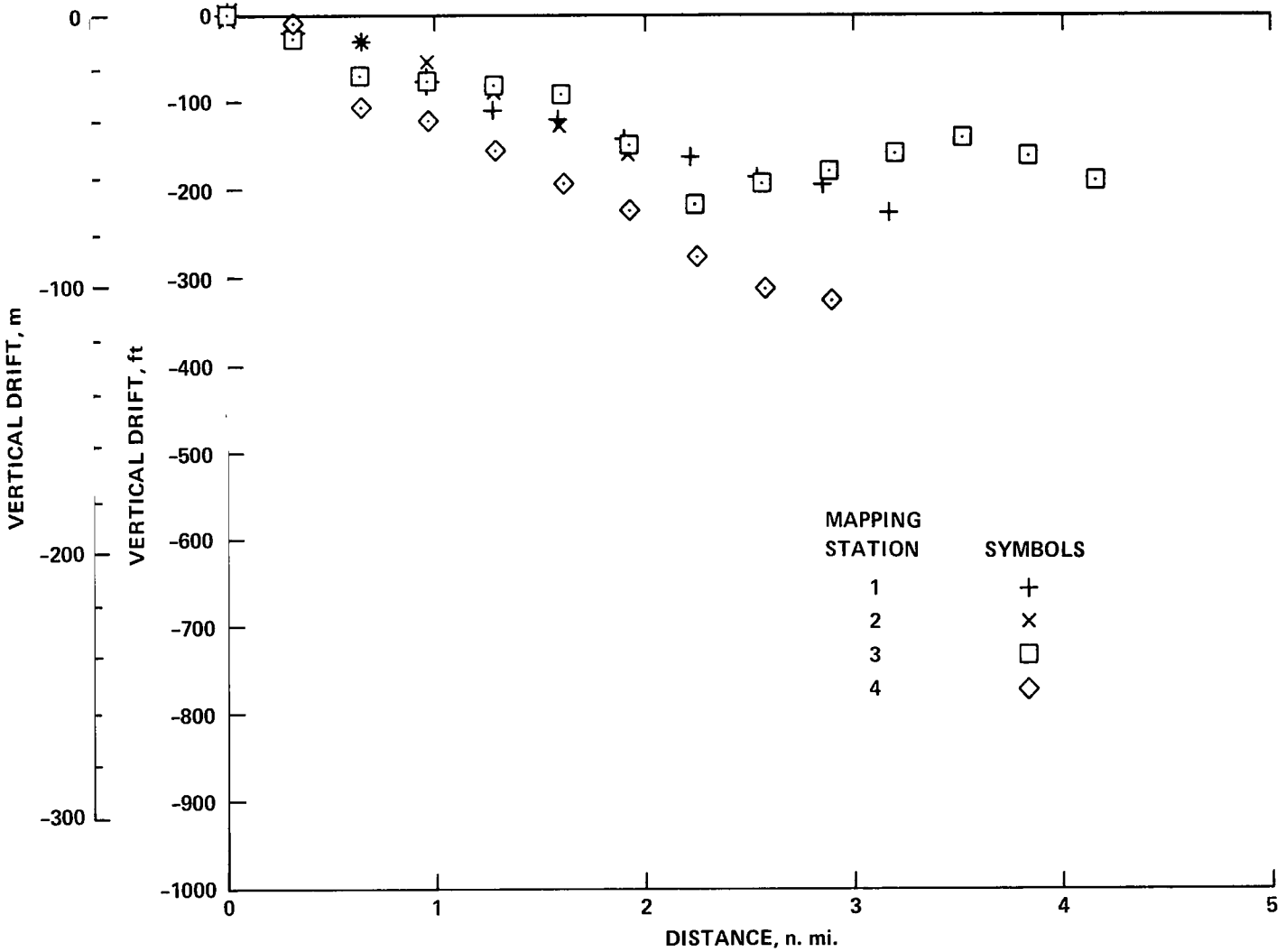

(e) Take-off; take-off configuration, 220 knots.

Figure 16.– Continued.

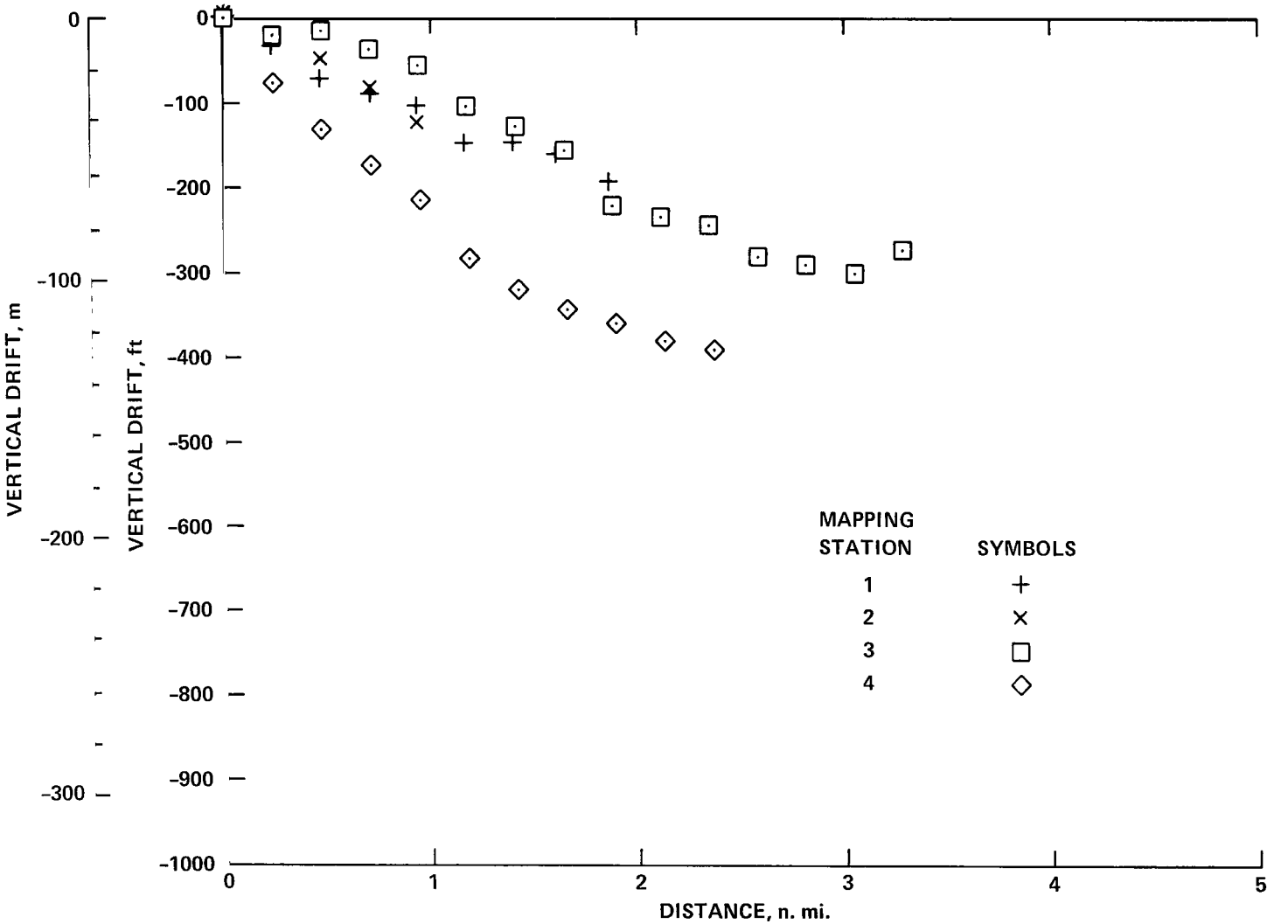

(f) Take-off; take-off configuration, 160 knots.

Figure 16.– Concluded.

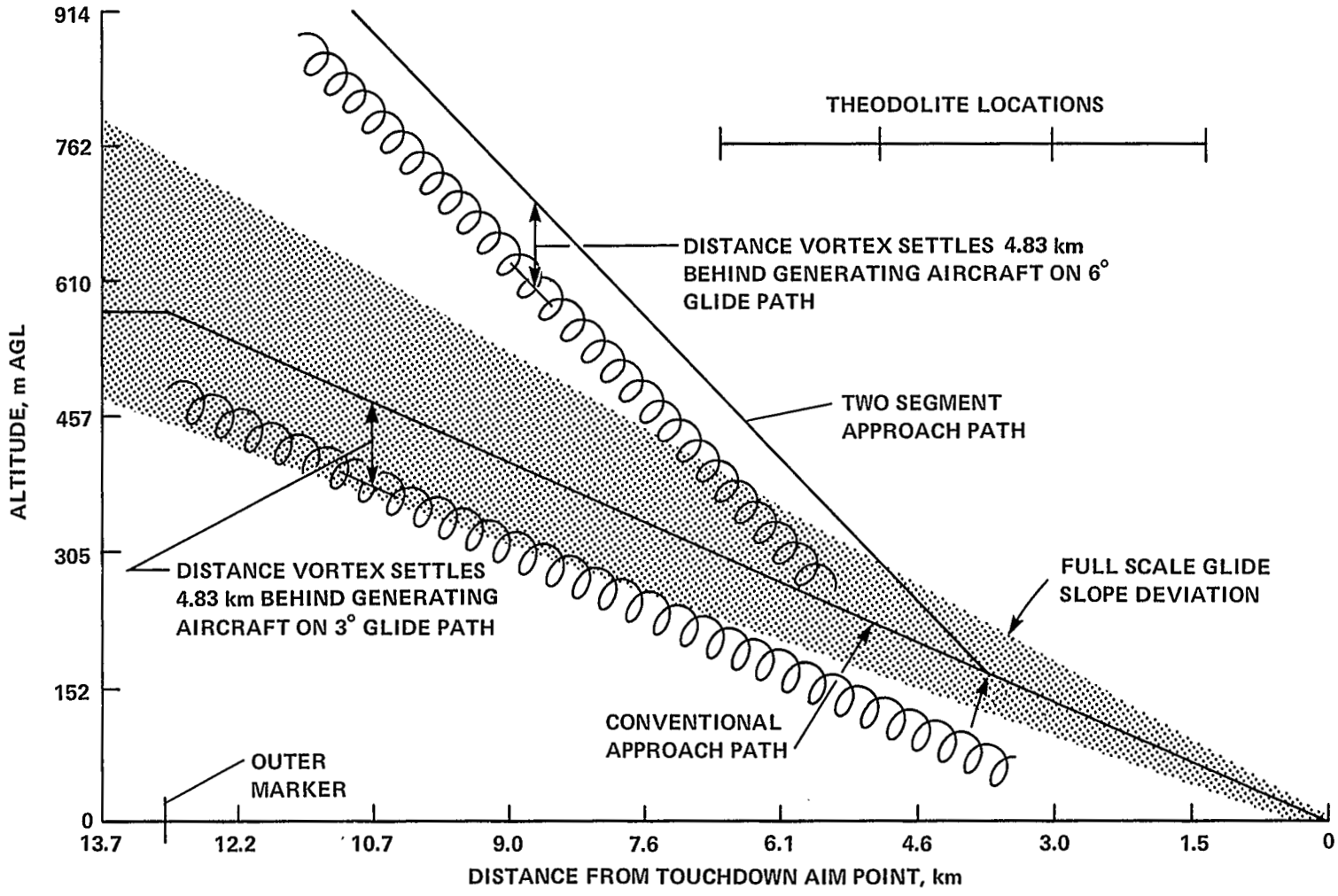

Figure 17.– Vortex location relative to approach path.

Figure 18.– B727 clean configuration vortex.

(a) Front view.

Figure 19.– B727 landing configuration vortex.

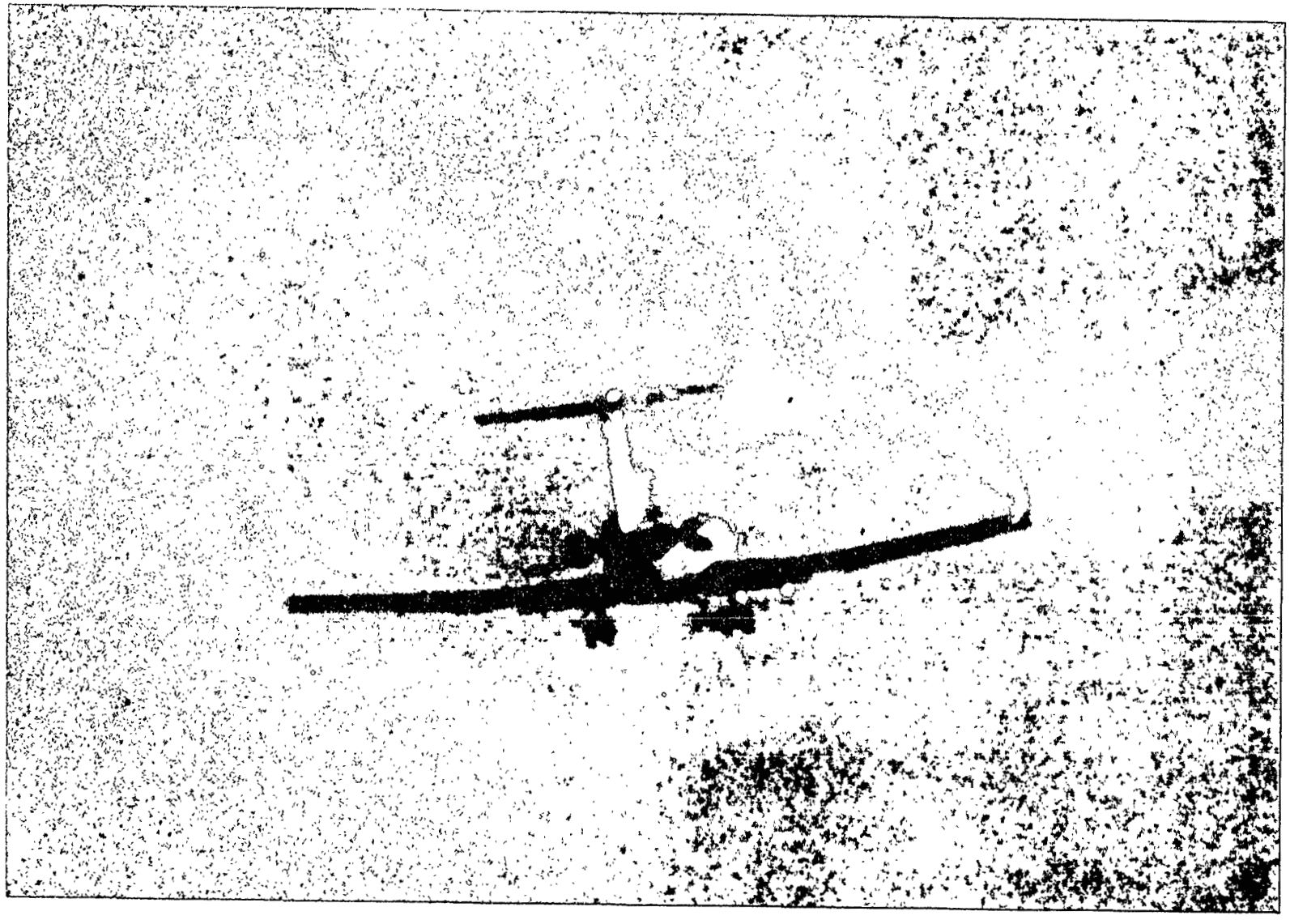

(b) Rear view.

Figure 19.– Concluded.

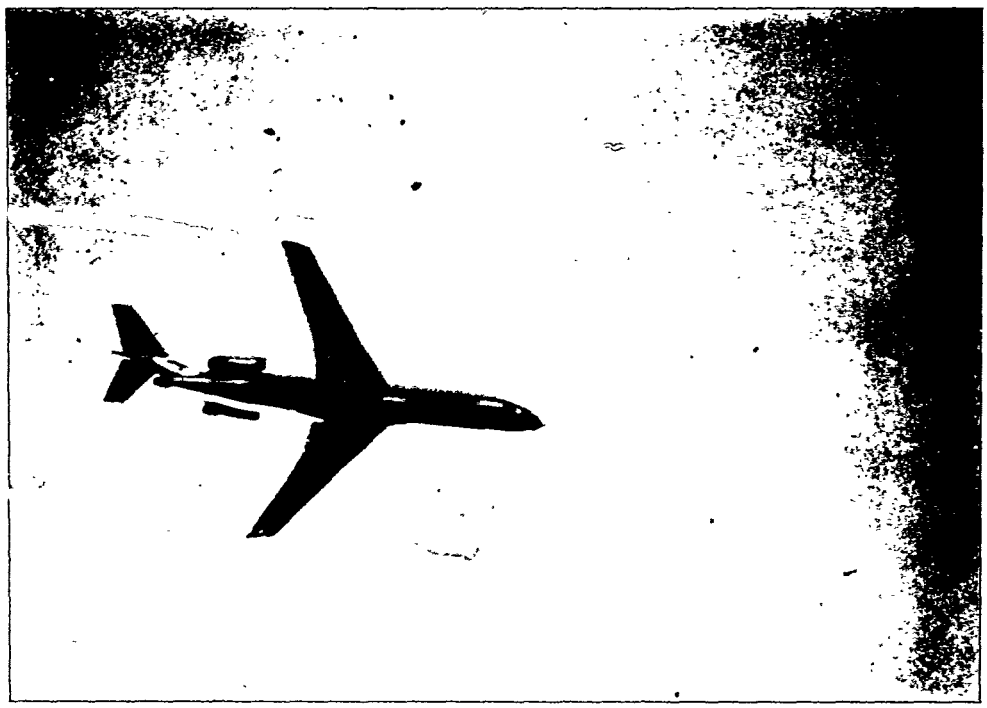

(a) Time = 0 sec.

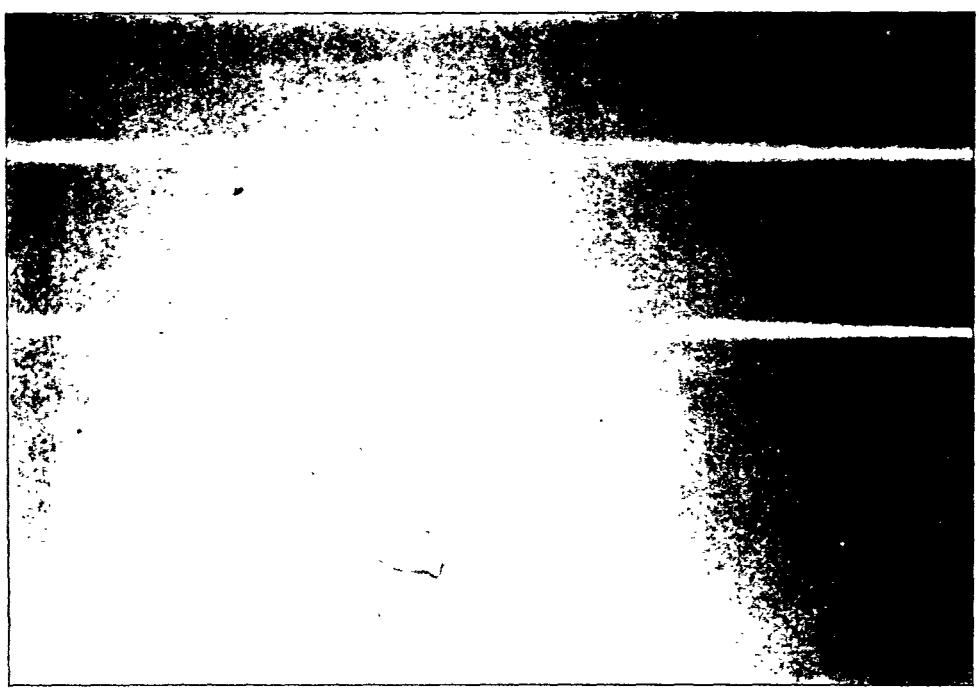

(b) Time = 5 sec.

Figure 20.— B727 wake vortex (clean configuration: weight = 334,000 kg (151,500 lb)).

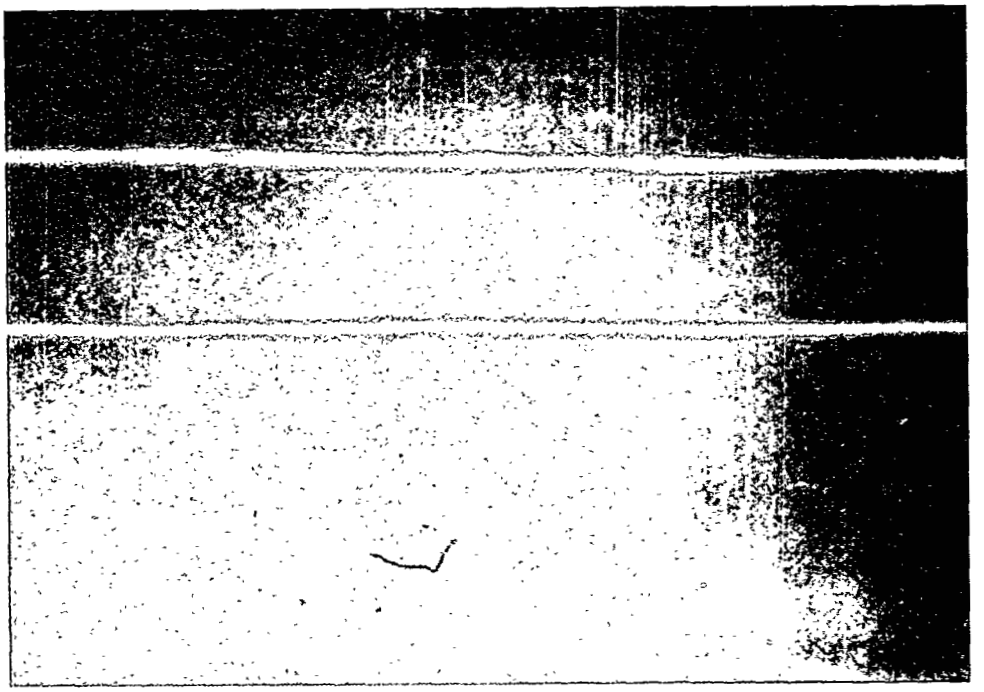

(c) Time = 10 sec.

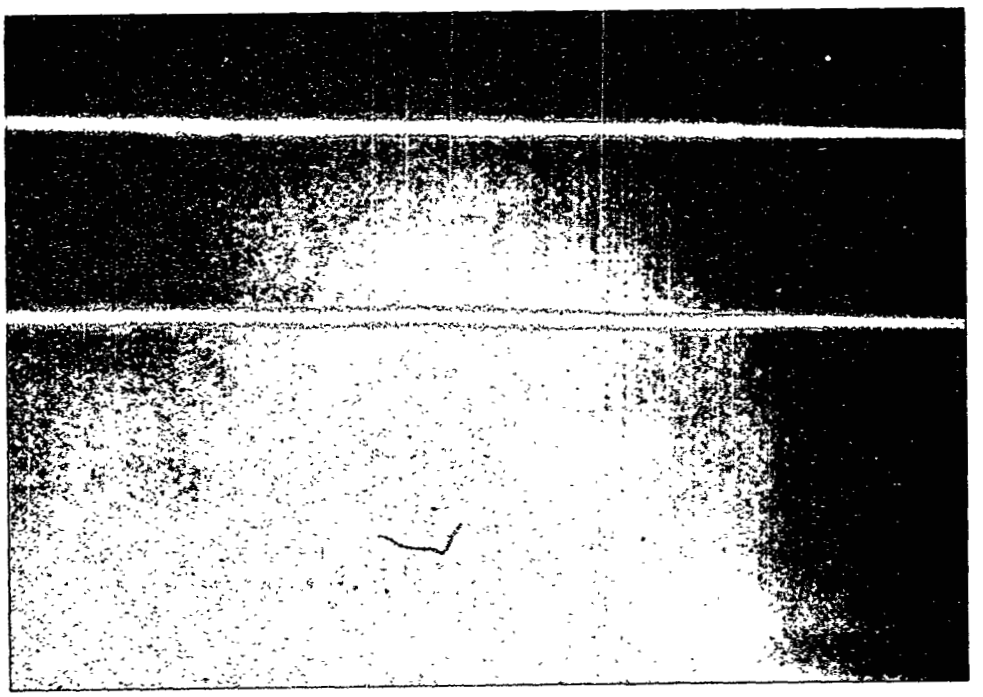

(d) Time = 15 sec.

Figure 20.– Continued.

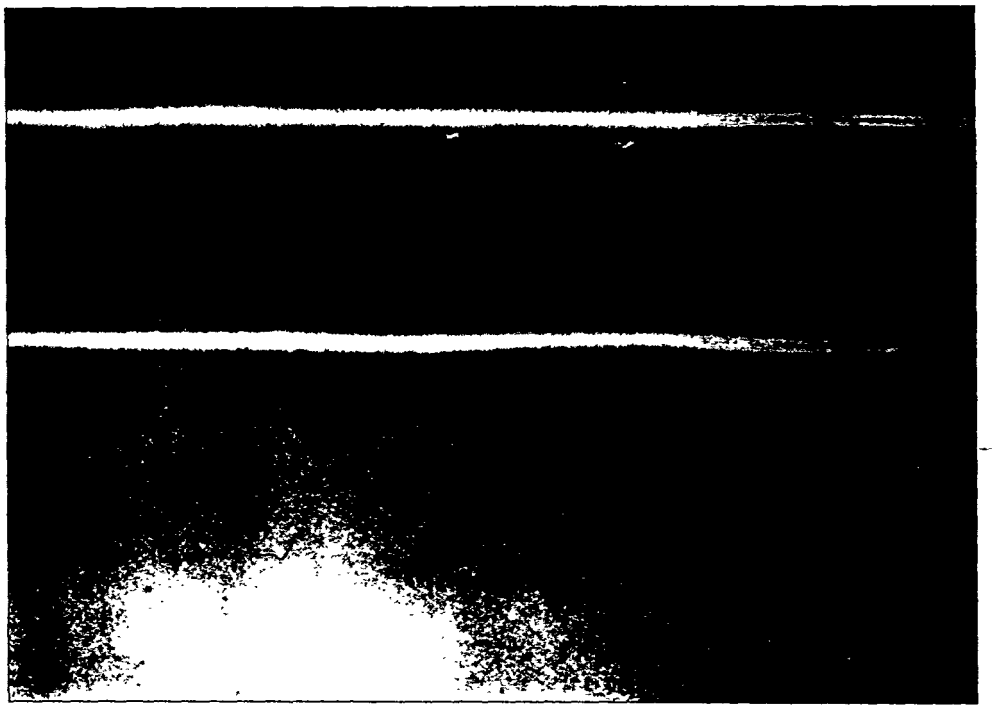

(e) Time = 20 sec.

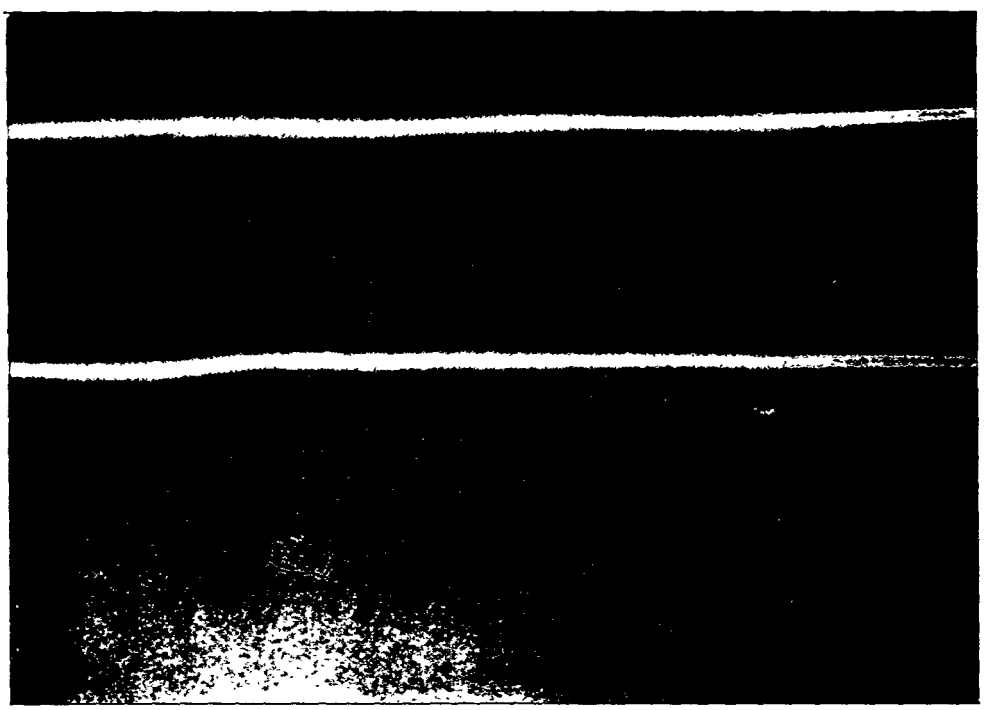

(f) Time = 25 sec.

Figure 20.– Continued.

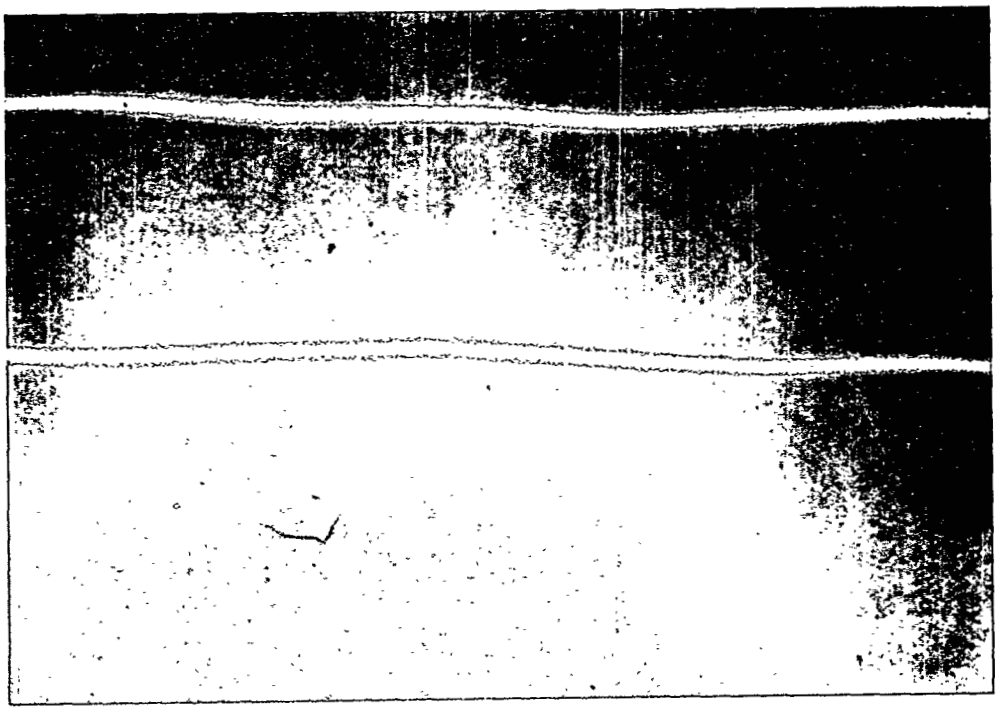

(g) Time = 30 sec.

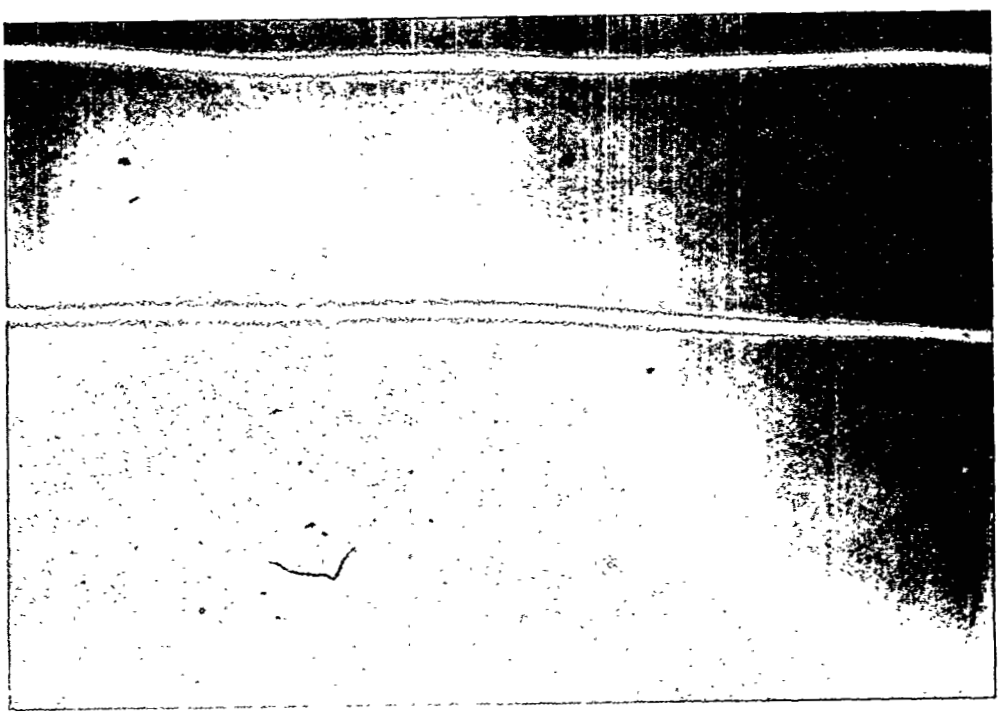

(h) Time = 35 sec.

Figure 20.– Continued.

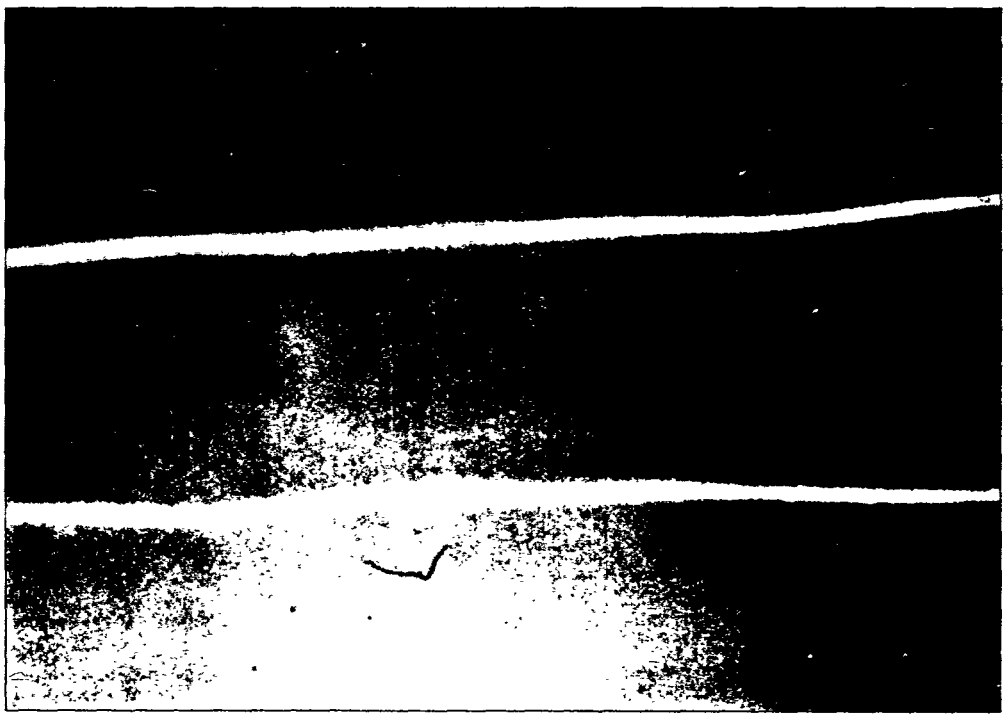

(i) Time = 40 sec.

(j) Time = 45 sec.

Figure 20.– Continued.

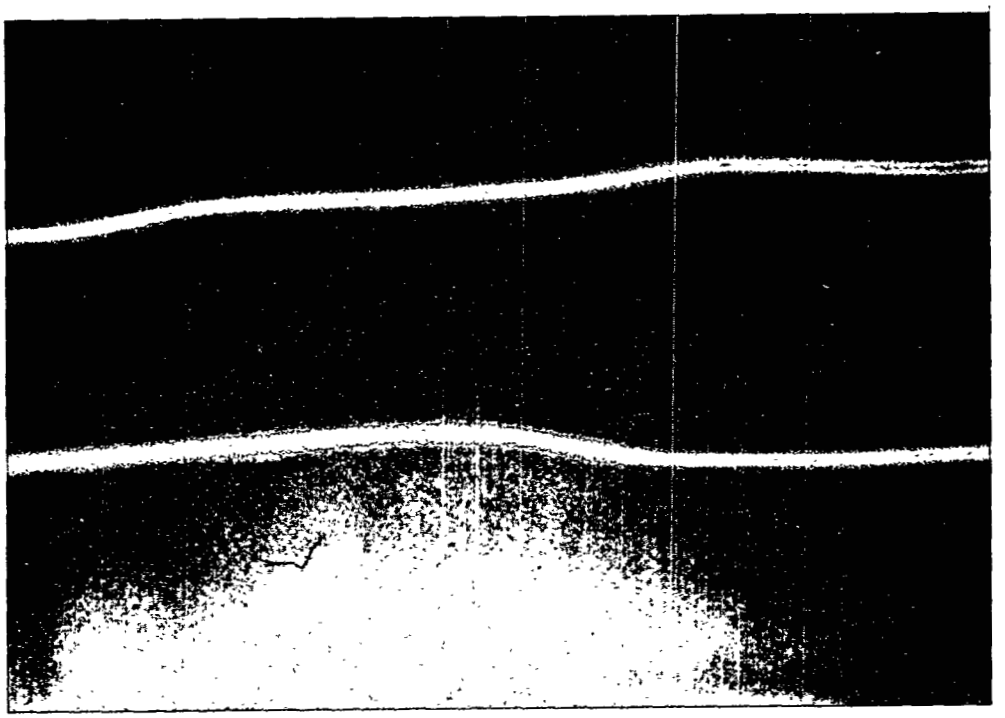

(k) Time = 50 sec.

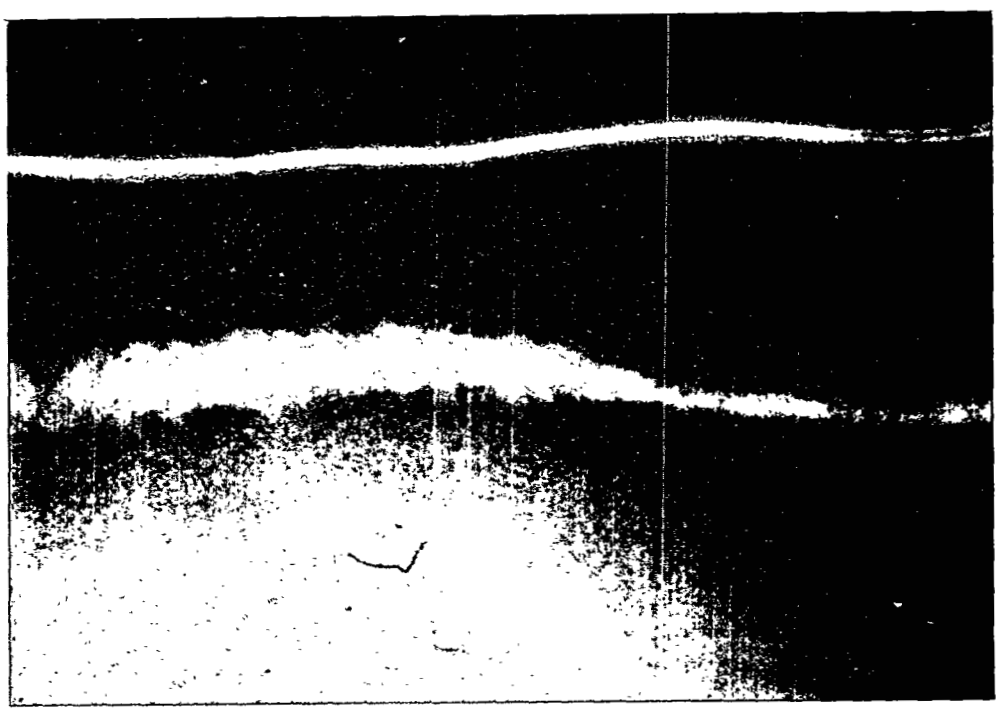

(l) Time = 55 sec.

Figure 20.– Continued.

(m) Time = 60 sec.

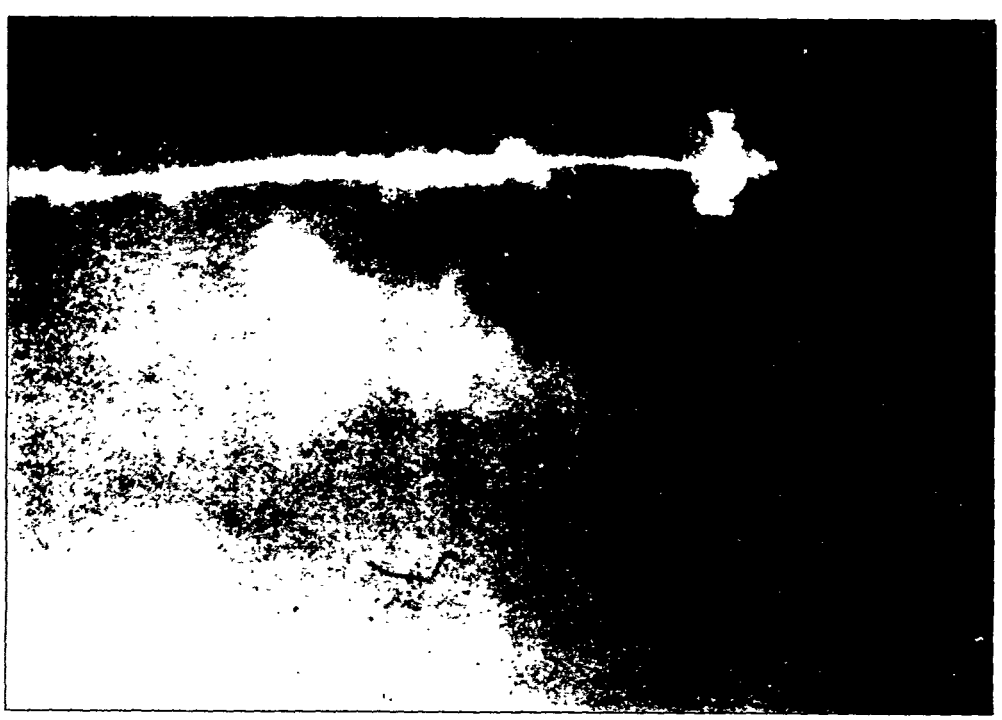

(n) Time = 65 sec.

Figure 20.– Continued.

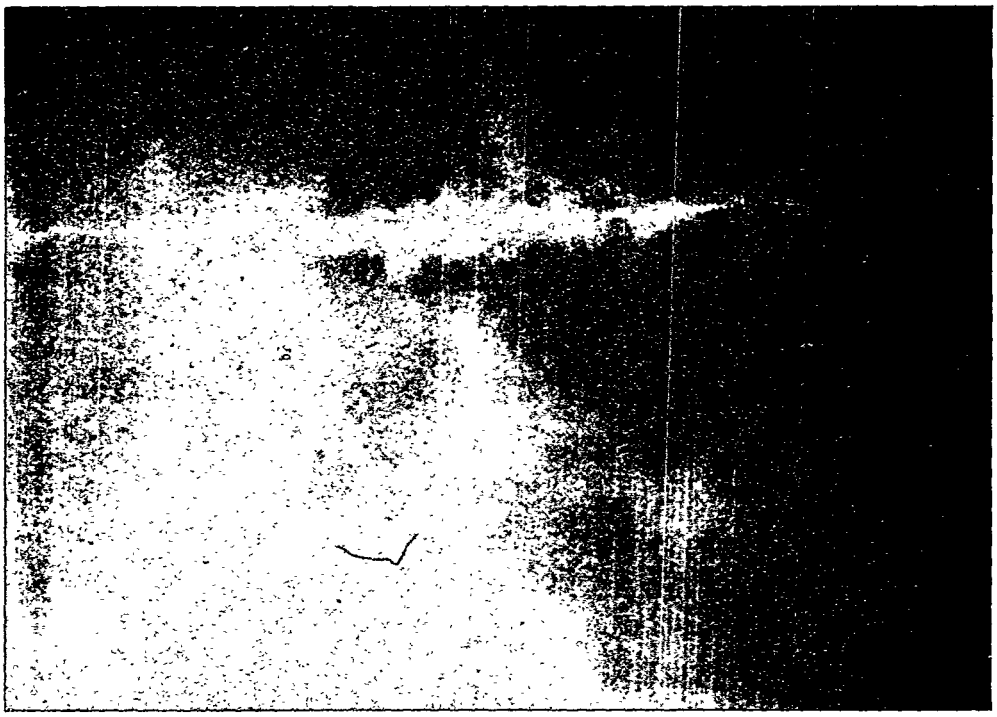

(o) Time = 70 sec.

Figure 20.– Concluded.

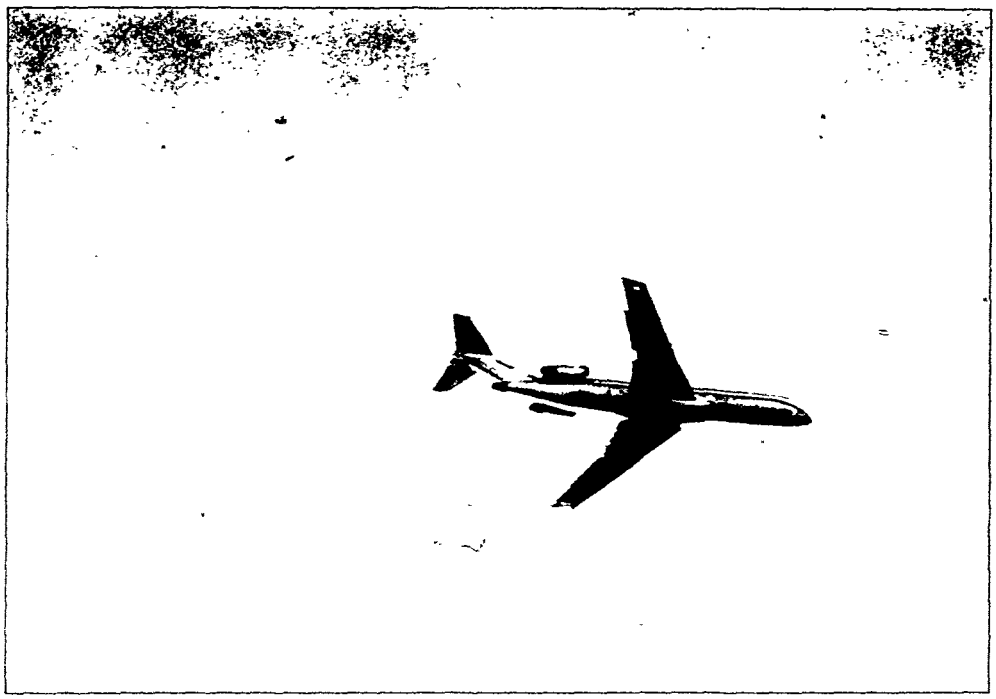

(a) Time = 0 sec.

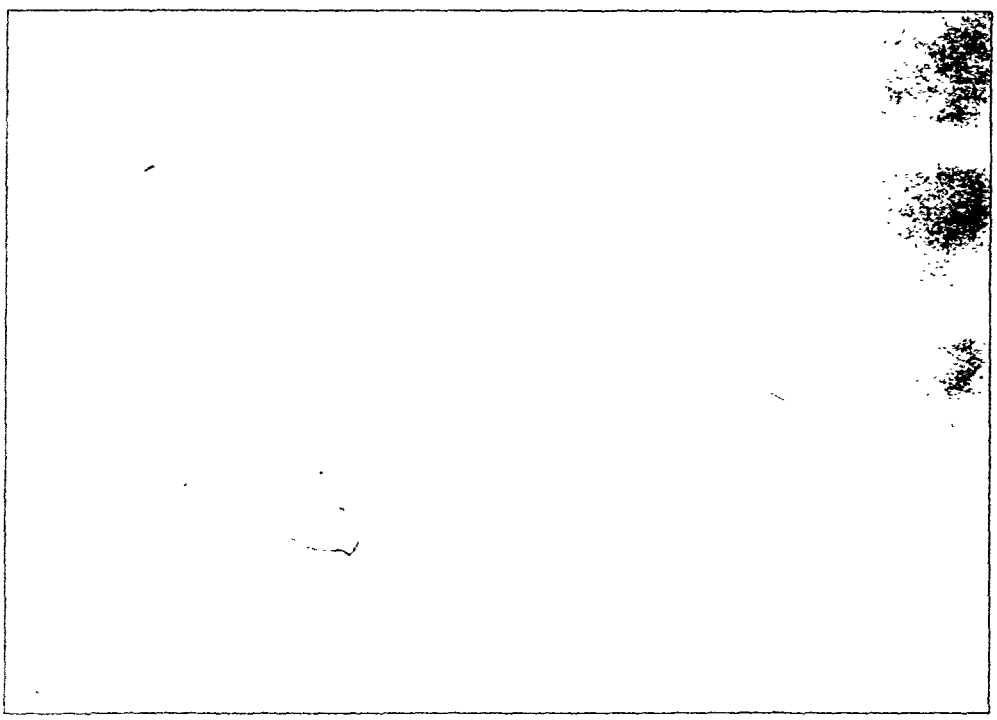

(b) Time = 5 sec.

Figure 21.– B727 wake vortex (take-off configuration: weight = 329,000 kg (149,000 lb)).

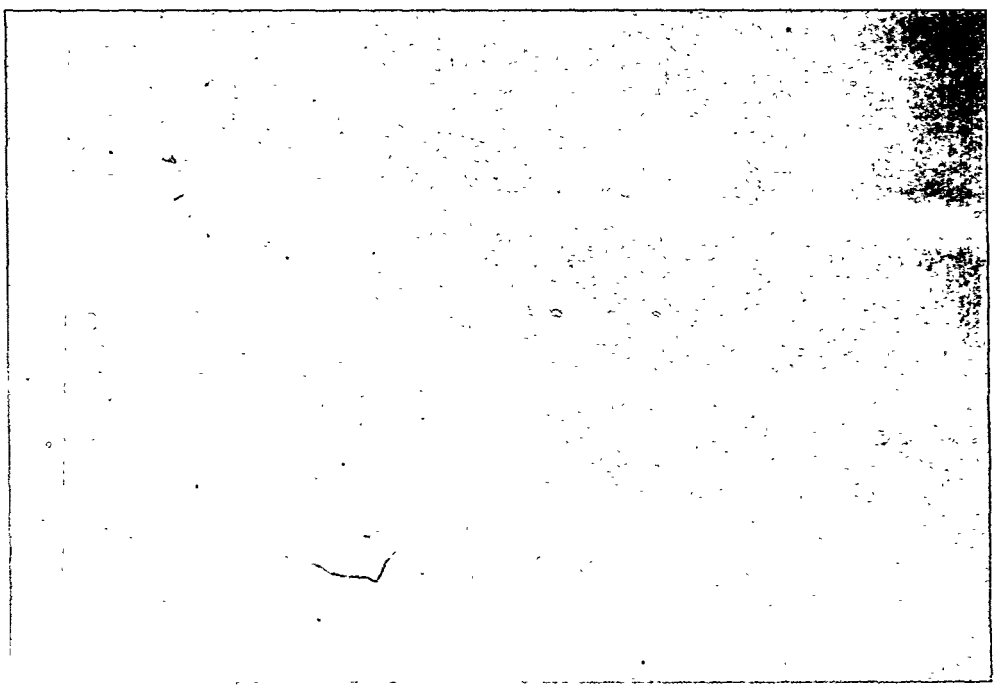

(c) Time = 10 sec.

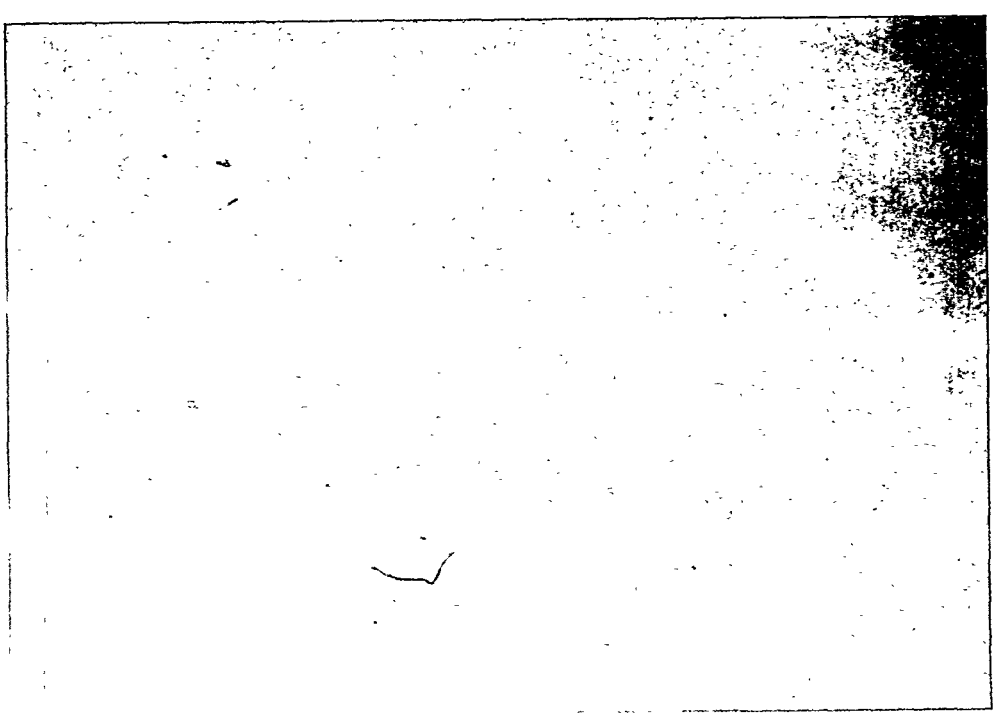

(d) Time = 15 sec.

Figure 21.– Continued.

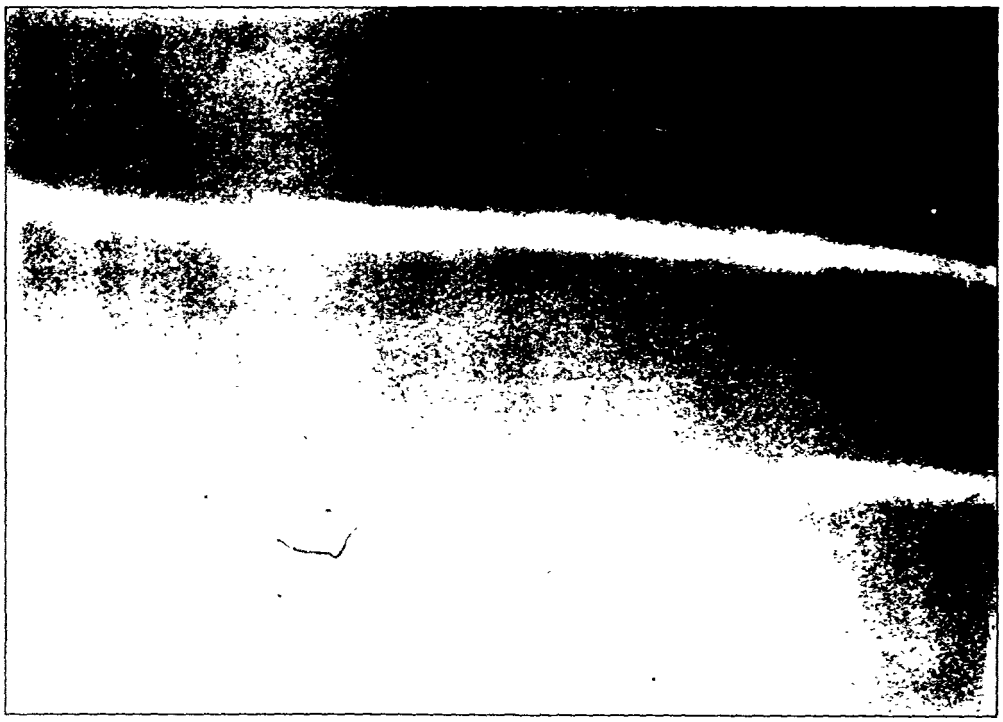

(e) Time = 20 sec.

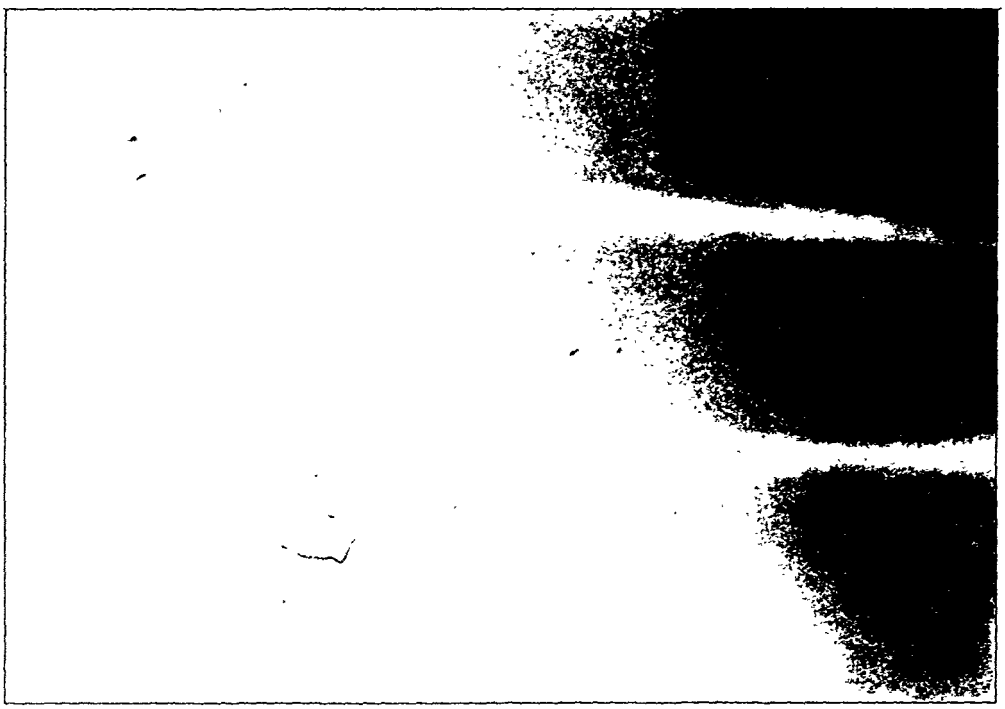

(f) Time = 25 sec.

Figure 21.– Continued.

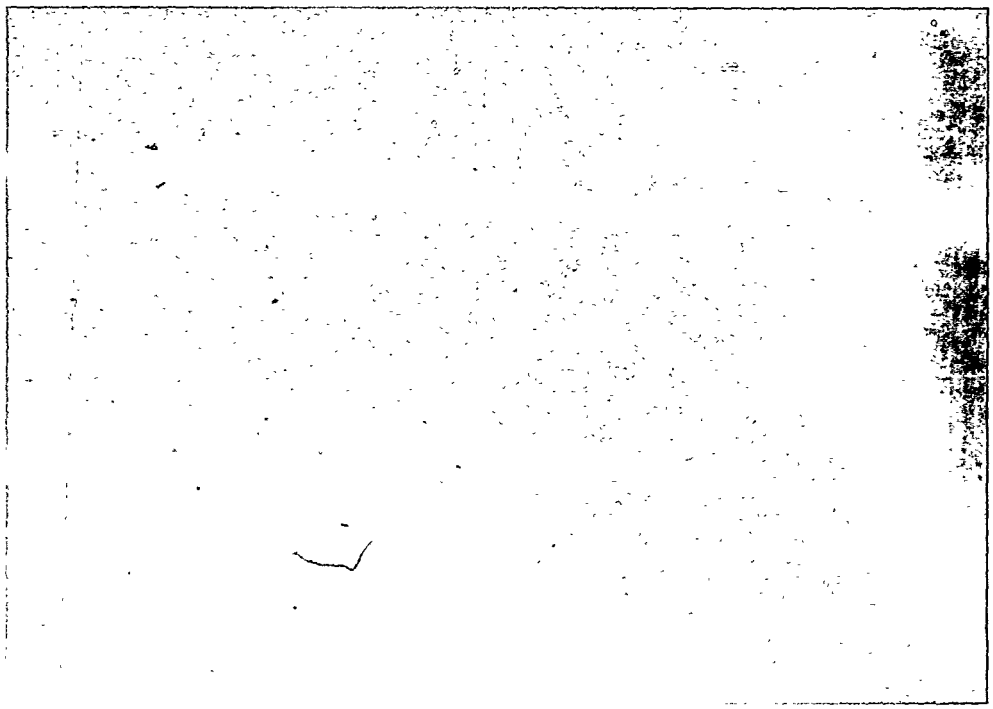

(g) Time = 30 sec.

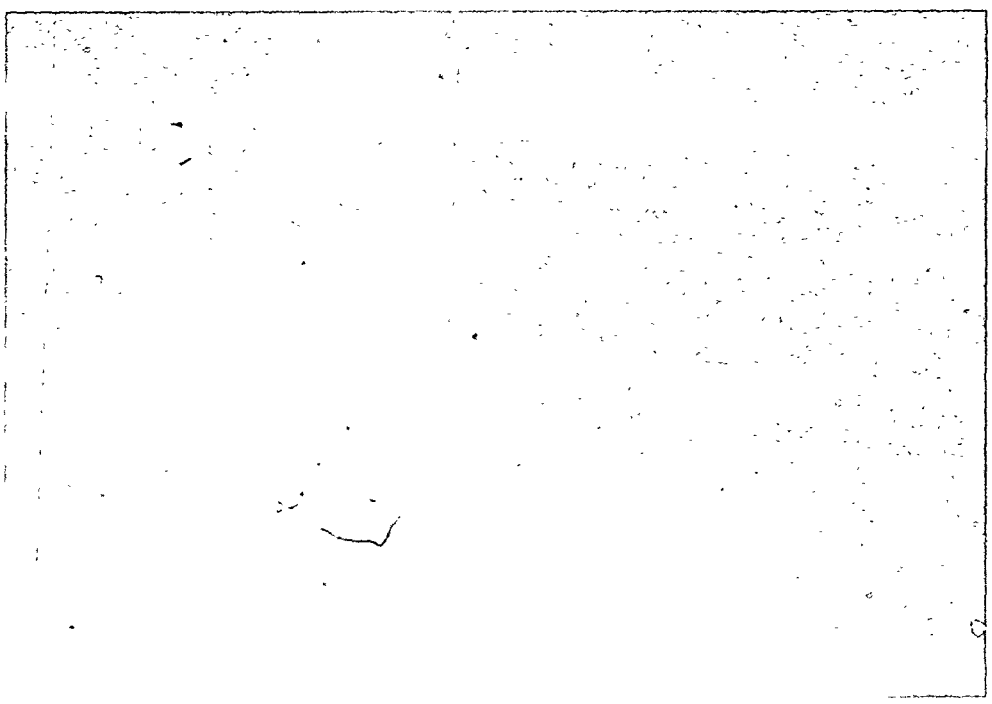

(h) Time = 35 sec.

Figure 21.– Continued.

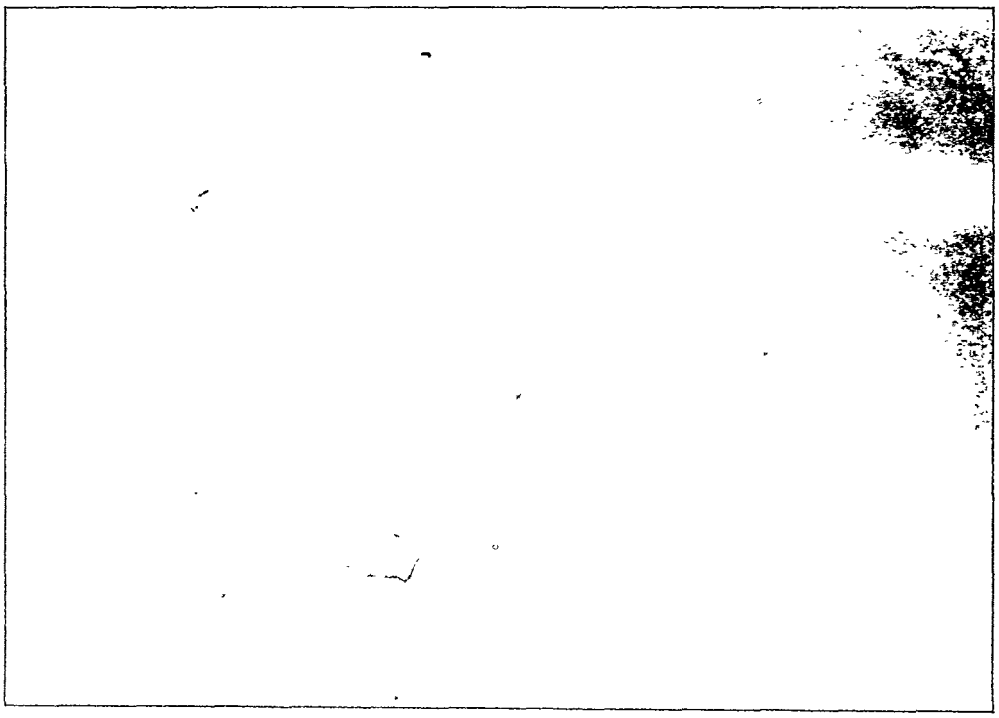

(i) Time = 40 sec.

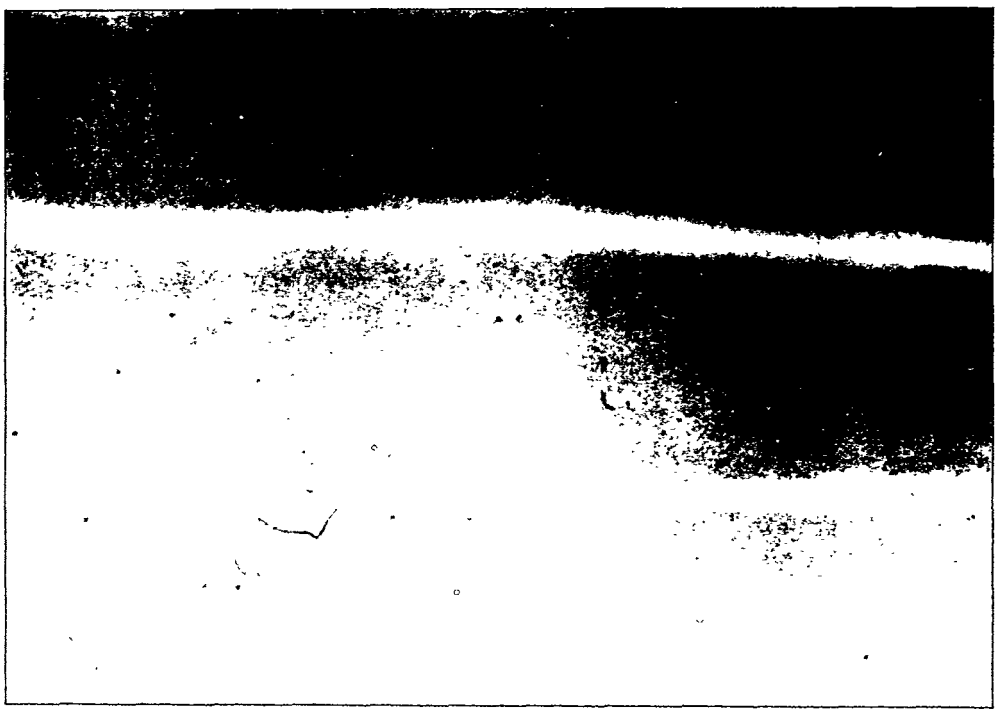

(j) Time = 45 sec.

Figure 21.– Continued.

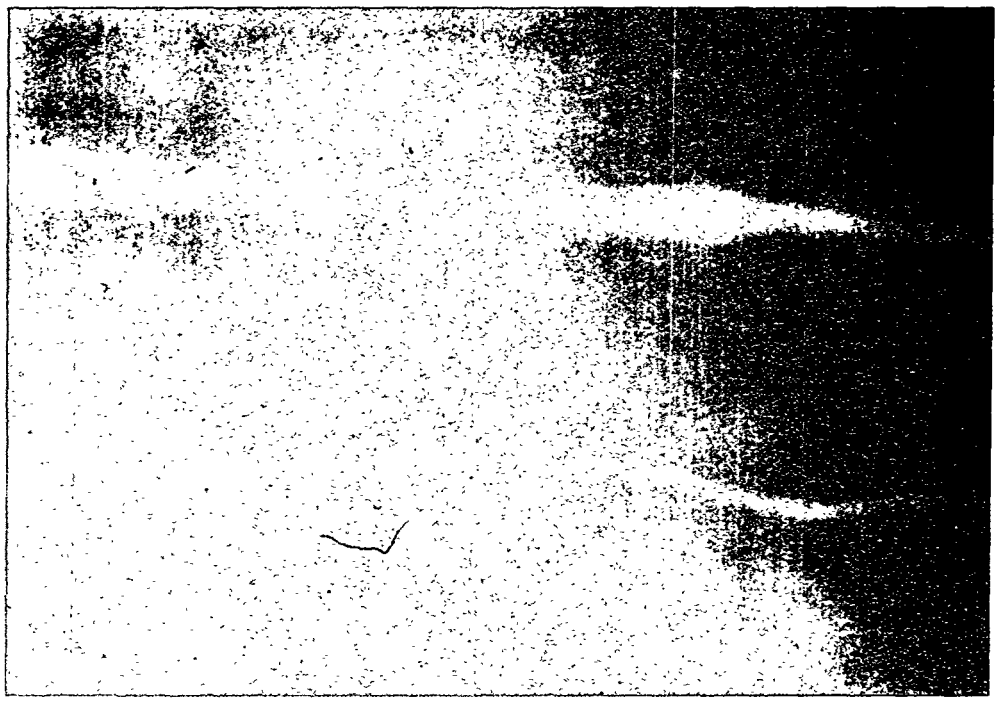

(k) Time = 50 sec.

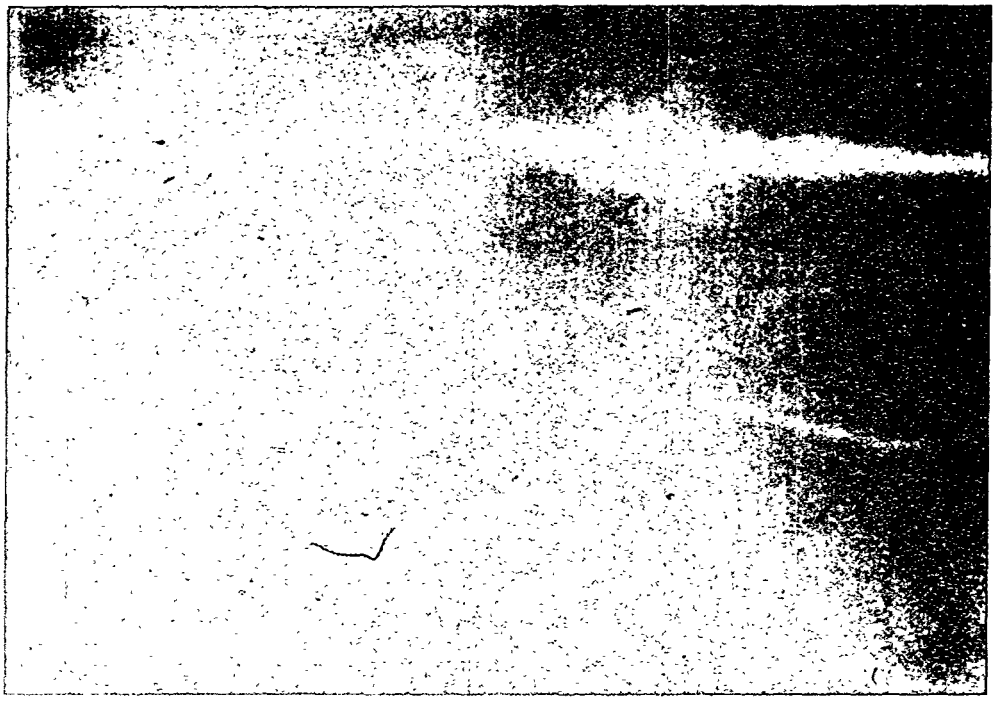

(l) Time = 55 sec.

Figure 21.– Continued.

(m) Time = 60 sec.

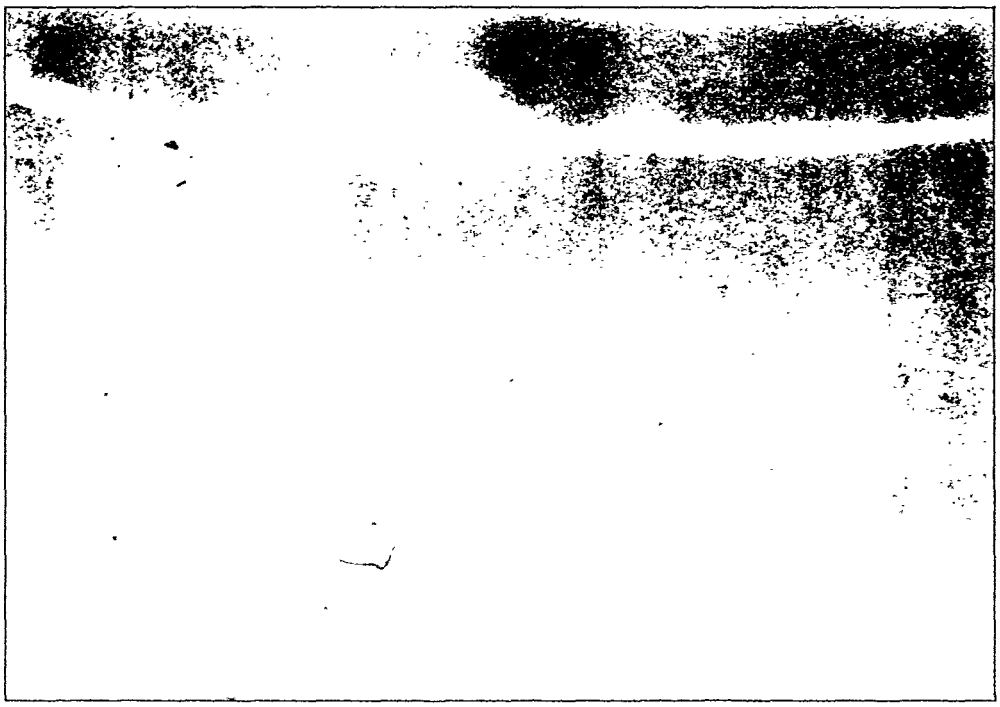

(n) Time = 65 sec.

Figure 21.– Continued.

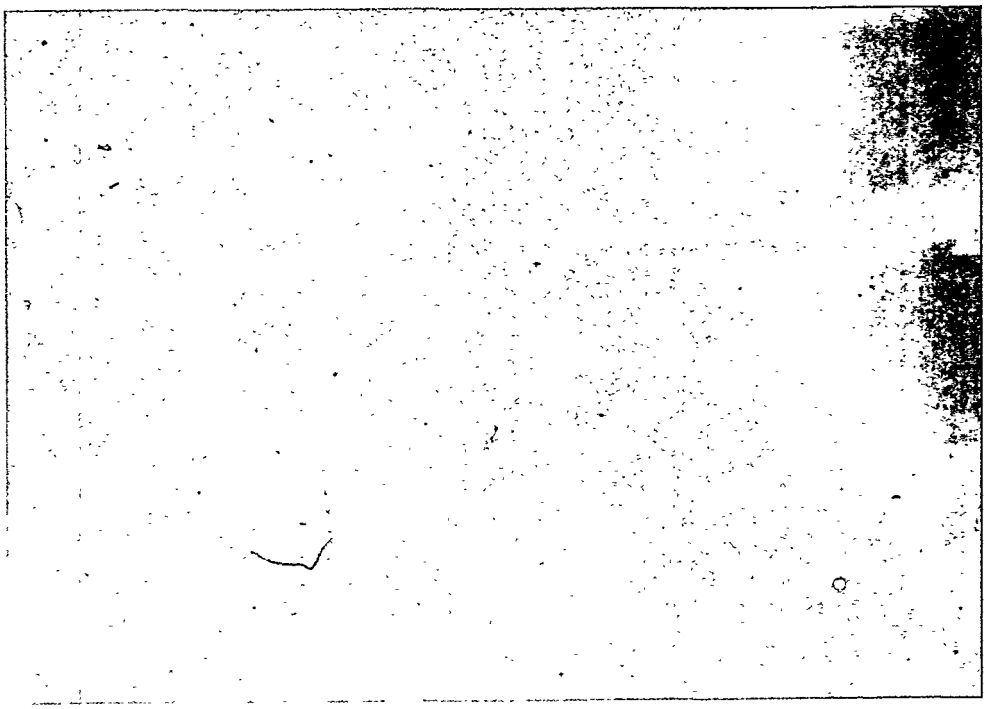

(o) Time = 70 sec.

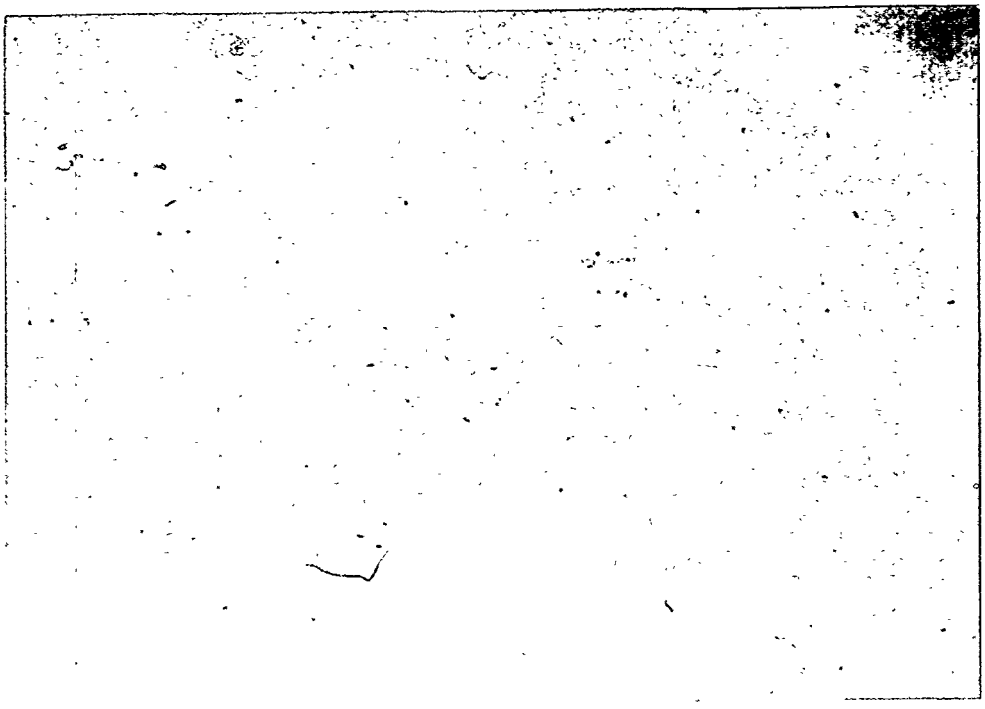

(p) Time = 75 sec.

Figure 21.– Concluded.

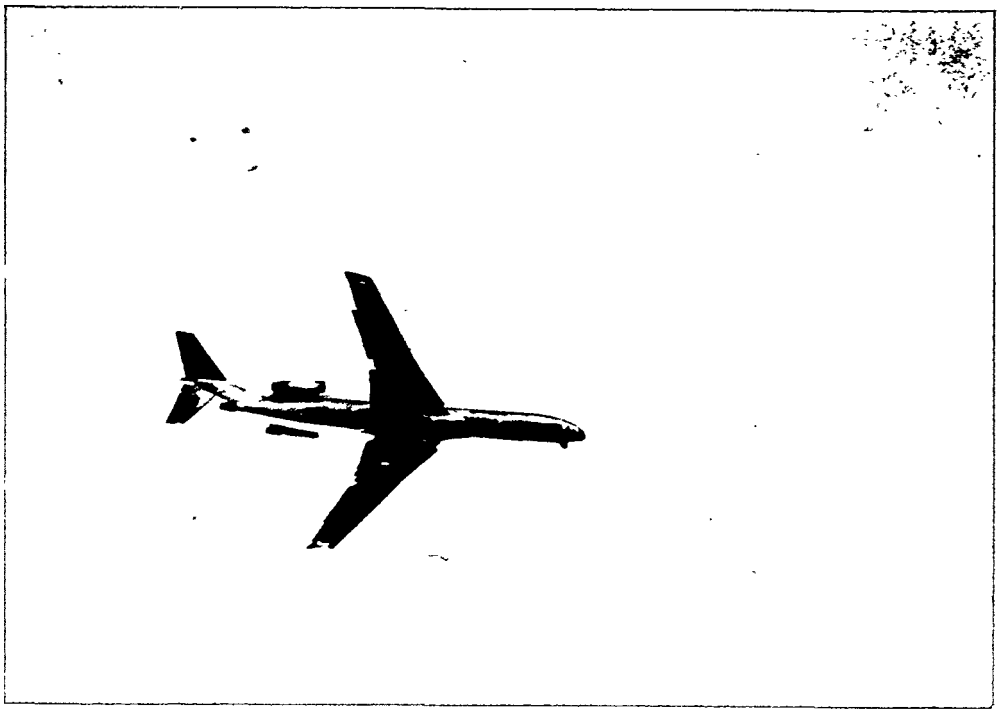

(a) Time = 0 sec.

(b) Time = 10 sec.

Figure 22.– B727 wake vortex (landing configuration: weight = 330,500 kg (150,000 lb)).

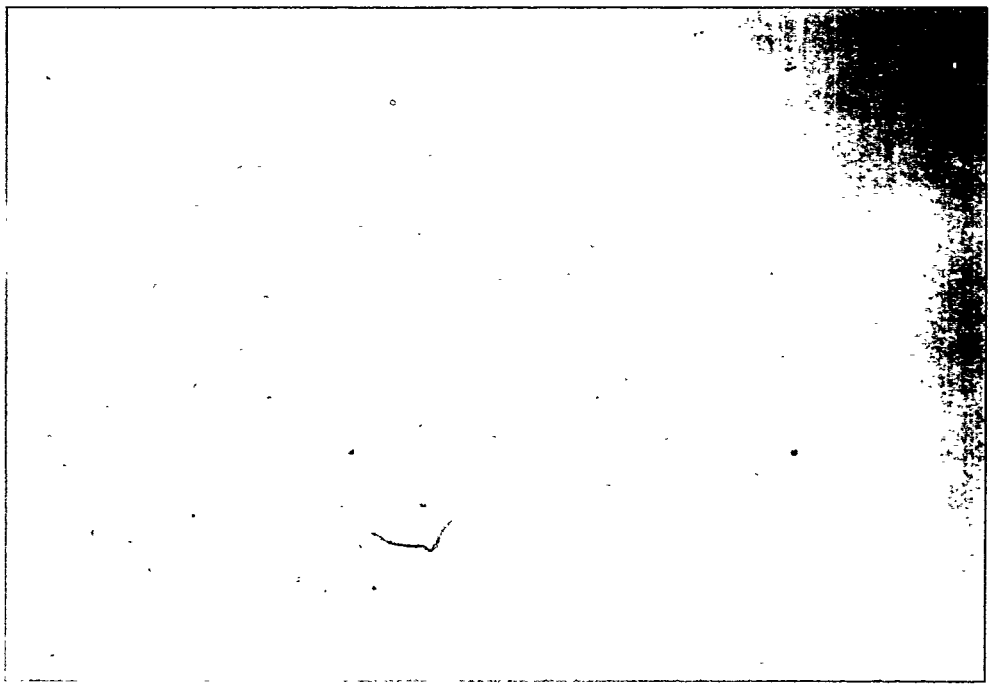

(c) Time = 15 sec.

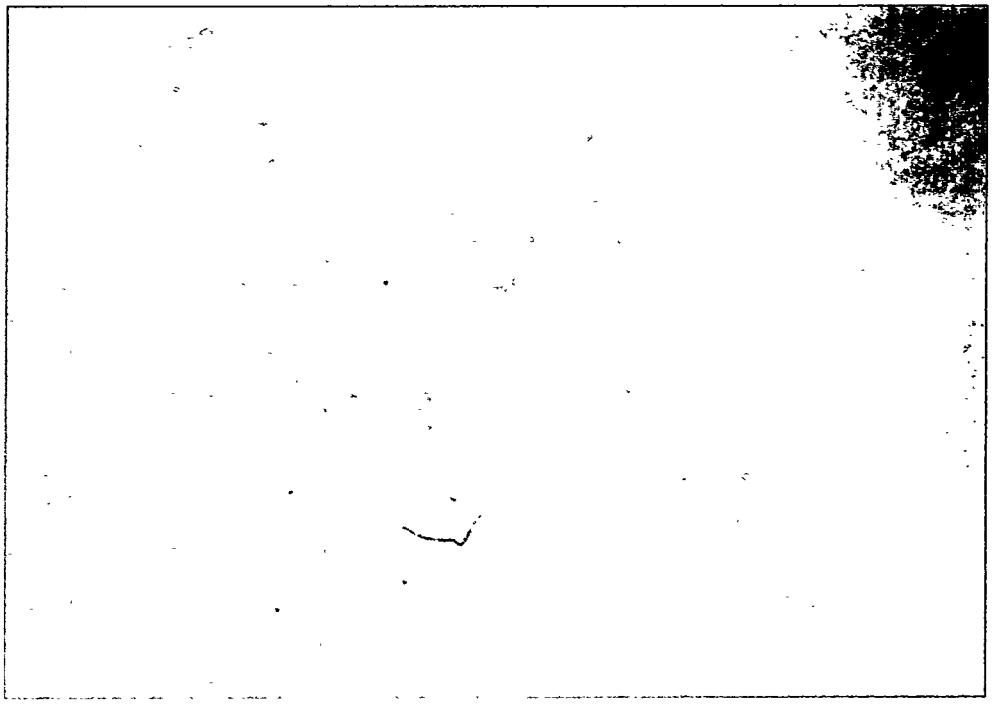

(d) Time = 20 sec.

Figure 22.– Continued.

(e) Time = 25 sec.

(f) Time = 30 sec.

Figure 22.– Continued.

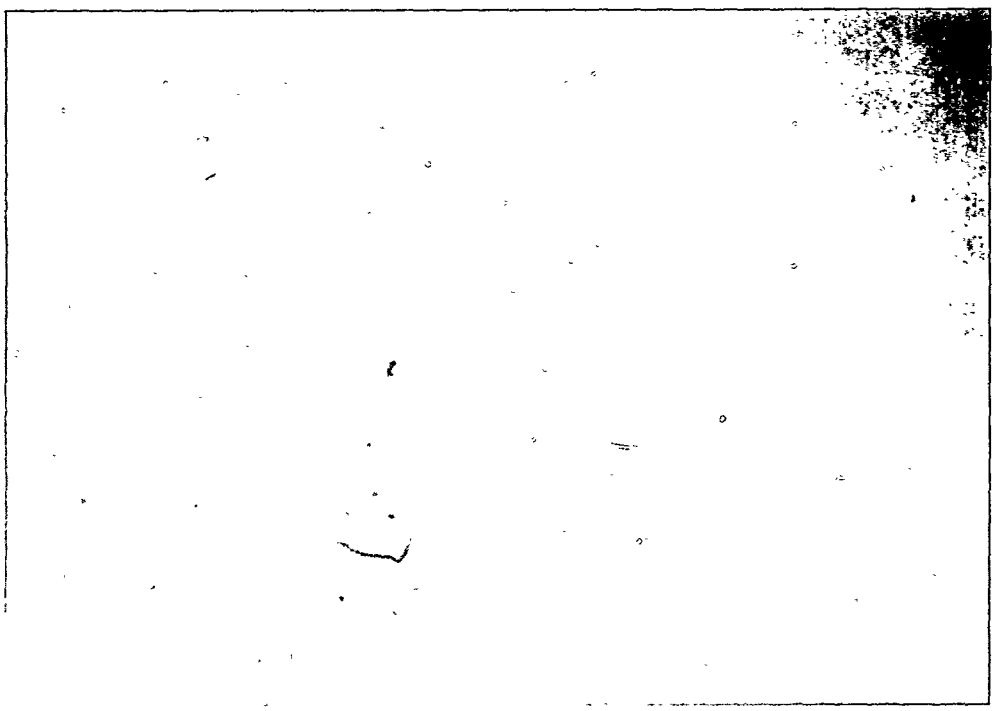

(g) Time = 35 sec.

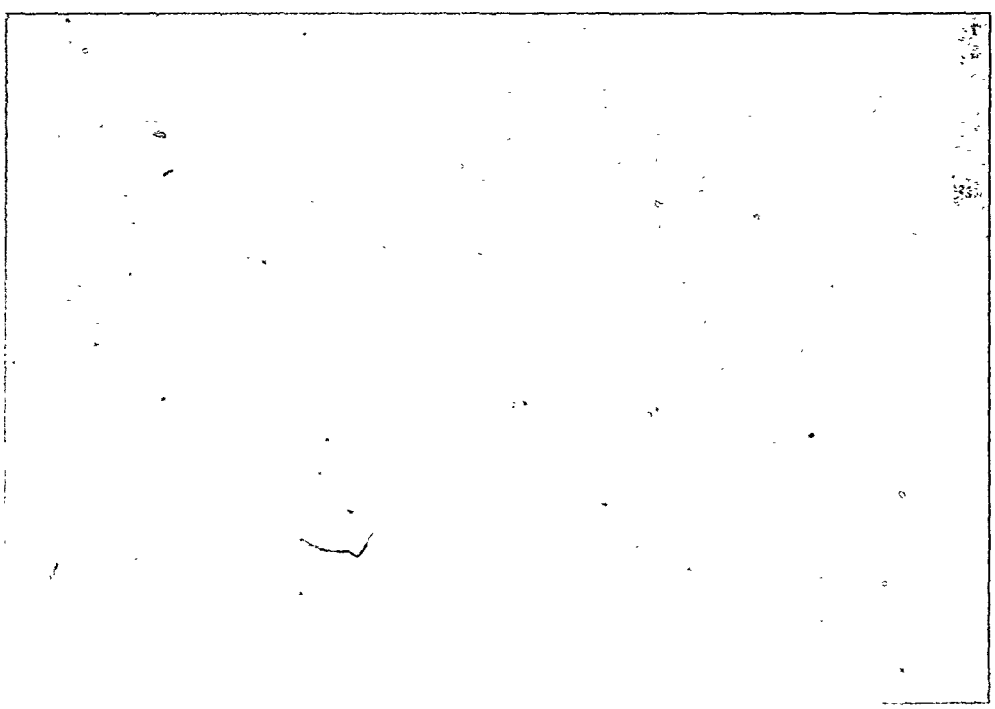

(h) Time = 40 sec.

Figure 22.– Concluded.

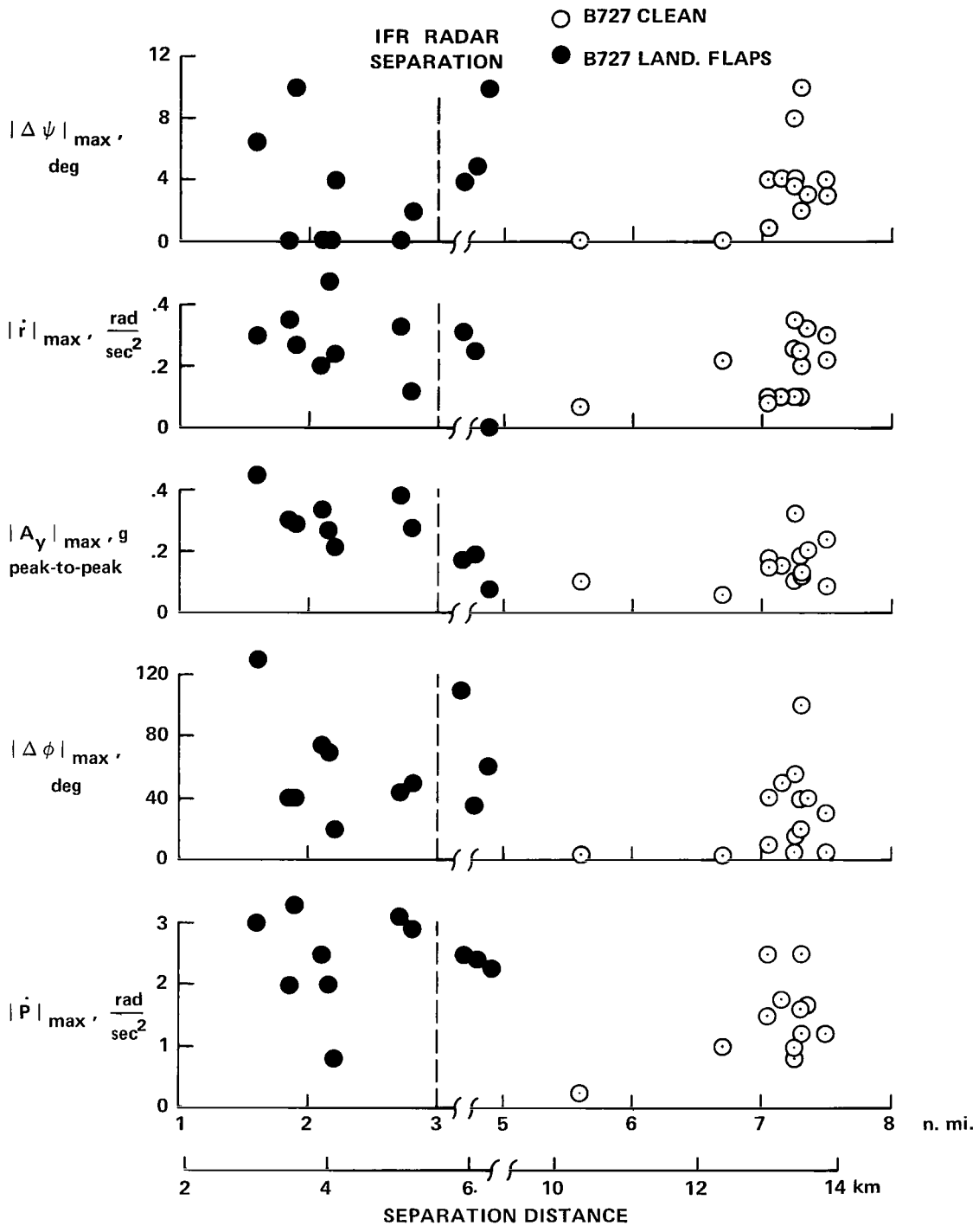

(a) Lateral-directional.

Figure 23.– Effect of generator flap configuration on maximum Lear Jet excursions versus separation distance.

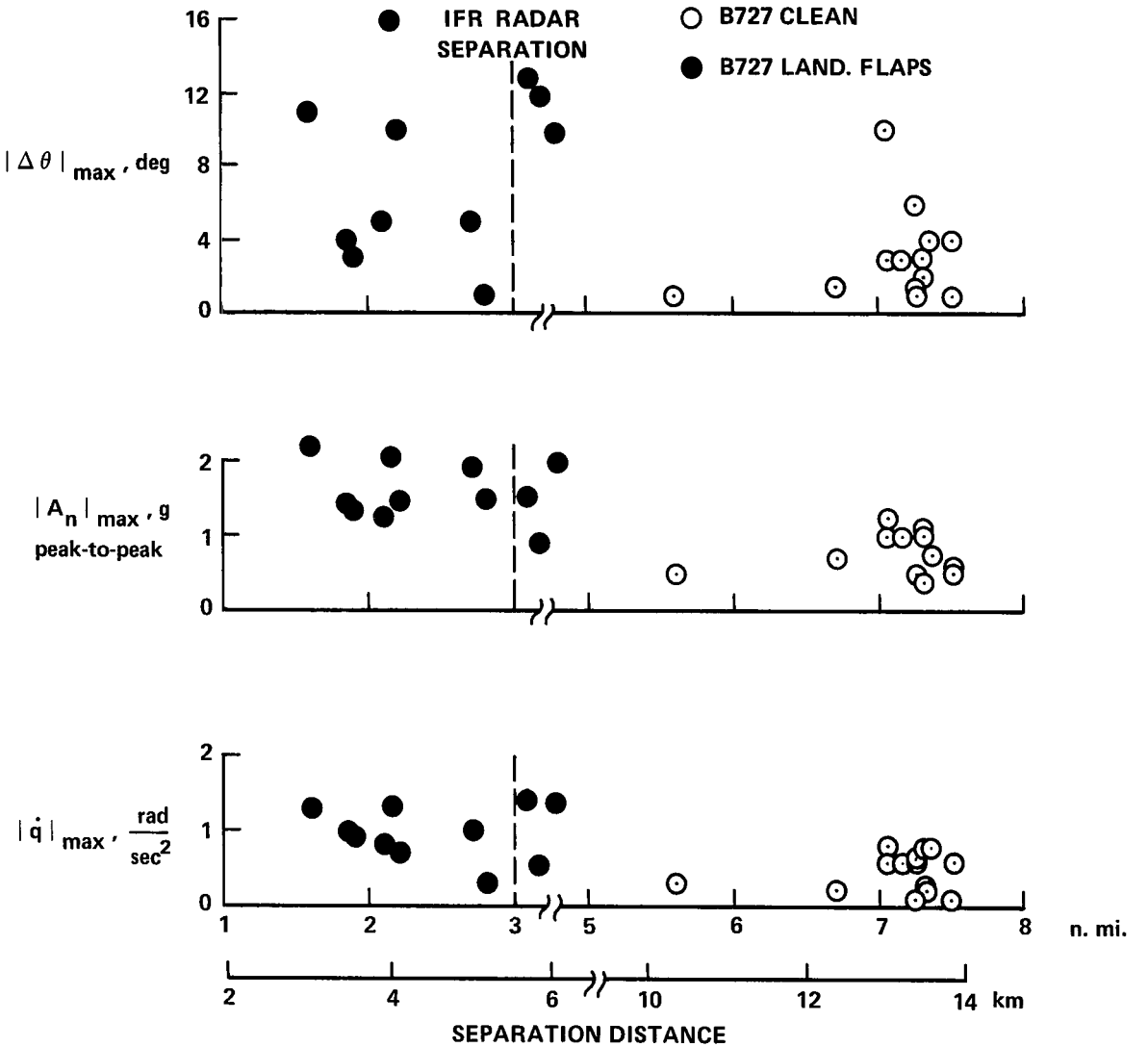

(b) Longitudinal.

Figure 23.– Concluded.

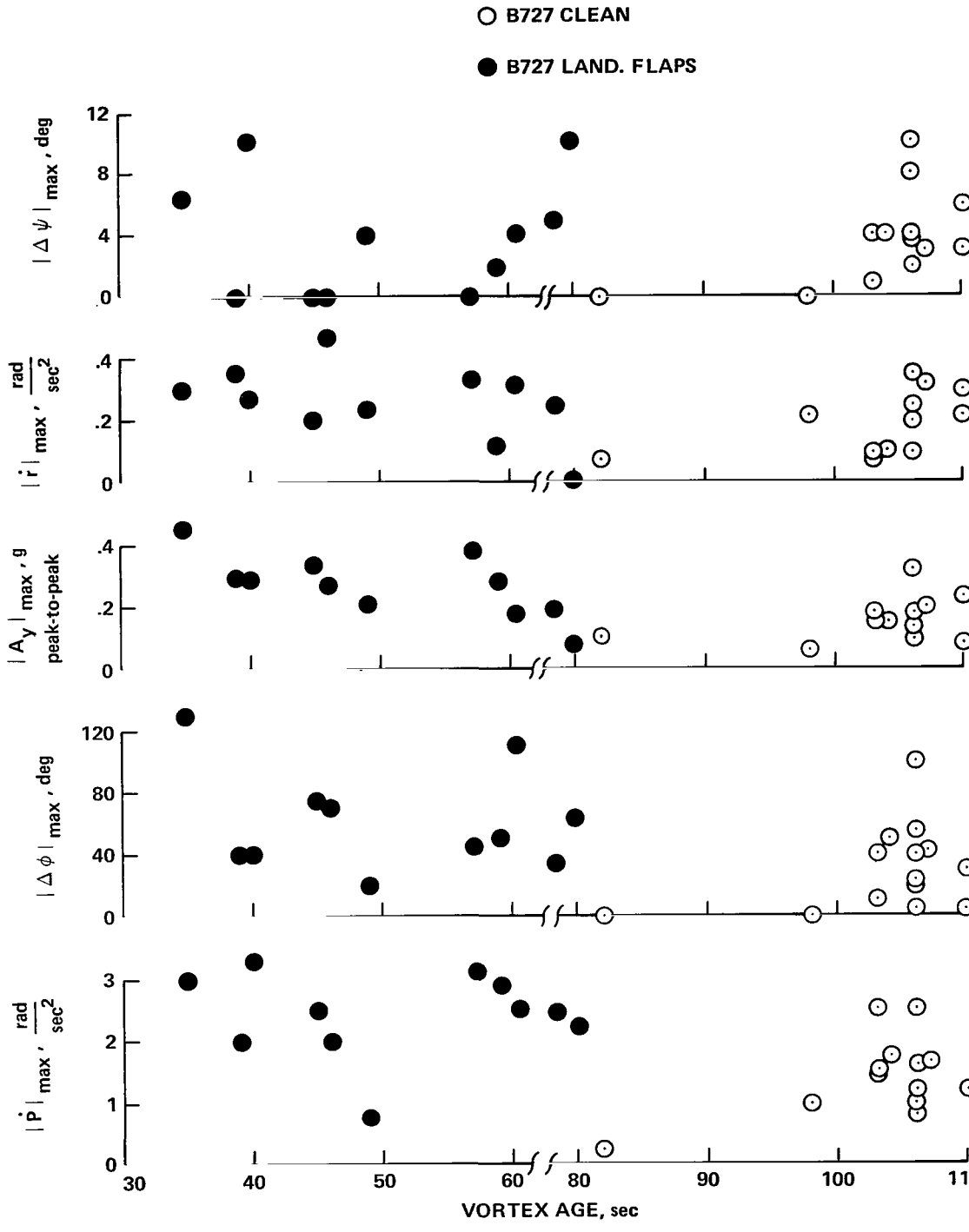

(a) Lateral-directional.

Figure 24.– Effect of generator flap configuration on maximum Lear Jet excursions versus vortex age.

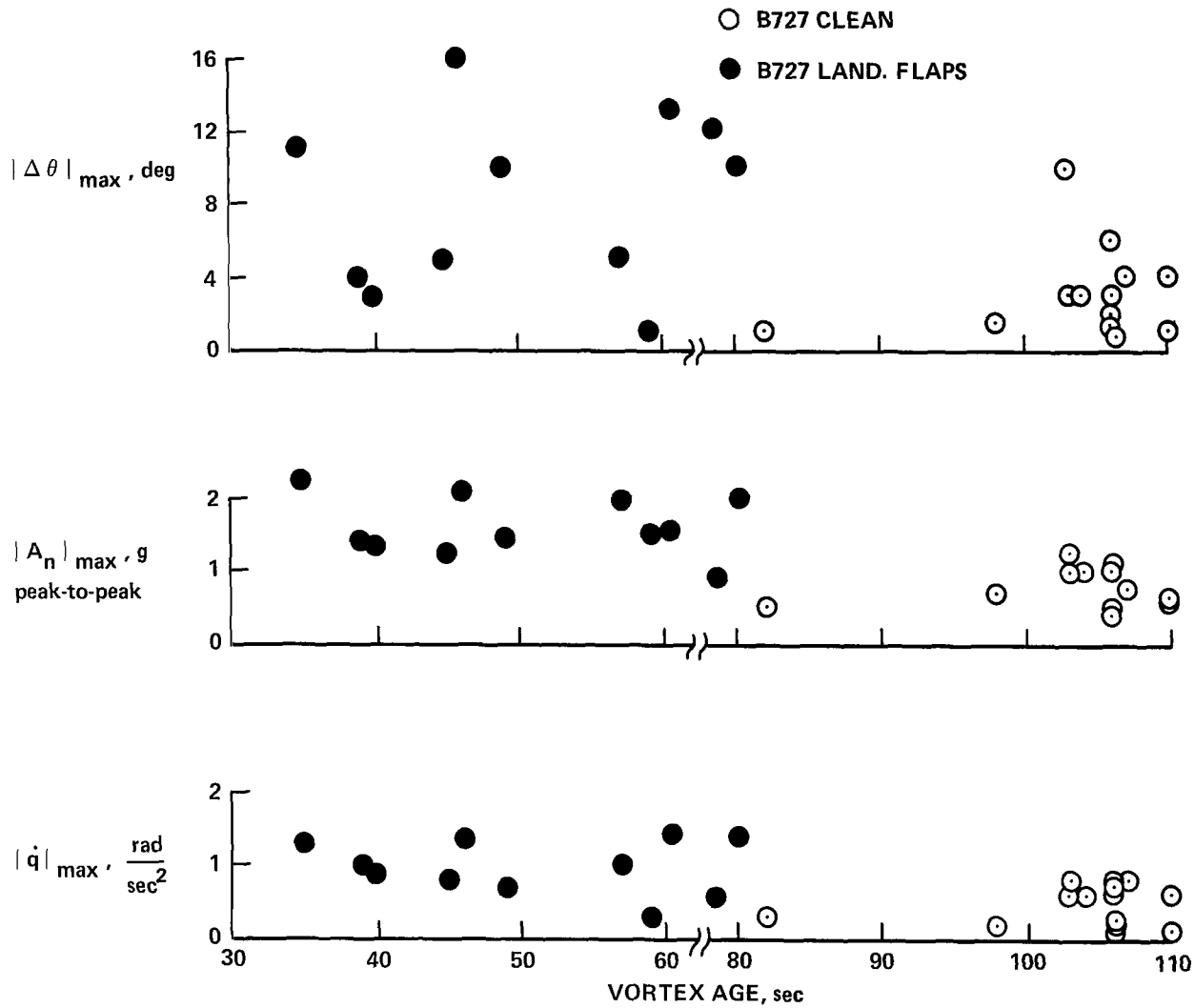

(b) Longitudinal.

Figure 24.– Concluded.

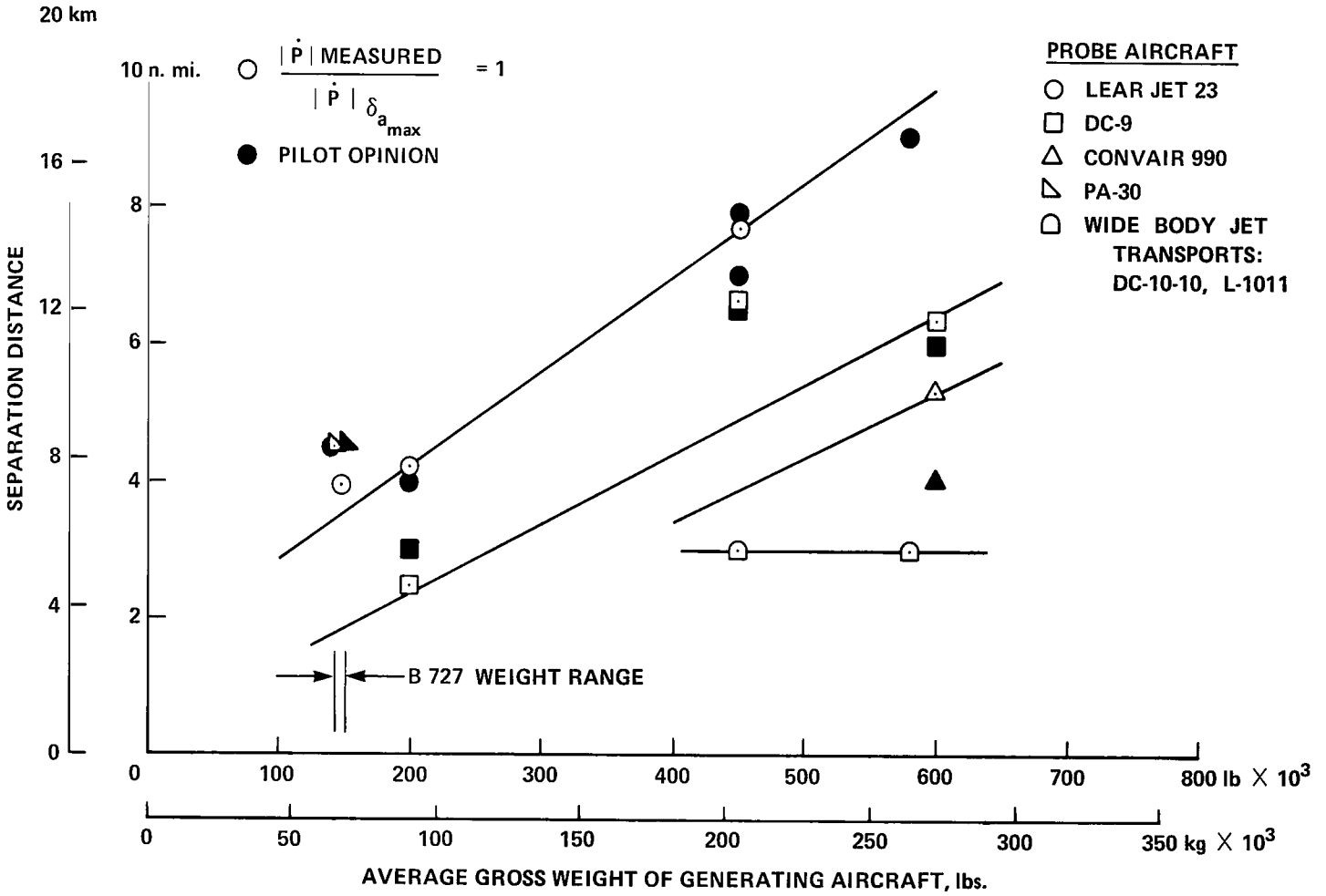

Figure 25.– Comparison of the minimum separation distances based on roll control criteria, for an operational encounter of the wake vortex of the B727 and other larger aircraft.

APPENDIX

VORTEX LOCATION MAPPING DATA

As stated earlier, the relative difference between the probabilities of wake vortex encounters for the two types of approach profiles cannot be determined only from this flight test. Additional information would be required to do this. All of the vortex location data from this flight test are included in figures 26–27 in order to aid such a probability analysis. The vortex mapping system was described earlier and the tracking stations are shown in figure 5. The vortex location data for the 14 mapping runs are presented. The data were obtained for five conventional approaches, five two-segment approaches to runway 22, and four take-off and climb-out cases using runway 04. The horizontal and vertical location of a cross section element of one of the vortex pairs is plotted for each of the four stations as a function both of (1) time after station passage, and (2) distance of the vortex element behind the B727 aircraft. The data were measured as a function of time, and calculated ground speed of the B727 was used to convert from time to distance in nautical miles. The figures are arranged as follows:

Figure	Flight condition	Independent parameter
26(a–e)	Conventional approaches	Distance
26(b–j)	Two-segment approaches	Distance
26(k–n)	Take-offs	Distance
27(a–e)	Conventional approaches	Time
27(f–j)	Two-segment approaches	Time
27(k–n)	Take-offs	Time

Indicated airspeeds are tabulated in the above figures; wind directions are referenced to magnetic north.

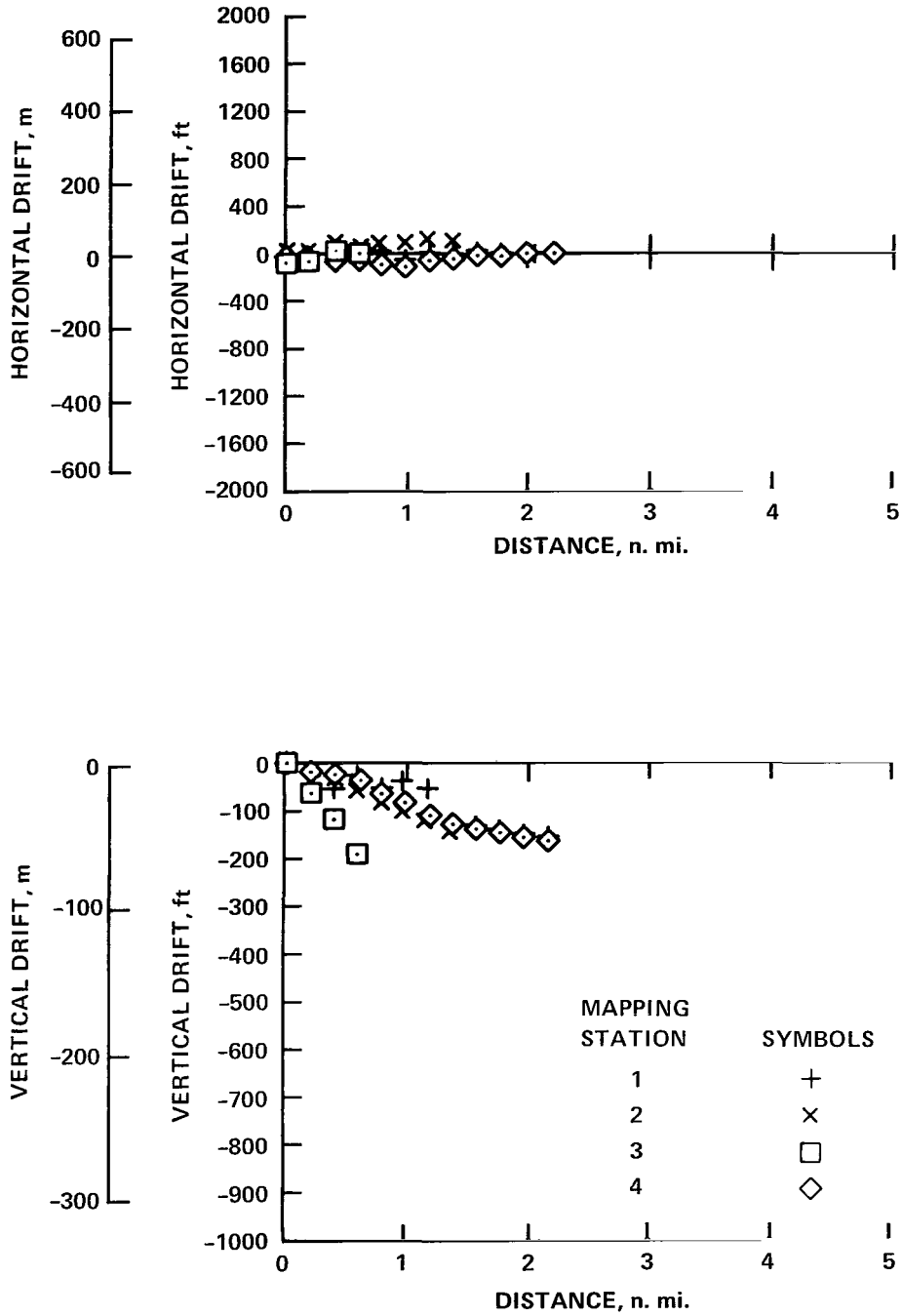

(a) Conventional approach: flaps, 30°; airspeed, 135 knots; weight, 64,000 kg (141,500 lb); winds, calm; turbulence, smooth.

Figure 26.– Vortex location behind a B727 aircraft.

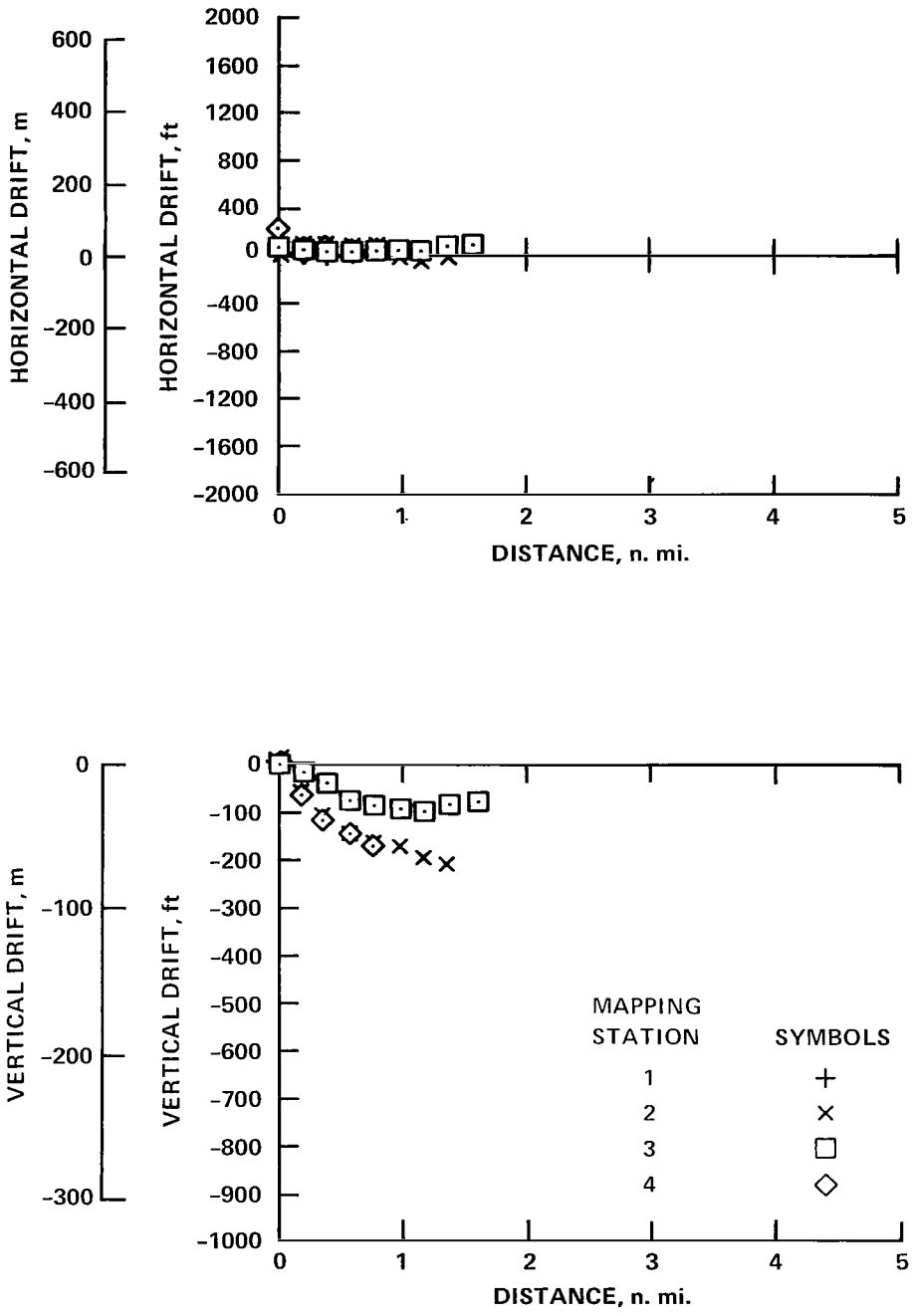

(b) Conventional approach: flaps, 30°; airspeed, 132 knots; weight, 66,000 kg (146,000 lb); winds, 240° at 12 knots; turbulence, light-moderate.

Figure 26.– Continued.

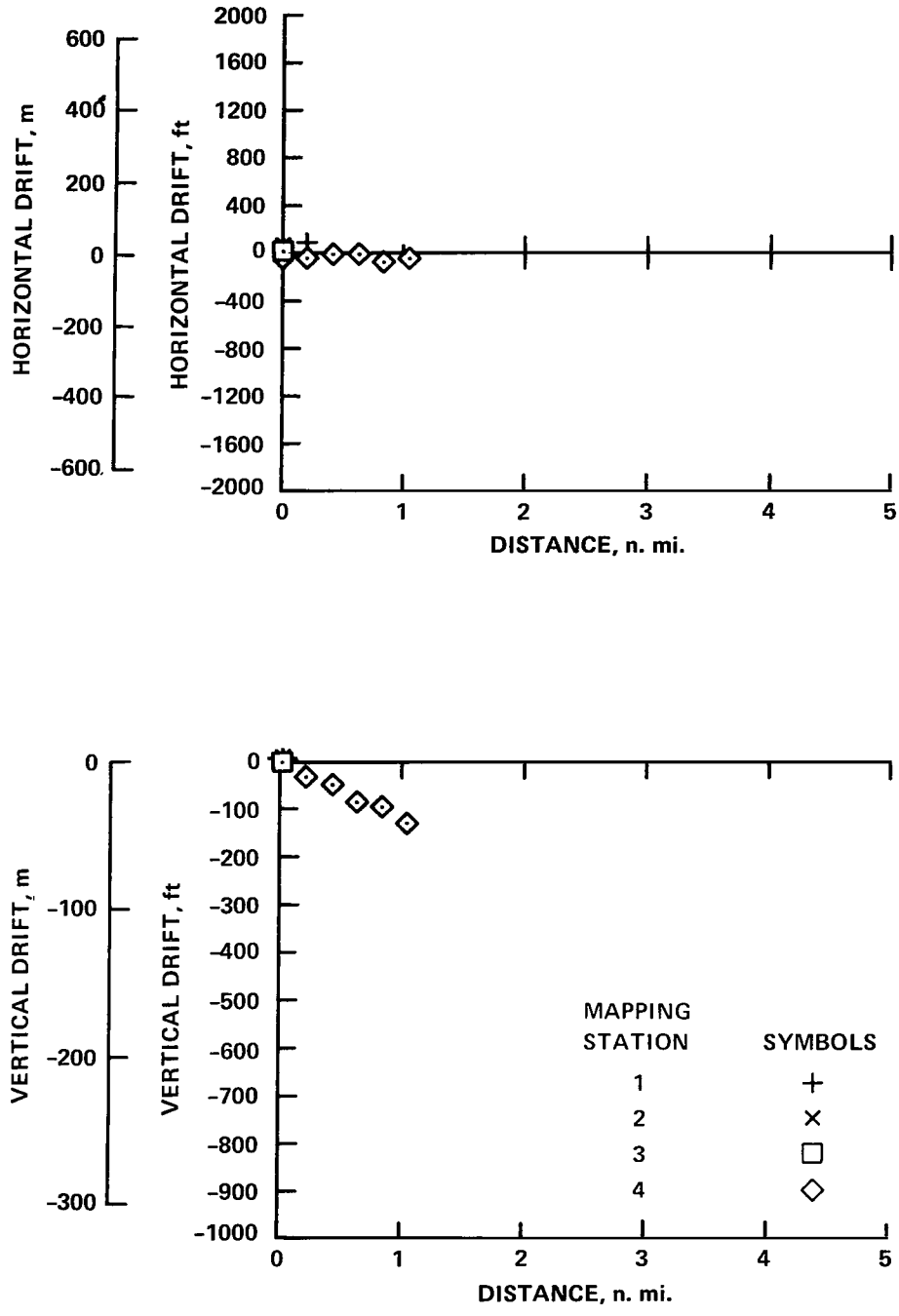

(c) Conventional approach: flaps, 30°; airspeed, 145 knots; weight, 68,000 kg (150,000 lb); winds, 230° at 5 knots; turbulence, light.

Figure 26.– Continued.

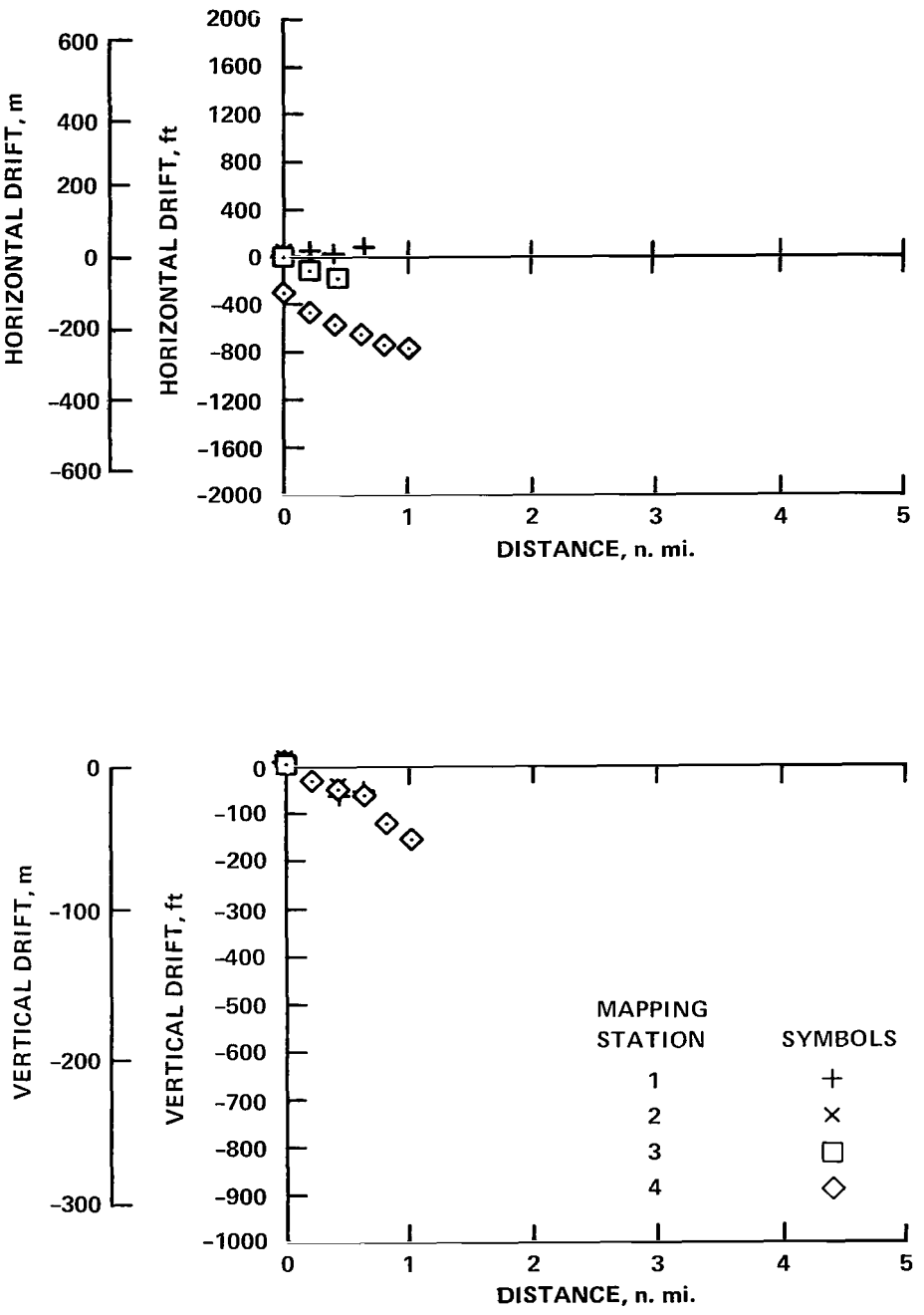

(d) Conventional approach: flaps, 30°; airspeed, 140 knots; weight, 64,500 kg (141,500 lb); winds, 240° at 10 knots; turbulence, light-moderate.

Figure 26.-- Continued.

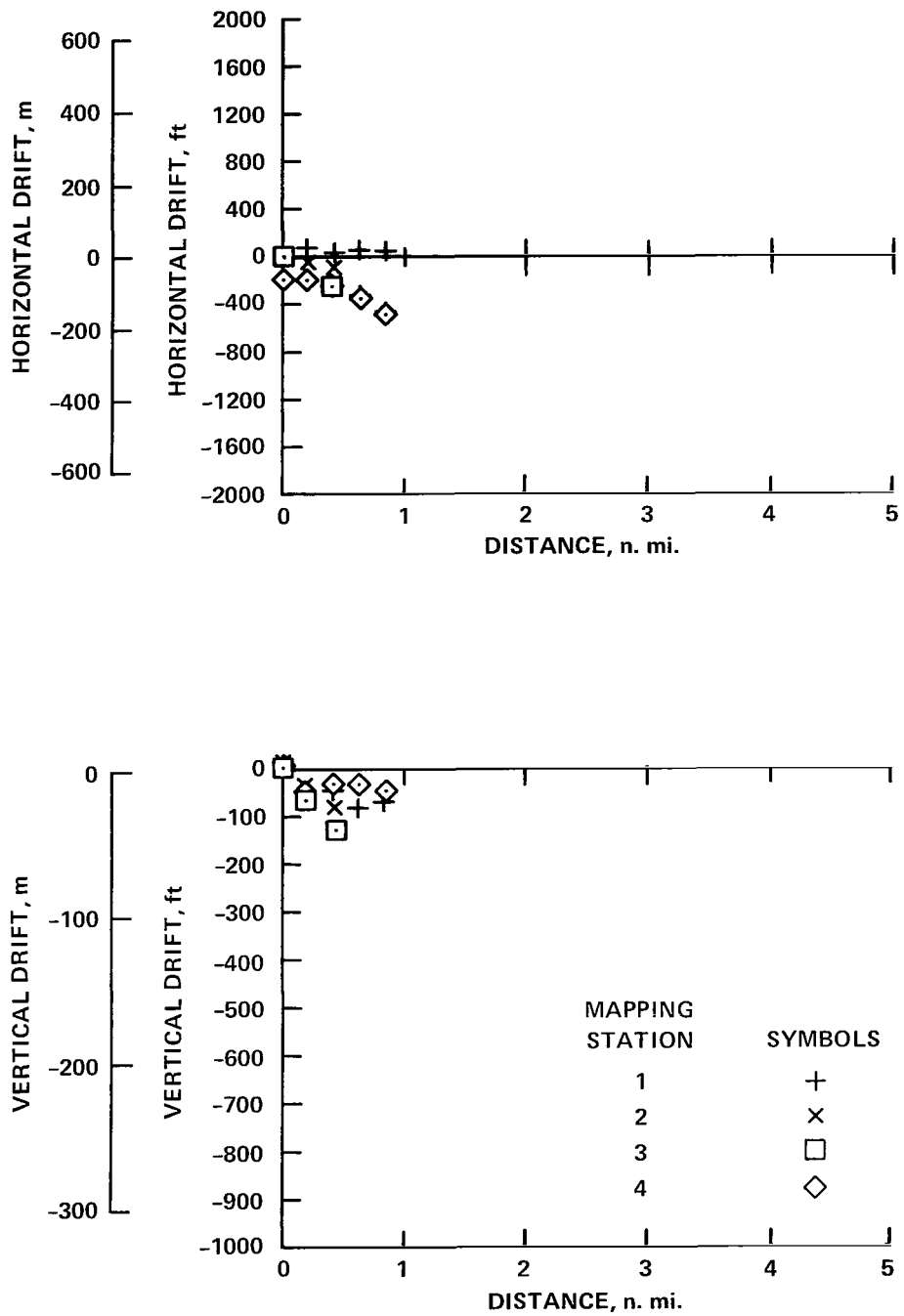

(e) Conventional approach: flaps, 30°; airspeed, 145 knots; weight, 67,000 kg (148,000 lb); winds, 230° at 8 knots; turbulence, light-moderate.

Figure 26.– Continued.

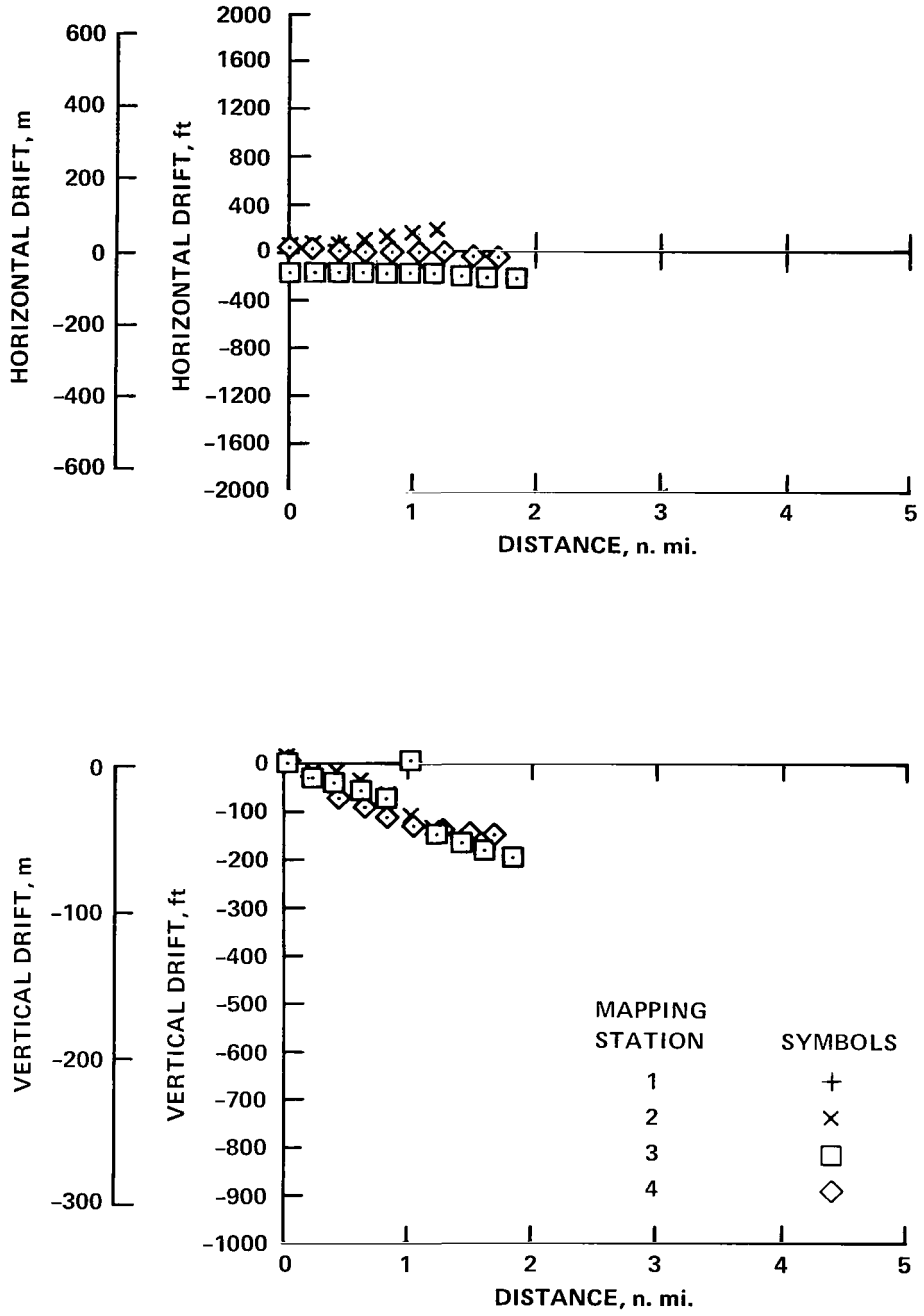

(f) Two-segment approach: flaps, 30°; airspeed, 138 knots; weight, 69,000 kg (151,500 lb); winds, calm; turbulence, smooth.

Figure 26.– Continued.

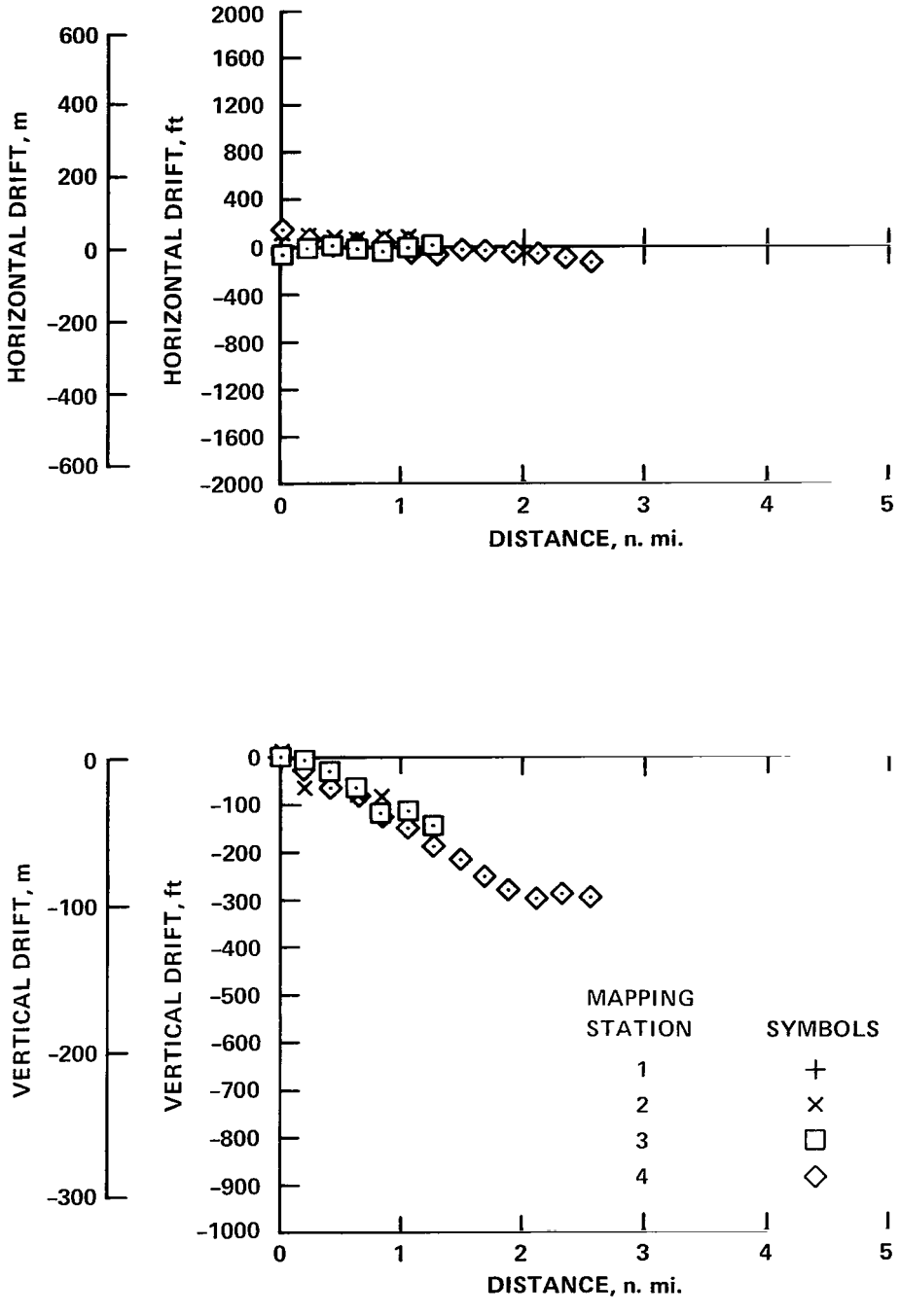

(g) Two-segment approach: flaps, 30°; airspeed, 144 knots; weight, 67,000 kg (148,000 lb); winds, 240° at 12 knots; turbulence, light-moderate.

Figure 26.– Continued.

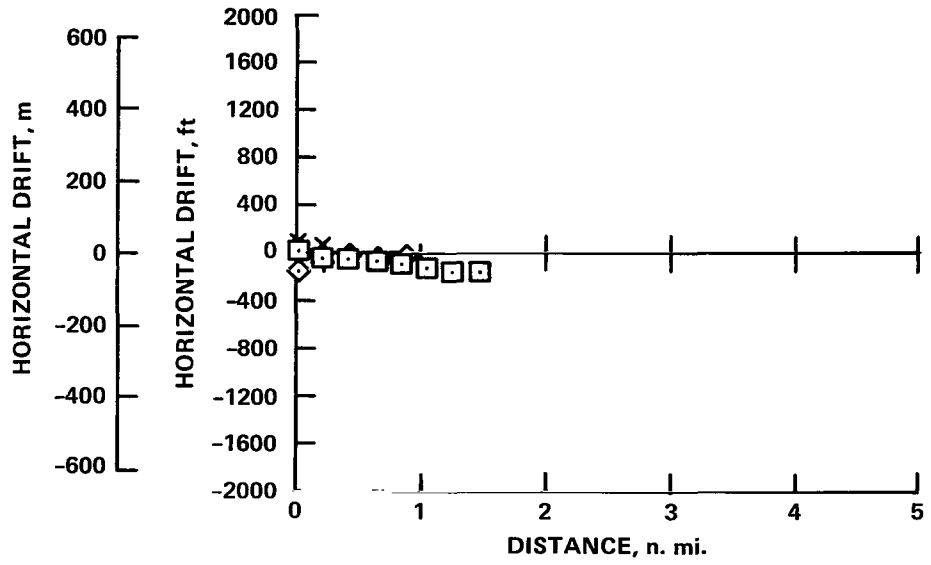

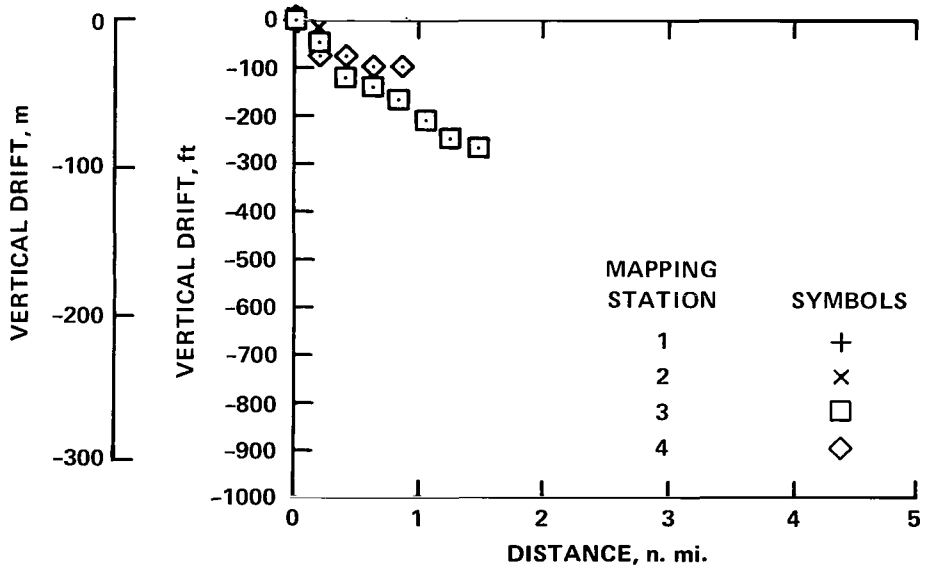

(h) Two-segment approach: flaps, 30°; airspeed, 144 knots; weight, 68,000 kg (150,000 lb); winds, 230° at 5 knots; turbulence, light.

Figure 26.– Continued.

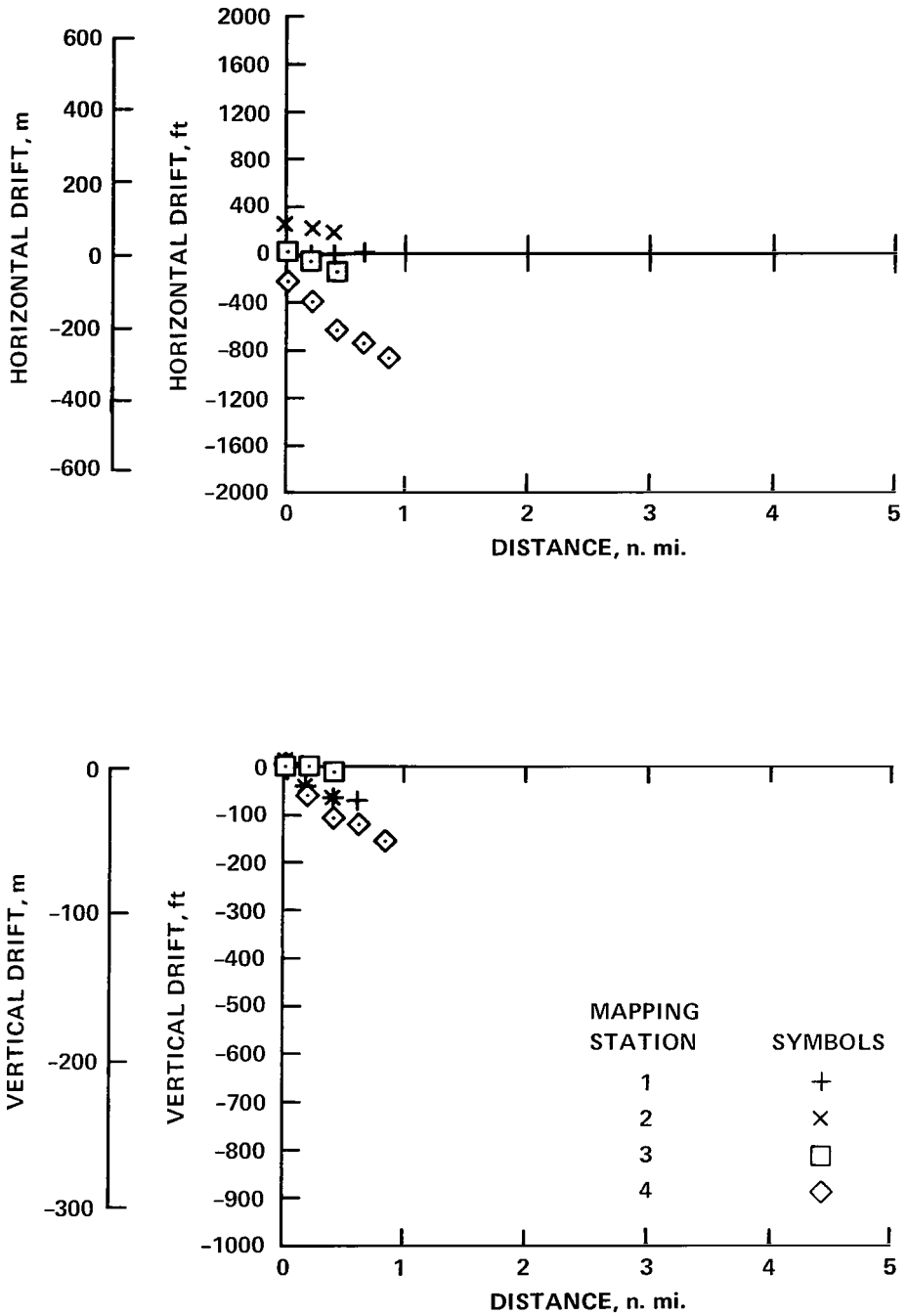

(i) Two-segment approach: flaps, 30°; airspeed, 145 knots; weight, 65,500 kg (144,000 lb); winds, 235° at 9 knots; turbulence, light-moderate.

Figure 26.– Continued.

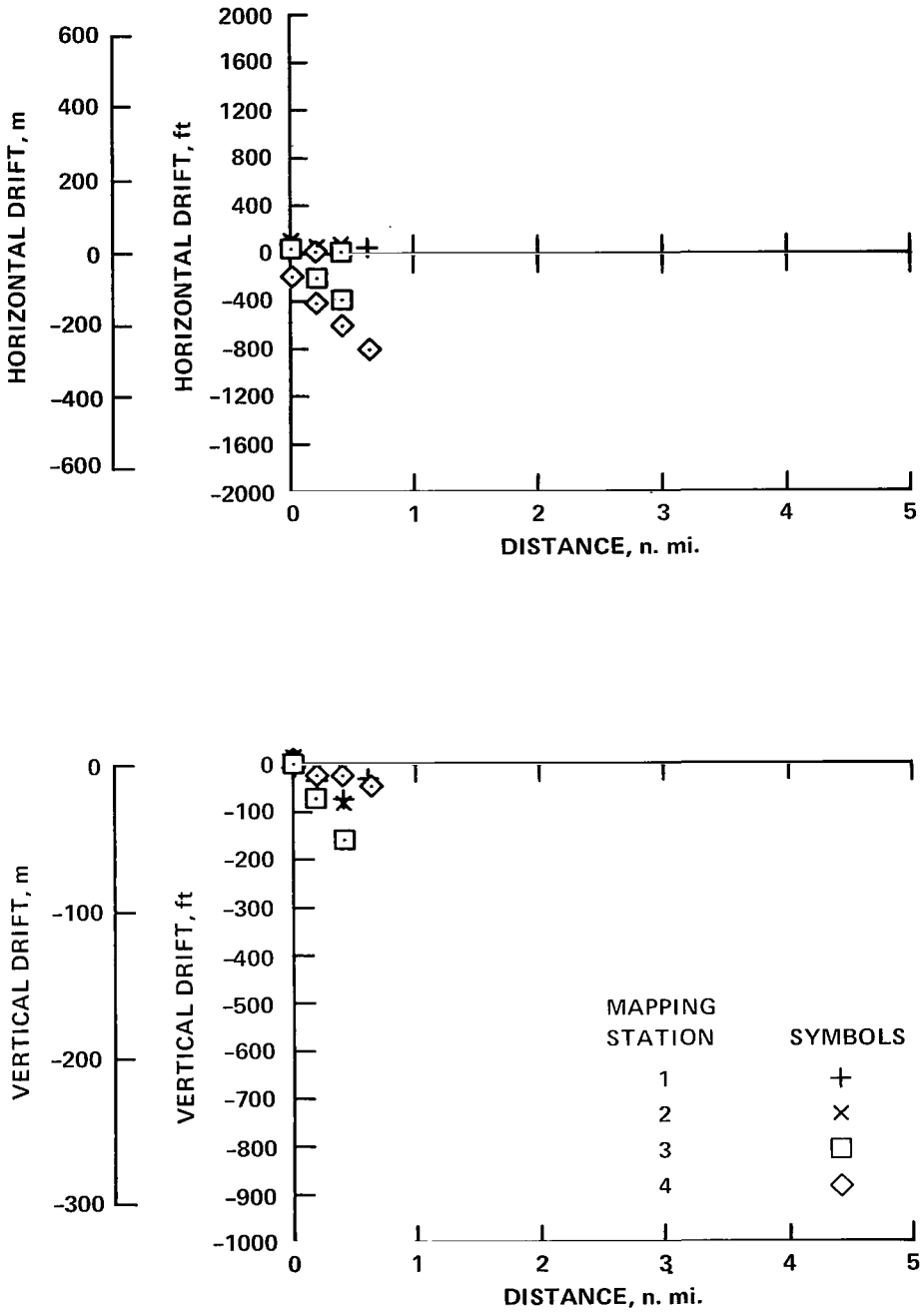

(j) Two-segment approach: flaps, 30°; airspeed, 145 knots; weight, 69,000 kg (151,500 lb); winds, 160° at 4 knots; turbulence, light.

Figure 26.– Continued.

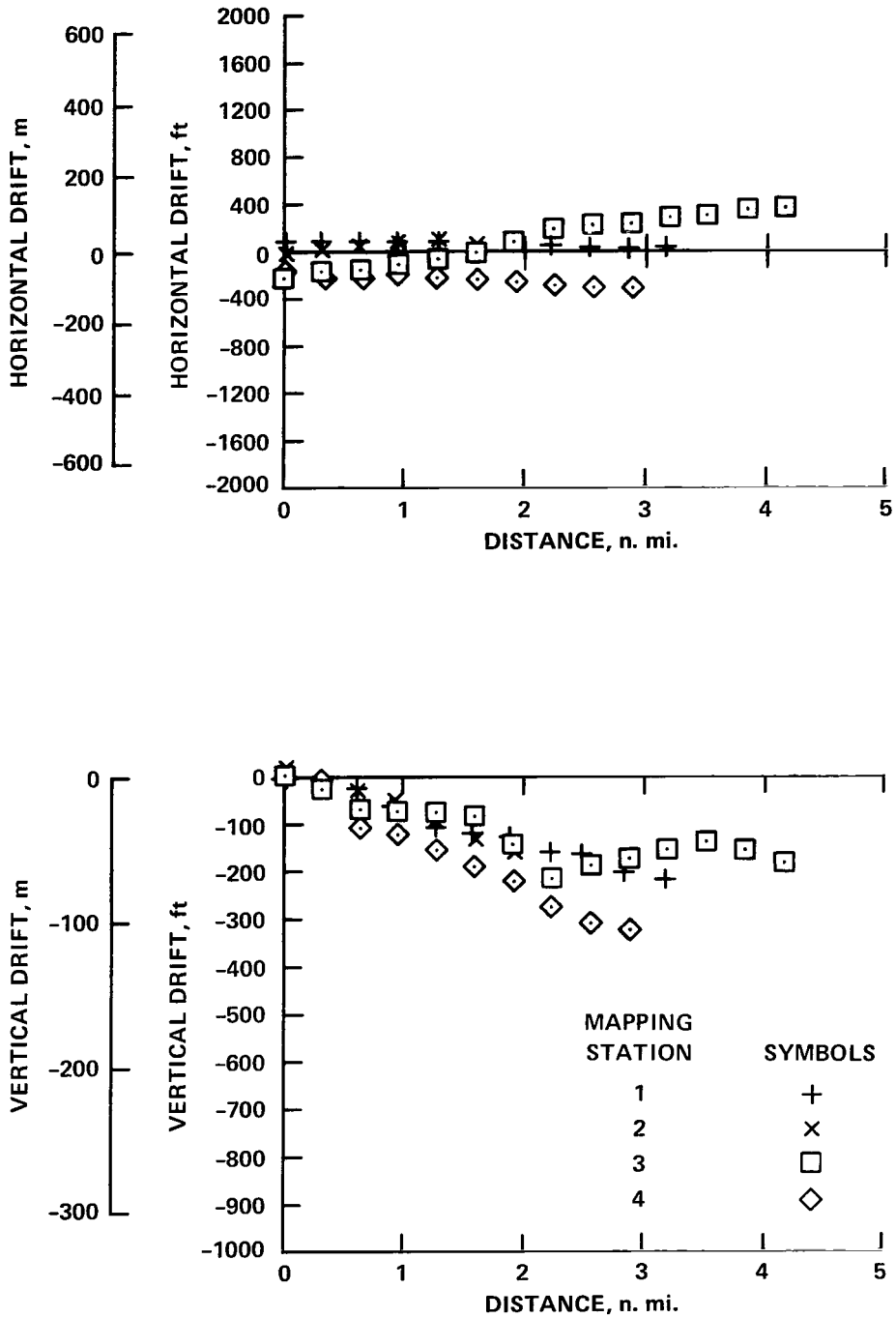

(k) Takeoff: flaps, 15°; airspeed, 220 knots; weight, 69,000 kg (153,000 lb); winds, calm; turbulence, smooth.

Figure 26.– Continued.

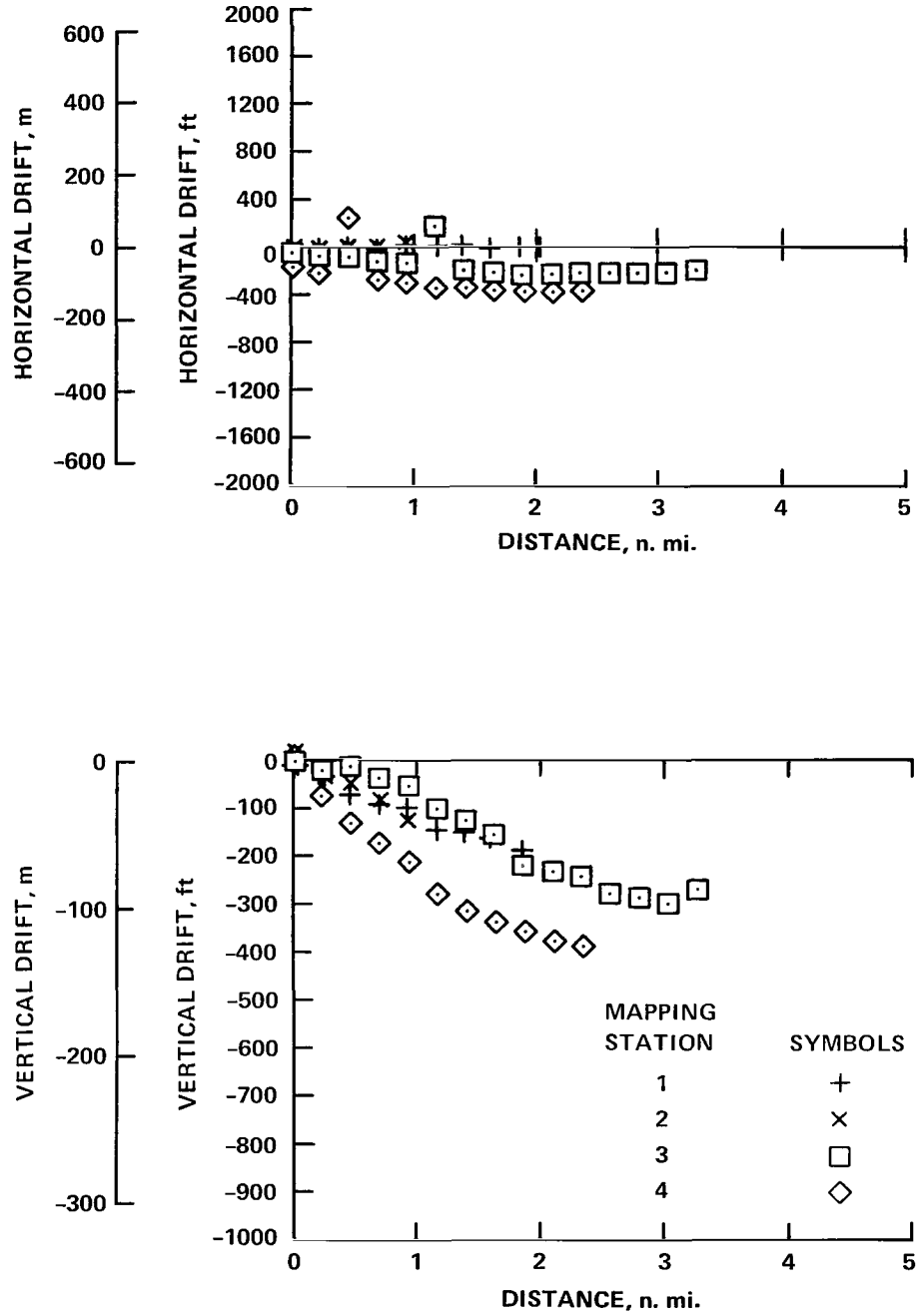

(l) Takeoff: flaps, 15°; airspeed, 160 knots; weight, 70,000 kg (159,000 lb); winds, 160° at 4 knots; turbulence, light.

Figure 26.– Continued.

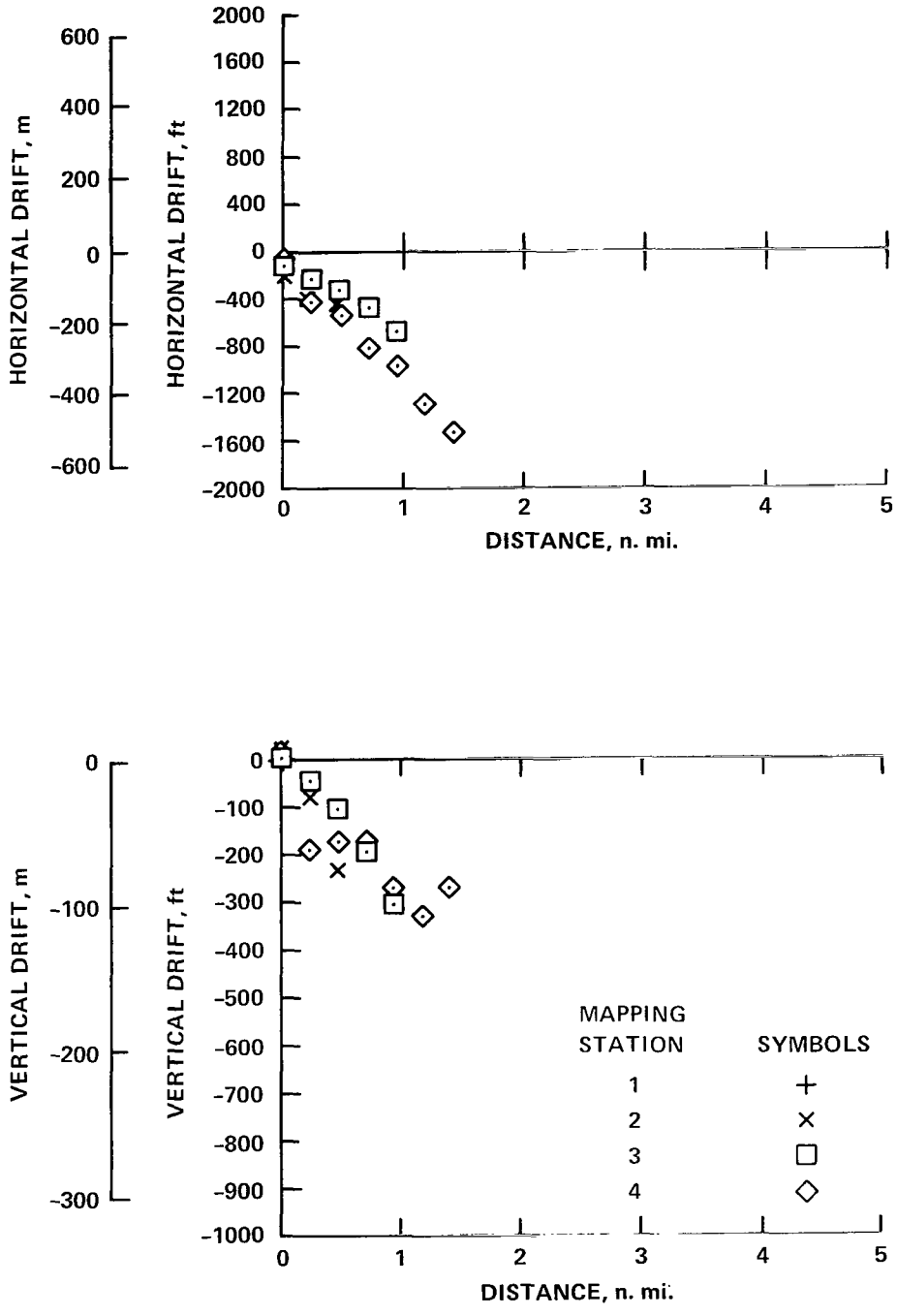

(m) Takeoff: flaps, 15°; airspeed, 160 knots; weight, 66,000 kg (145,500 lb); winds, 230° at 8 knots; turbulence, light.

Figure 26.– Continued.

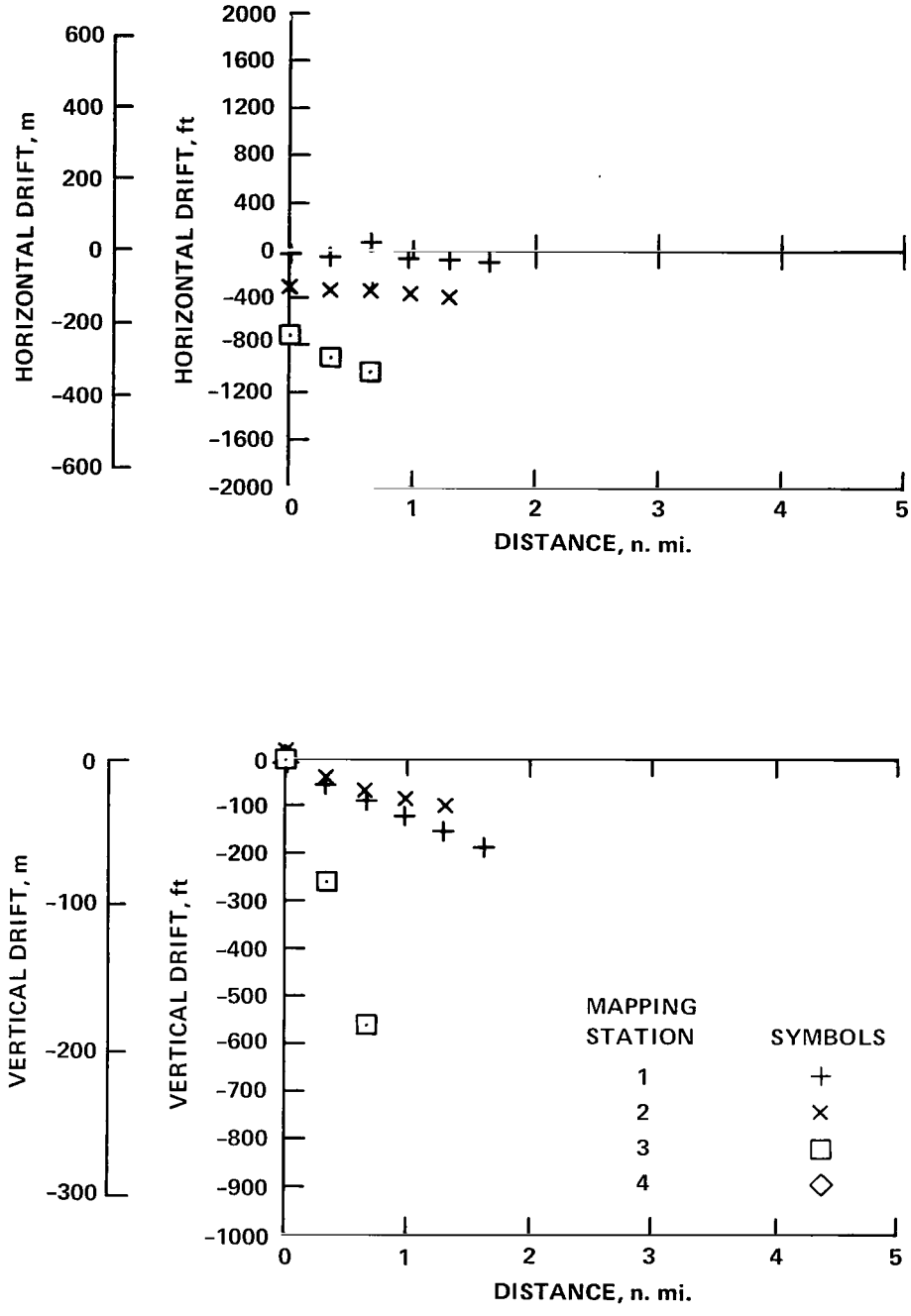

(n) Takeoff: flaps, 15°; airspeed, 200 knots; weight, 69,000 kg (155,000 lb); winds, 160° at 4 knots; turbulence, light.

Figure 26.– Concluded.

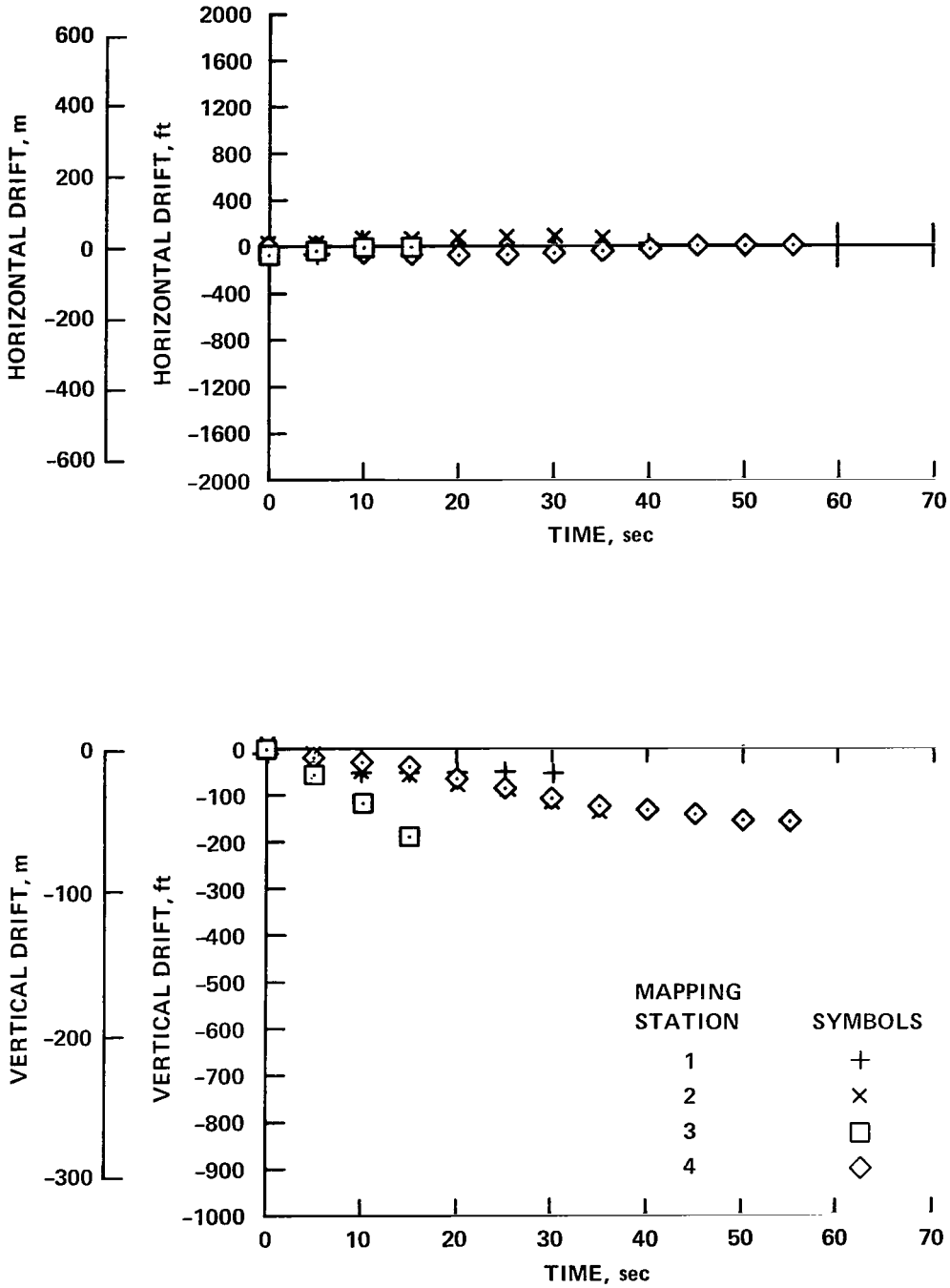

(a) Conventional approach: flaps, 30°; airspeed, 135 knots; weight, 64,000 kg (141,500 lb); winds, calm; turbulence, smooth.

Figure 27.– Vortex location after B727 passage.

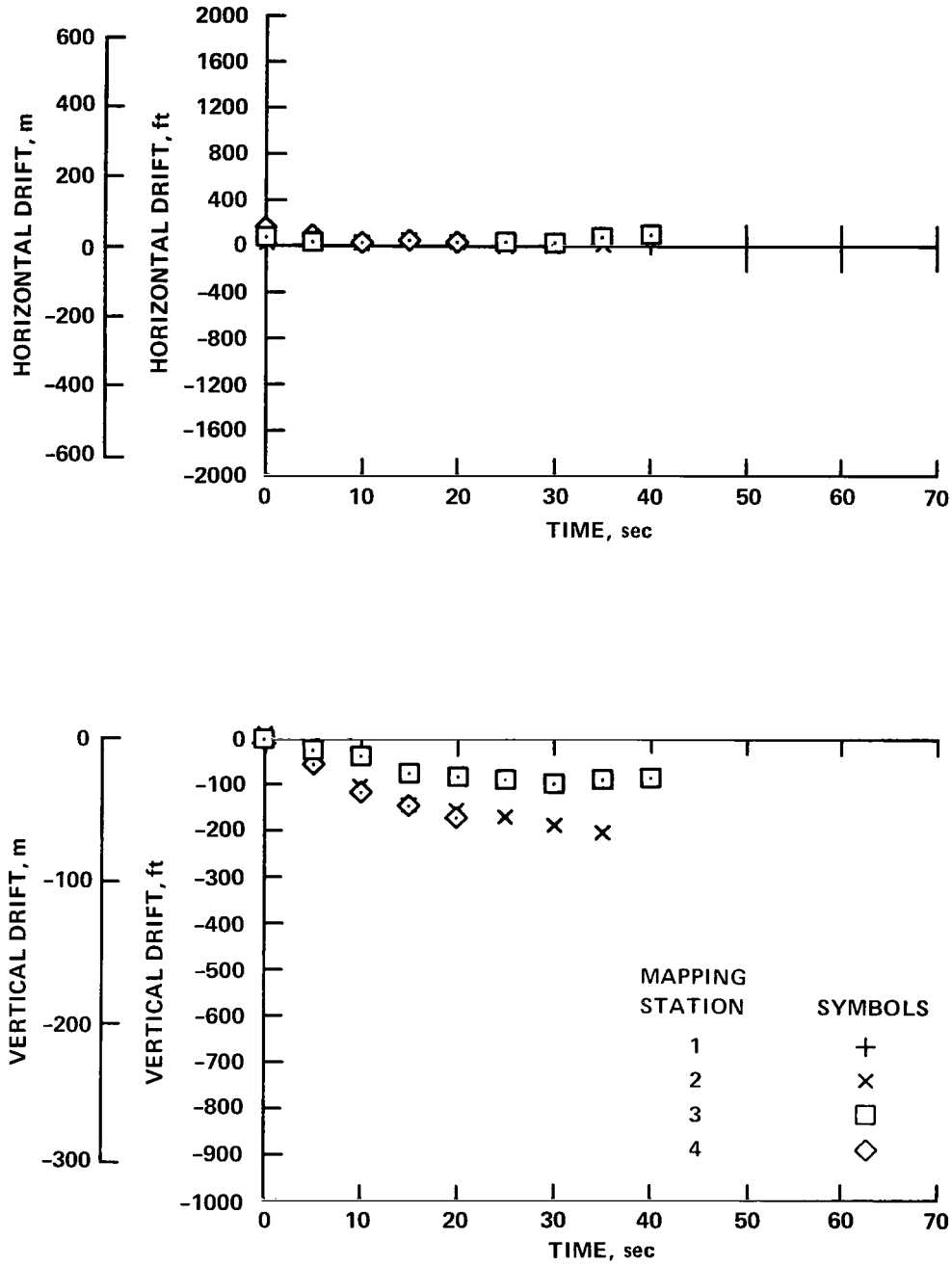

(b) Conventional approach: flaps, 30°; airspeed, 132 knots; weight, 66,000 kg (146,000 lb); winds, 240° at 12 knots; turbulence, light-moderate.

Figure 27.– Continued.

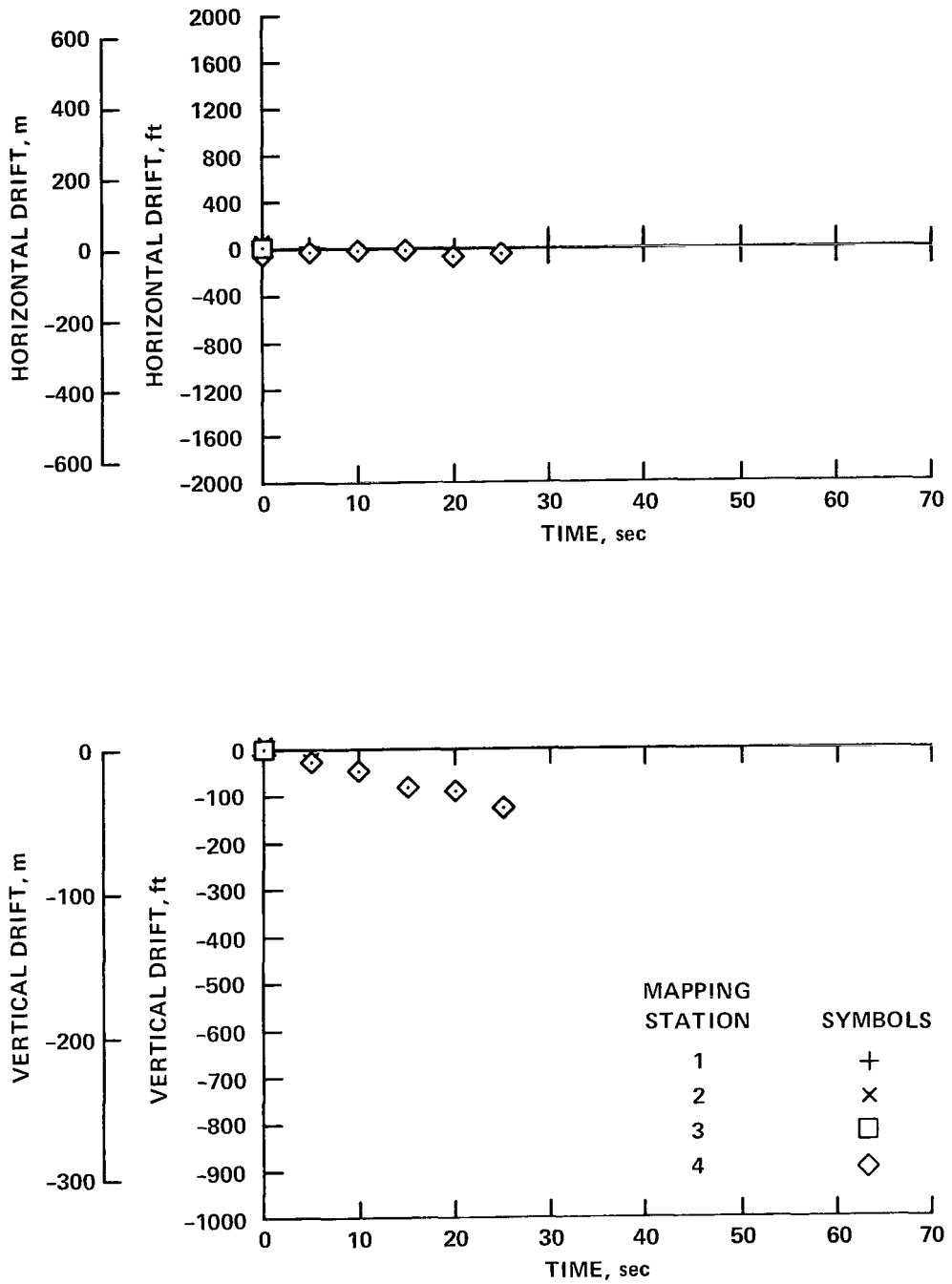

(c) Conventional approach: flaps, 30°; airspeed, 145 knots; weight, 68,000 kg (150,000 lb); winds, 230° at 5 knots; turbulence, light.

Figure 27.– Continued.

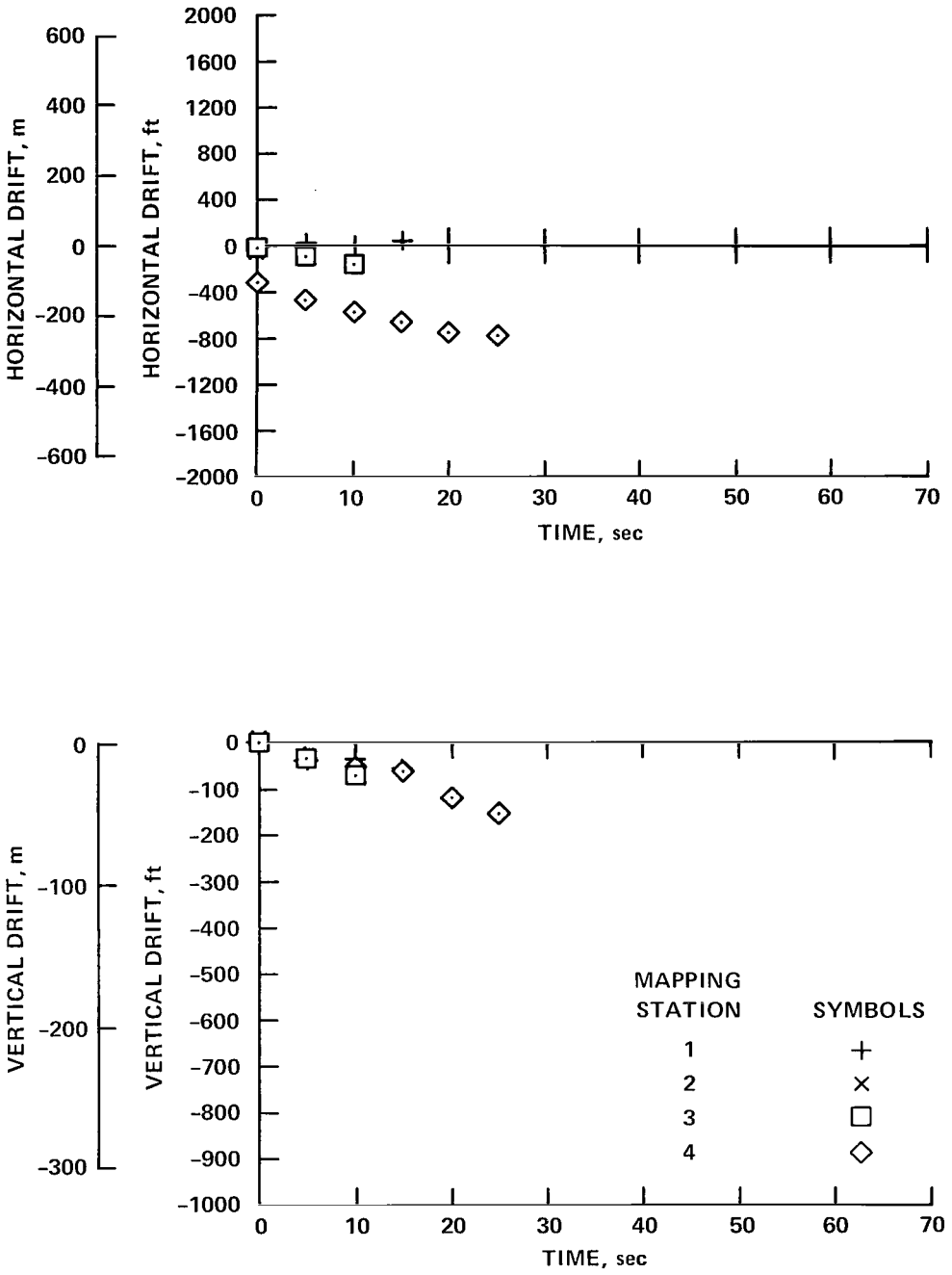

(d) Conventional approach: flaps, 30°; airspeed, 140 knots; weight, 64,500 kg (141,500 lb); winds, 240° at 10 knots; turbulence, light-moderate.

Figure 27.– Continued.

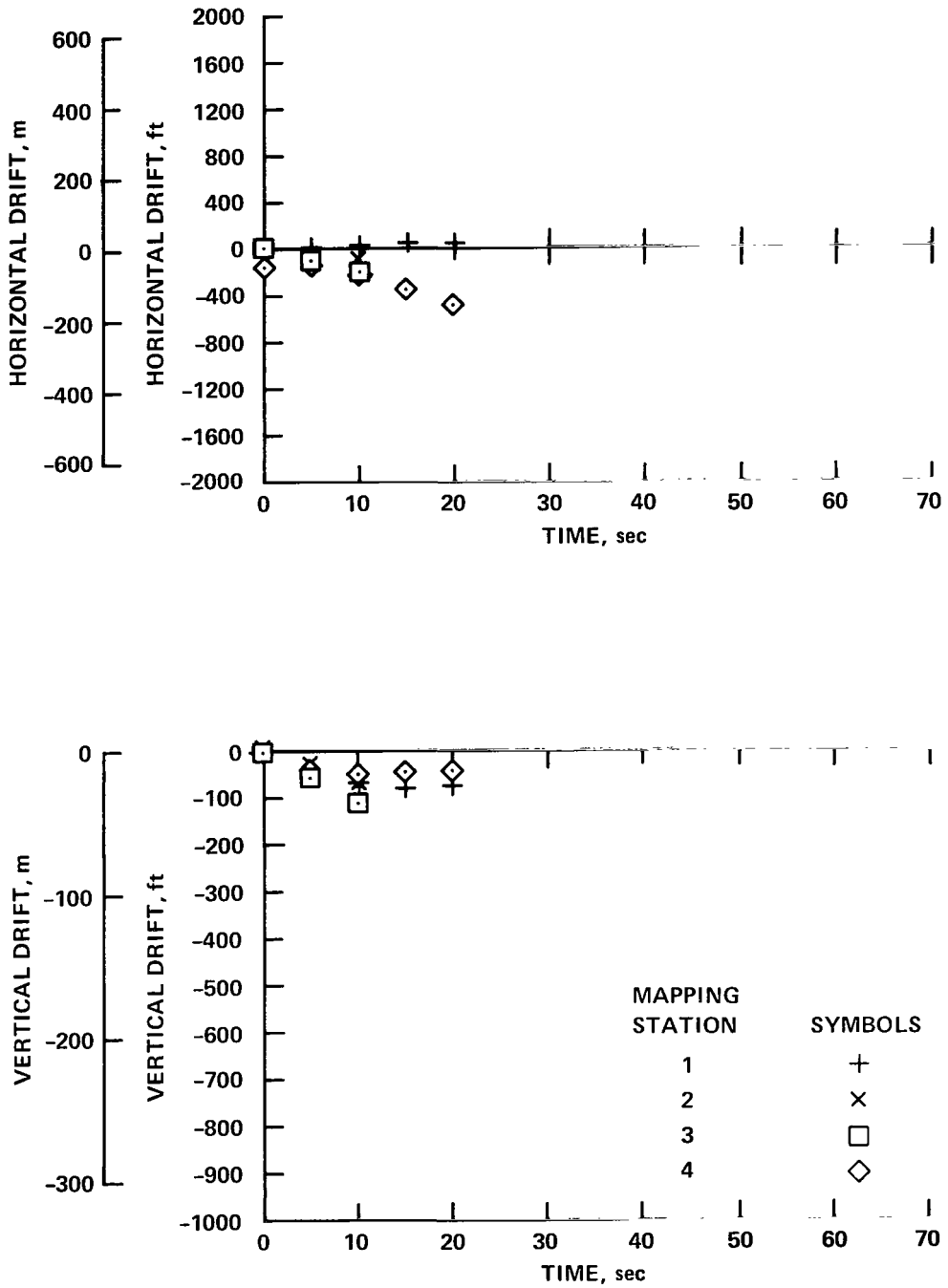

(e) Conventional approach: flaps, 30°; airspeed, 145 knots; weight, 67,000 kg (148,000 lb); winds, 230° at 8 knots; turbulence, light-moderate.

Figure 27.– Continued.

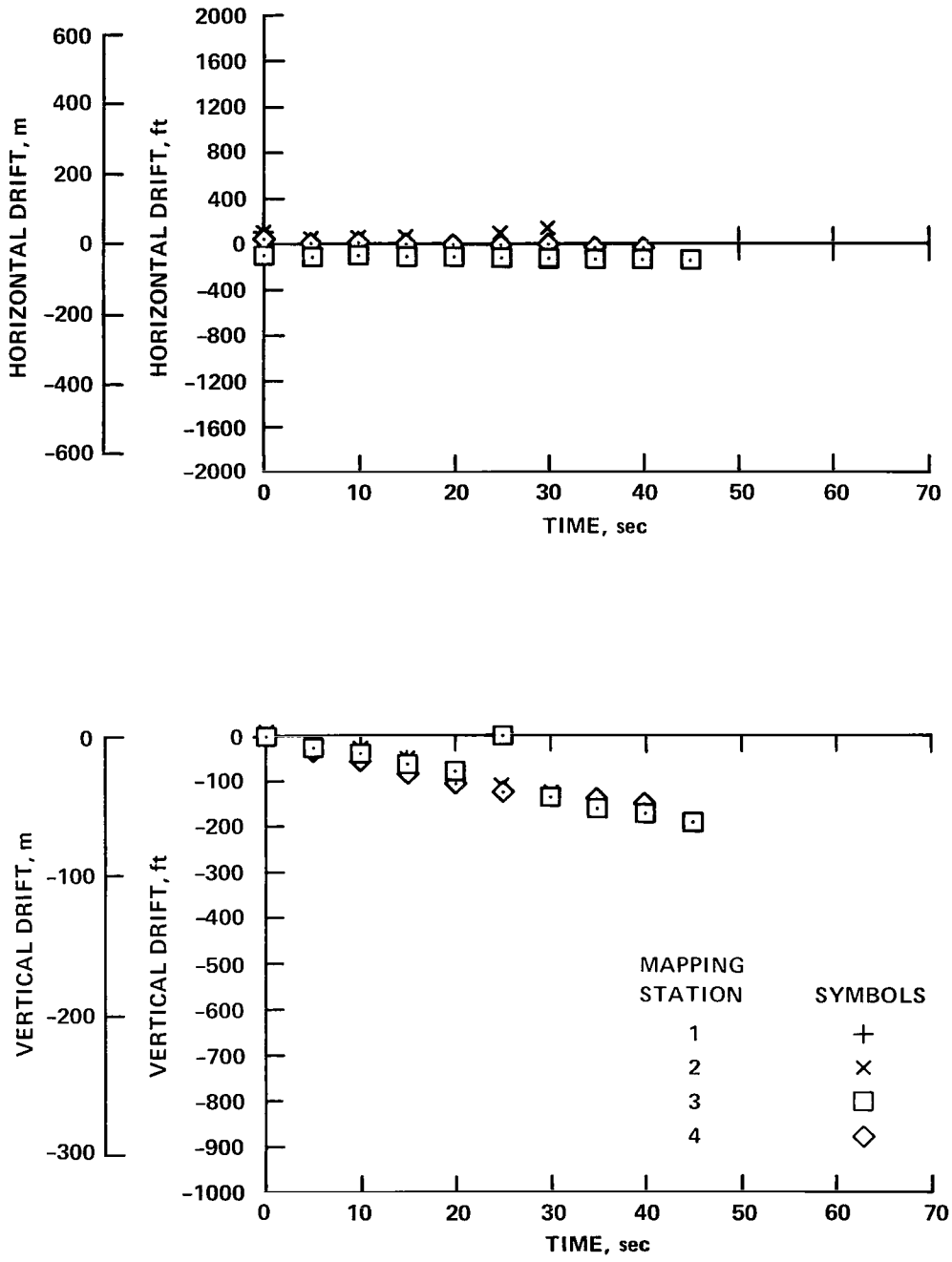

(f) Two-segment approach: flaps, 30°; airspeed, 138 knots; weight, 69,000 kg (151,500 lb); winds, calm; turbulence, smooth.

Figure 27.– Continued.

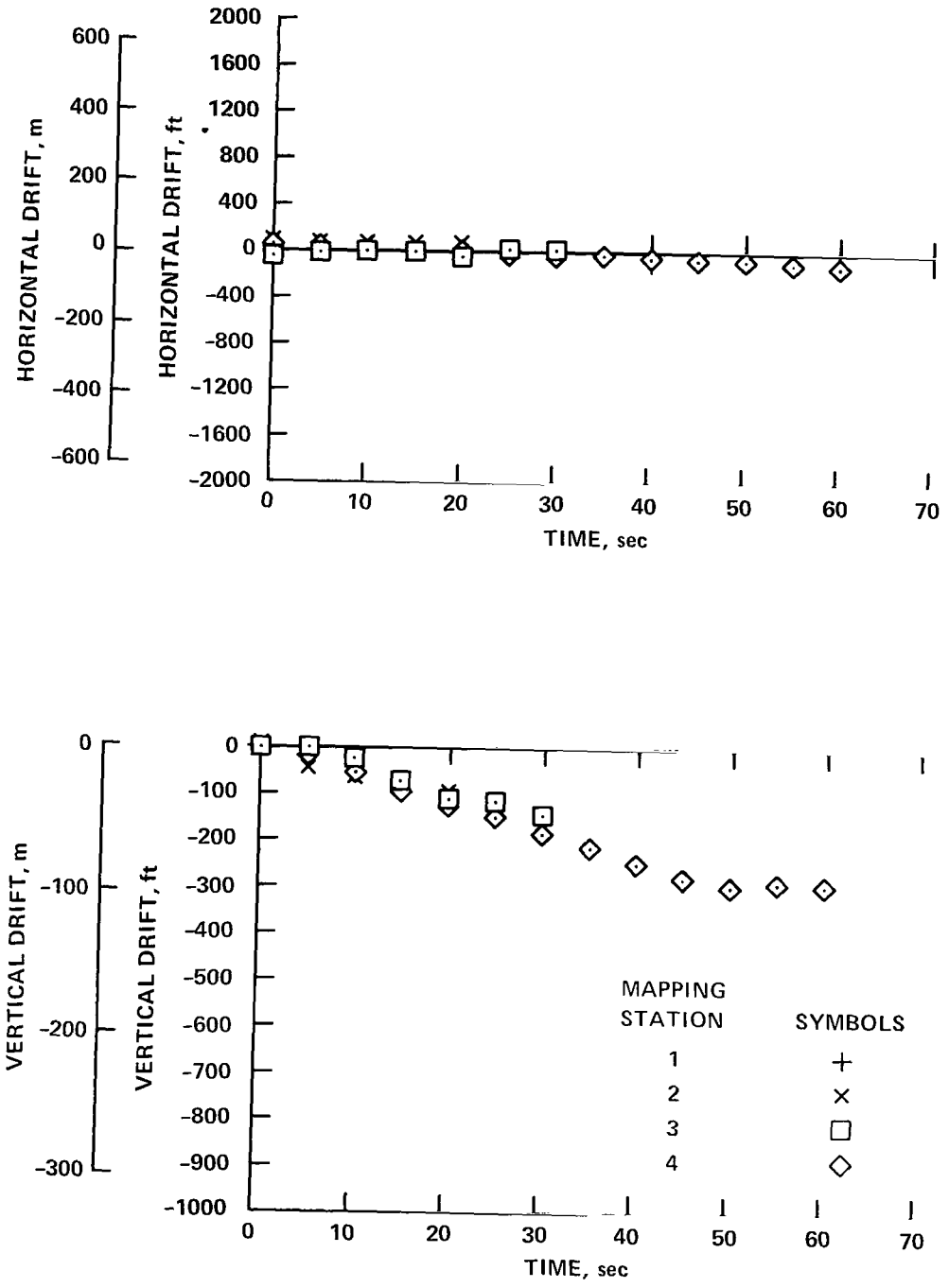

(g) Two-segment approach: flaps, 30°; airspeed, 144 knots; weight, 67,000 kg (148,000 lb); winds, 240° at 12 knots; turbulence, light-moderate.

Figure 27.– Continued.

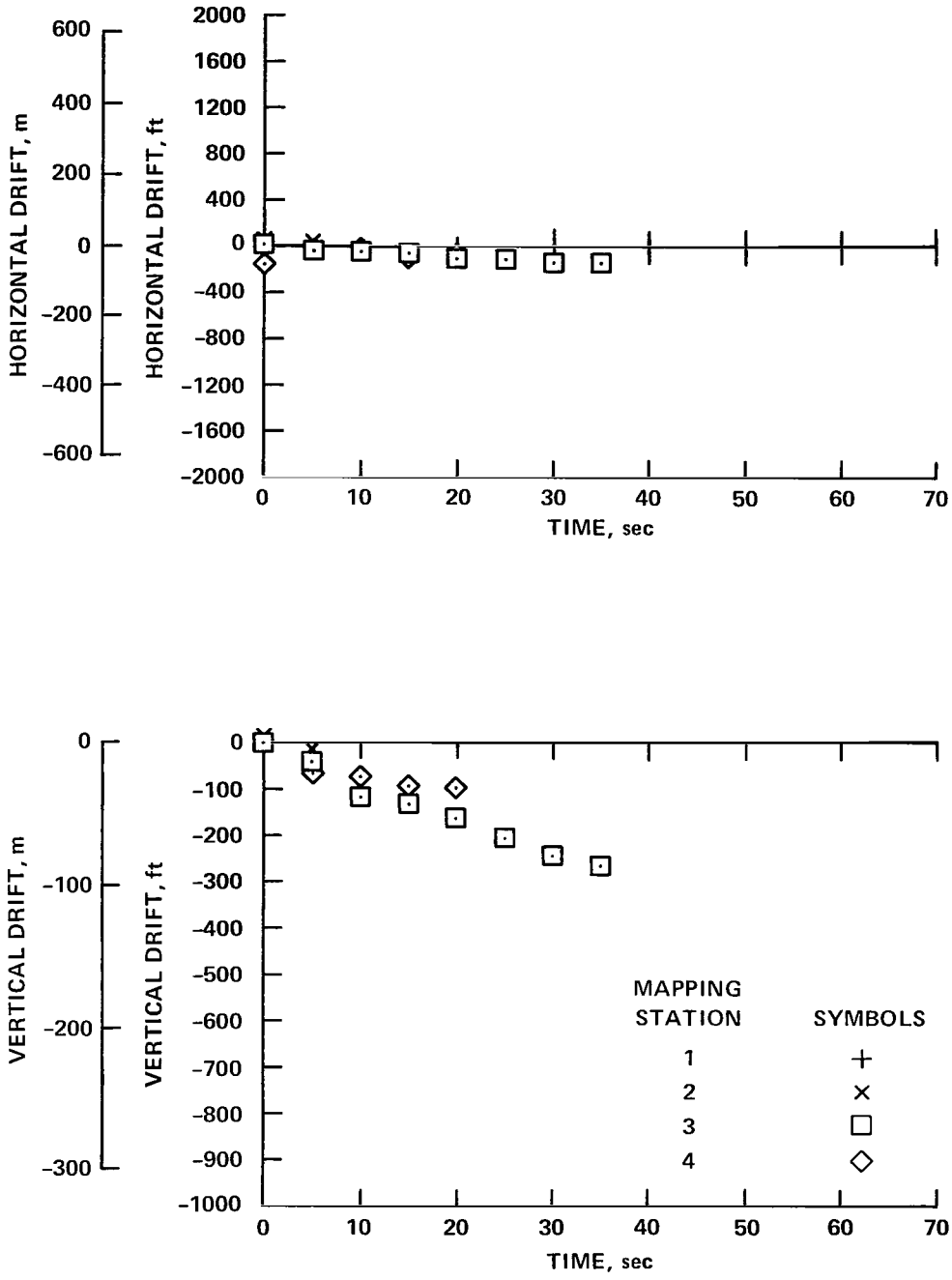

(h) Two-segment approach: flaps, 30°; airspeed, 144 knots; weight, 68,000 kg (150,000 lb); winds, 230° at 5 knots; turbulence, light.

Figure 27.– Continued.

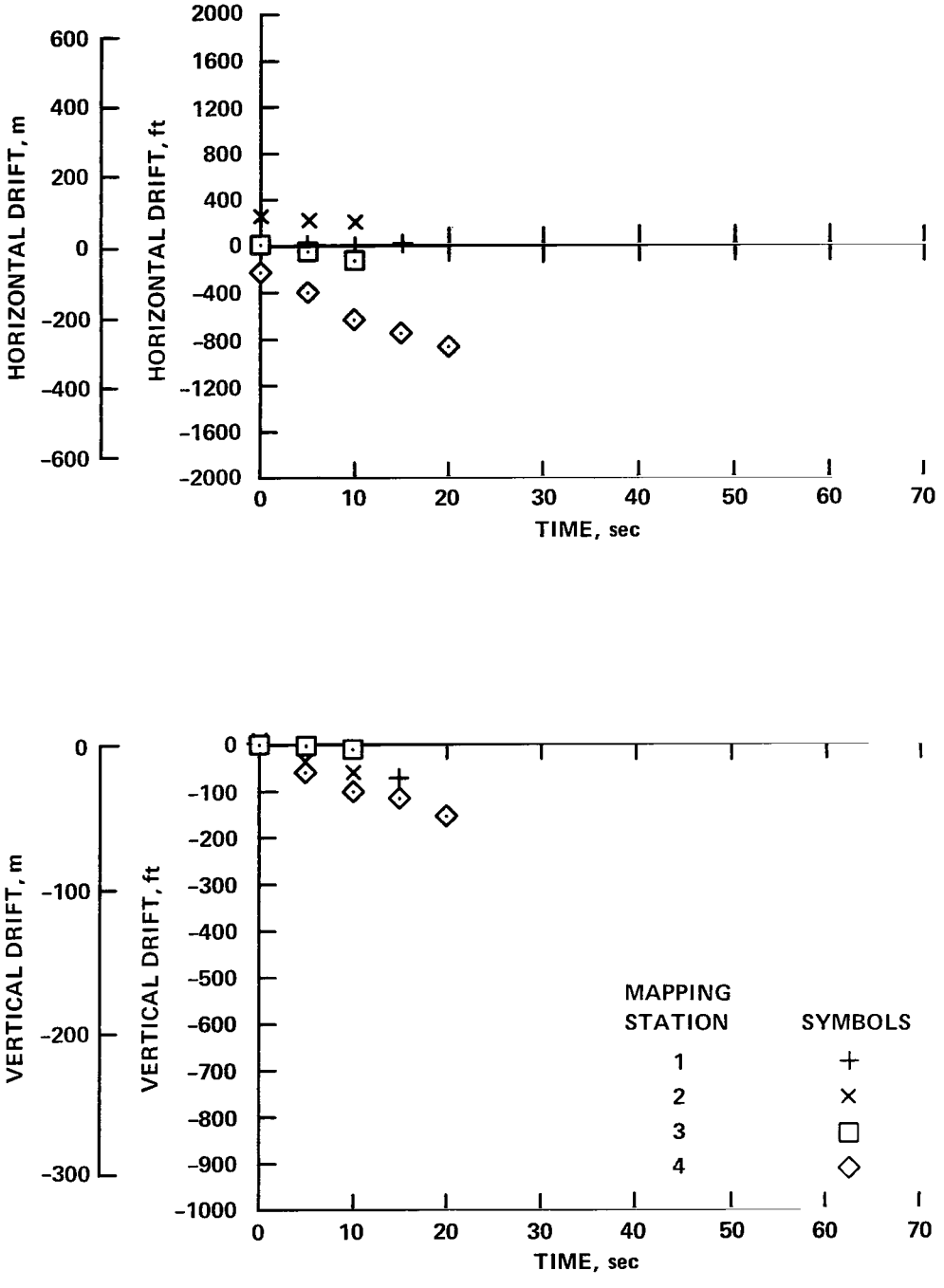

(i) Two-segment approach: flaps, 30°; airspeed, 145 knots; weight, 65,500 kg (144,000 lb); winds, 235° at 9 knots; turbulence, light-moderate.

Figure 27.– Continued.

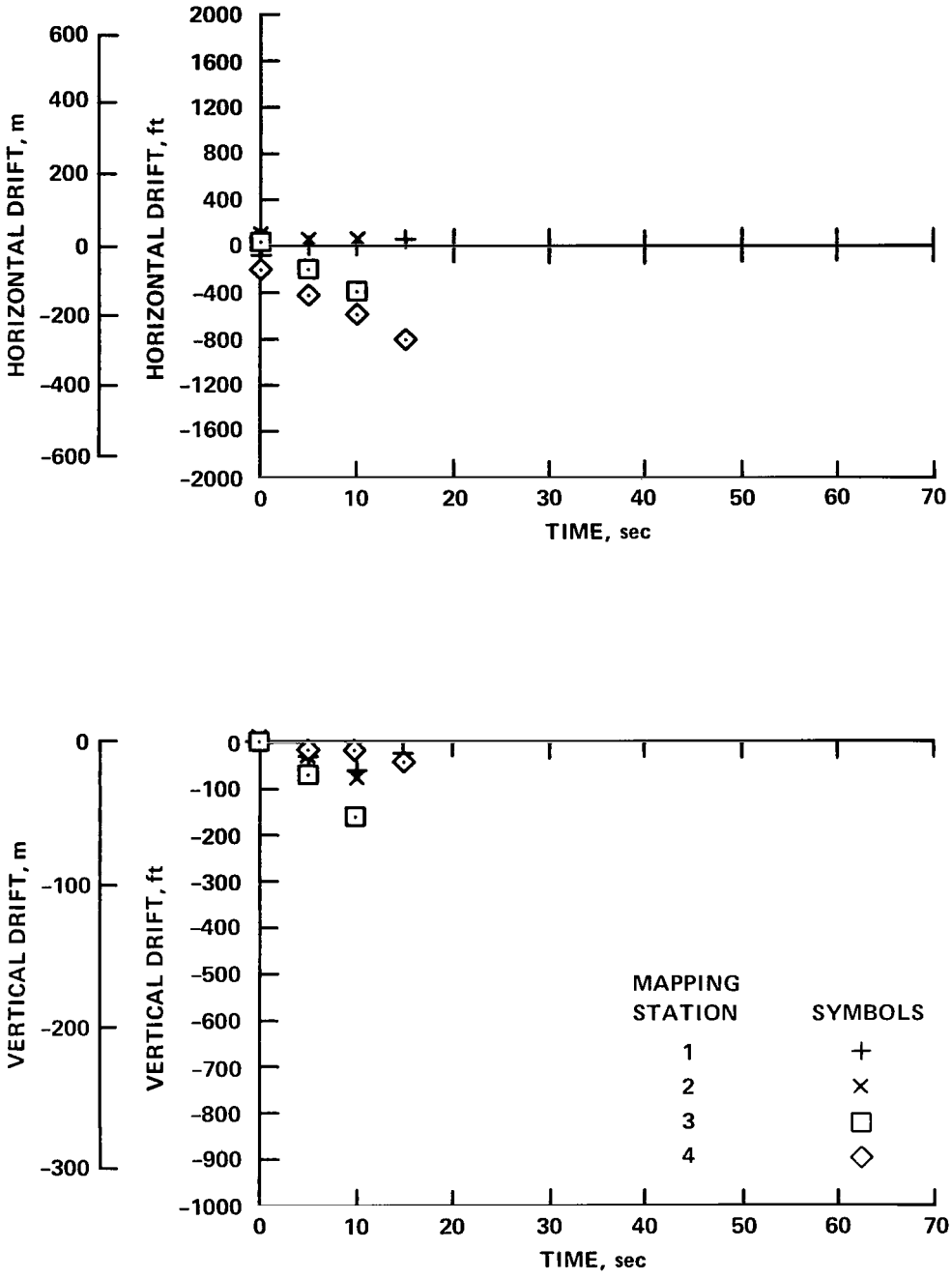

(j) Two-segment approach: flaps, 30°; airspeed, 145 knots; weight, 69,000 kg (151,500 lb); winds, 160° at 4 knots; turbulence, light.

Figure 27.– Continued.

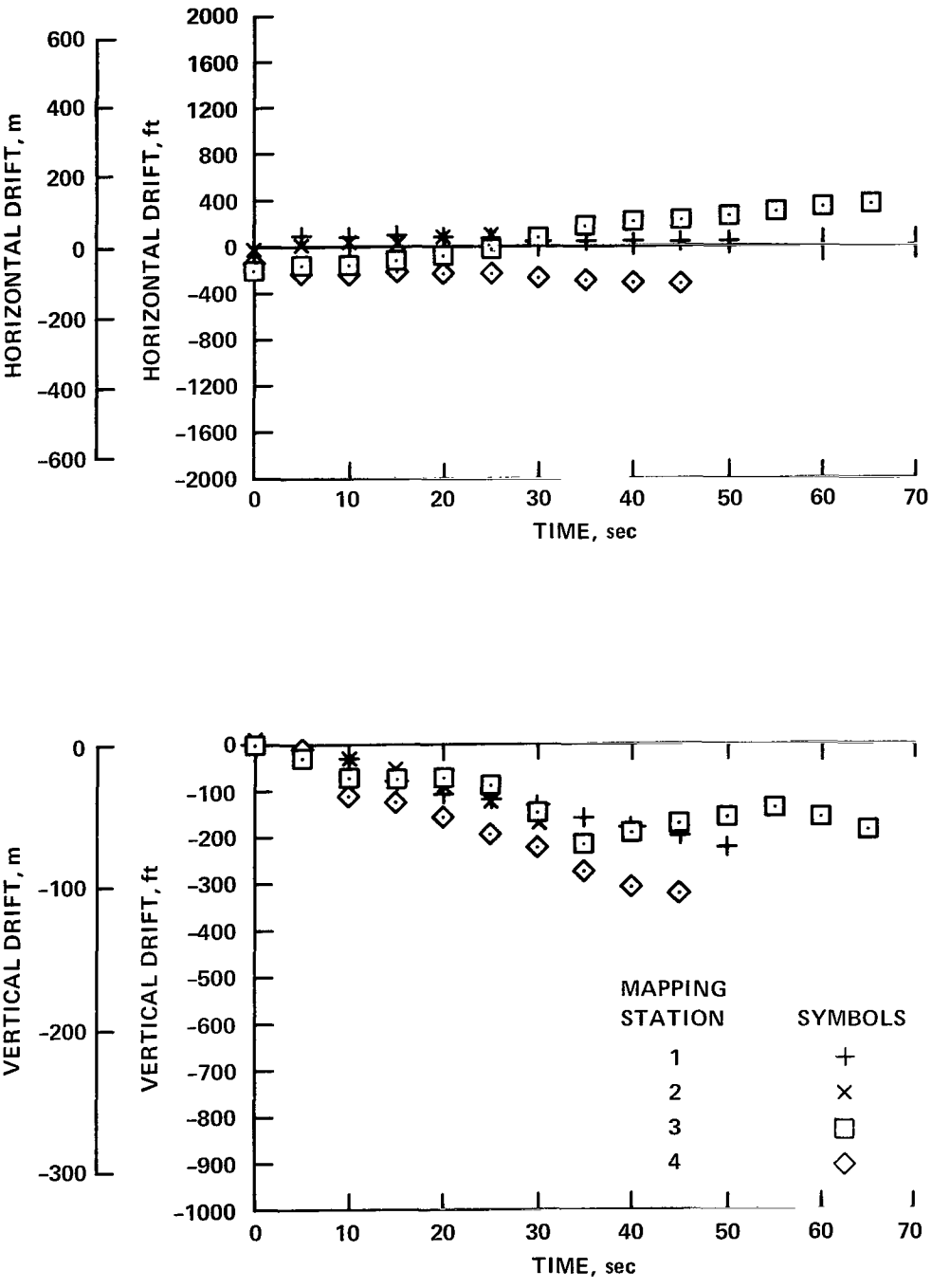

(k) Takeoff: flaps, 15°; airspeed, 220 knots; weight, 69,000 kg (153,000 lb); winds, calm; turbulence, smooth.

Figure 27.– Continued.

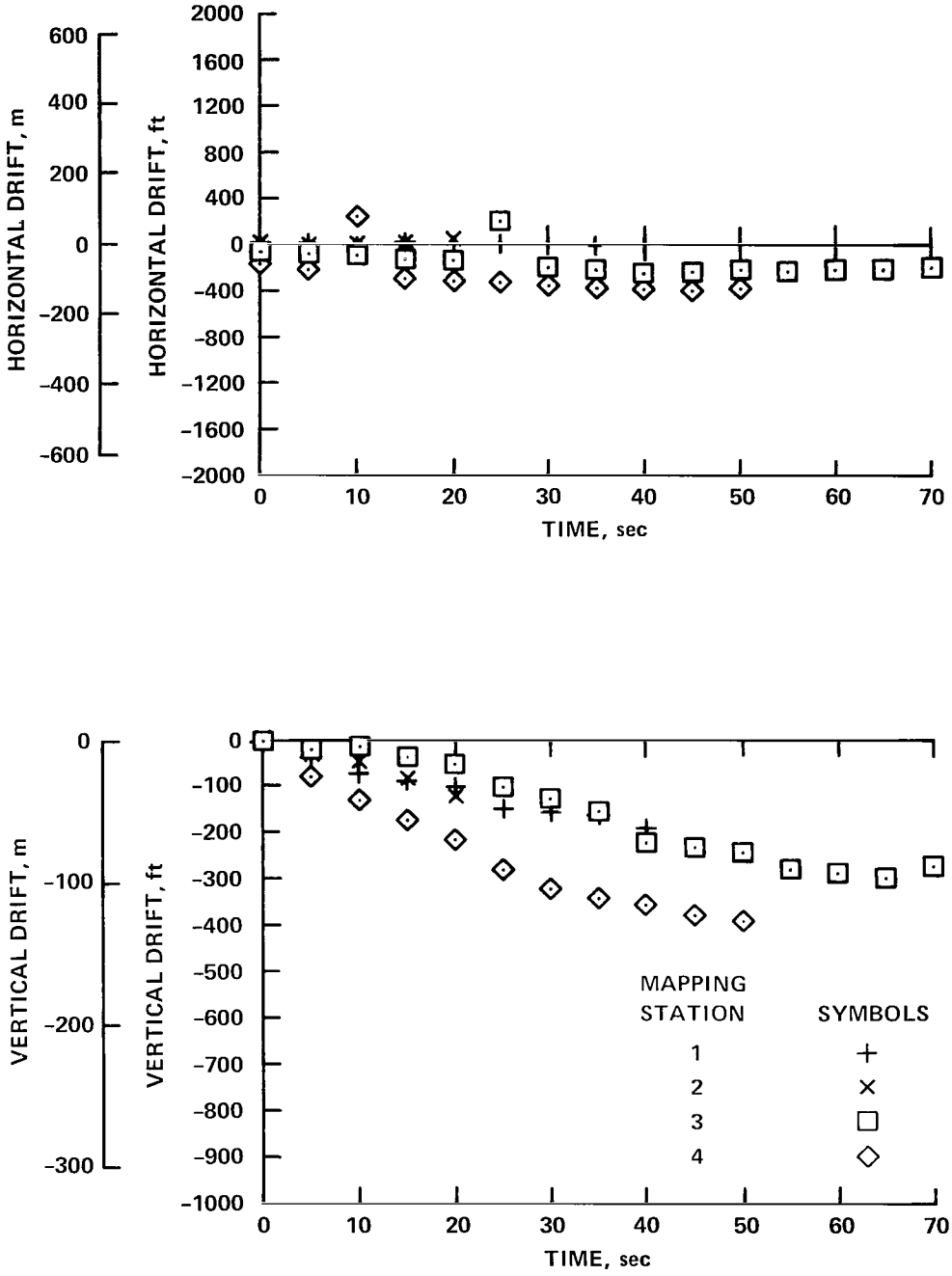

(l) Takeoff: flaps, 15°; airspeed, 160 knots; weight, 70,000 kg (159,000 lb); winds, 160° at 4 knots; turbulence, light.

Figure 27.– Continued.

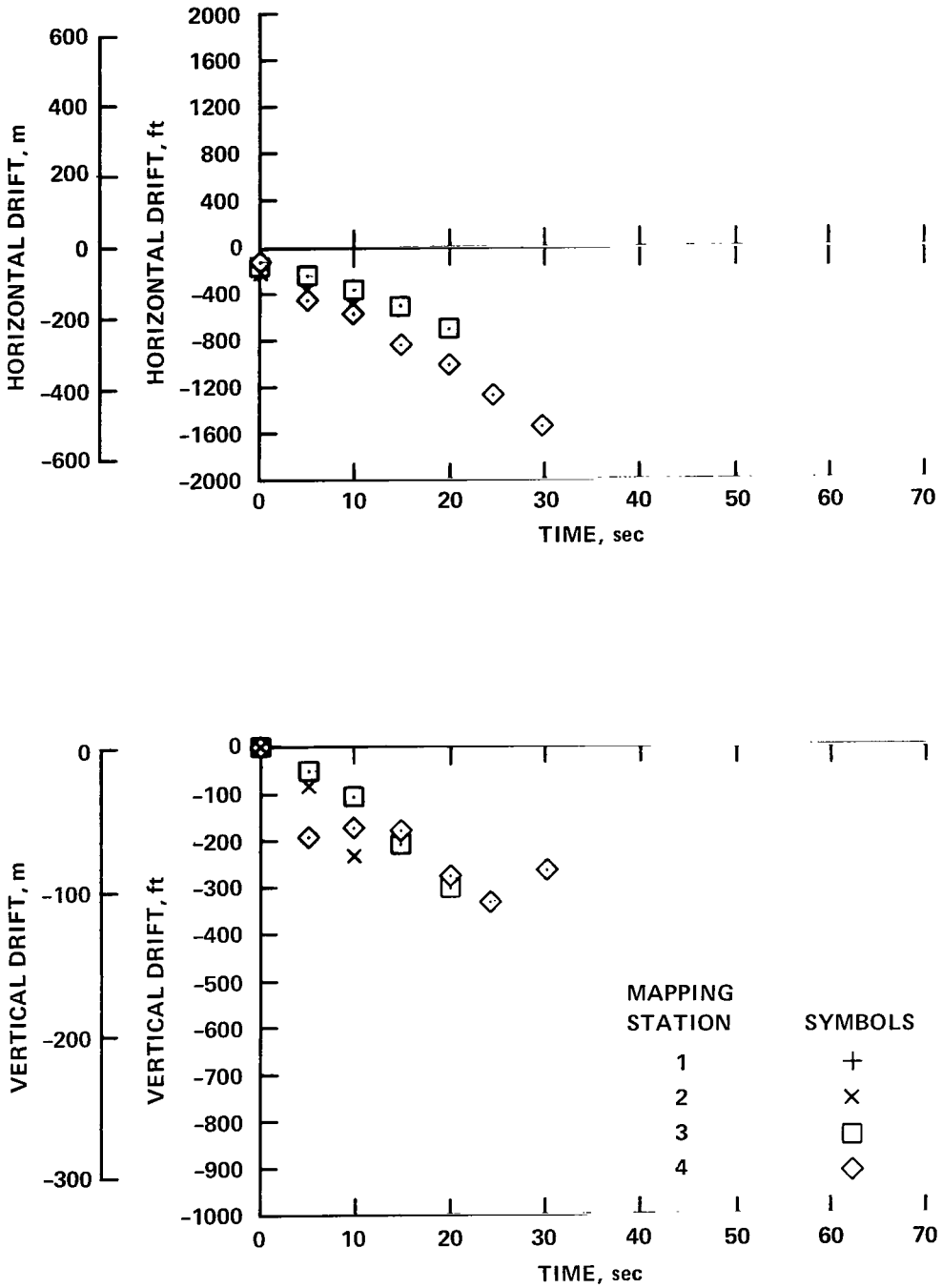

(m) Takeoff: flaps, 15°; airspeed, 160 knots; weight, 66,000 kg (145,500 lb); winds, 230° at 8 knots; turbulence, light.

Figure 27.– Continued.

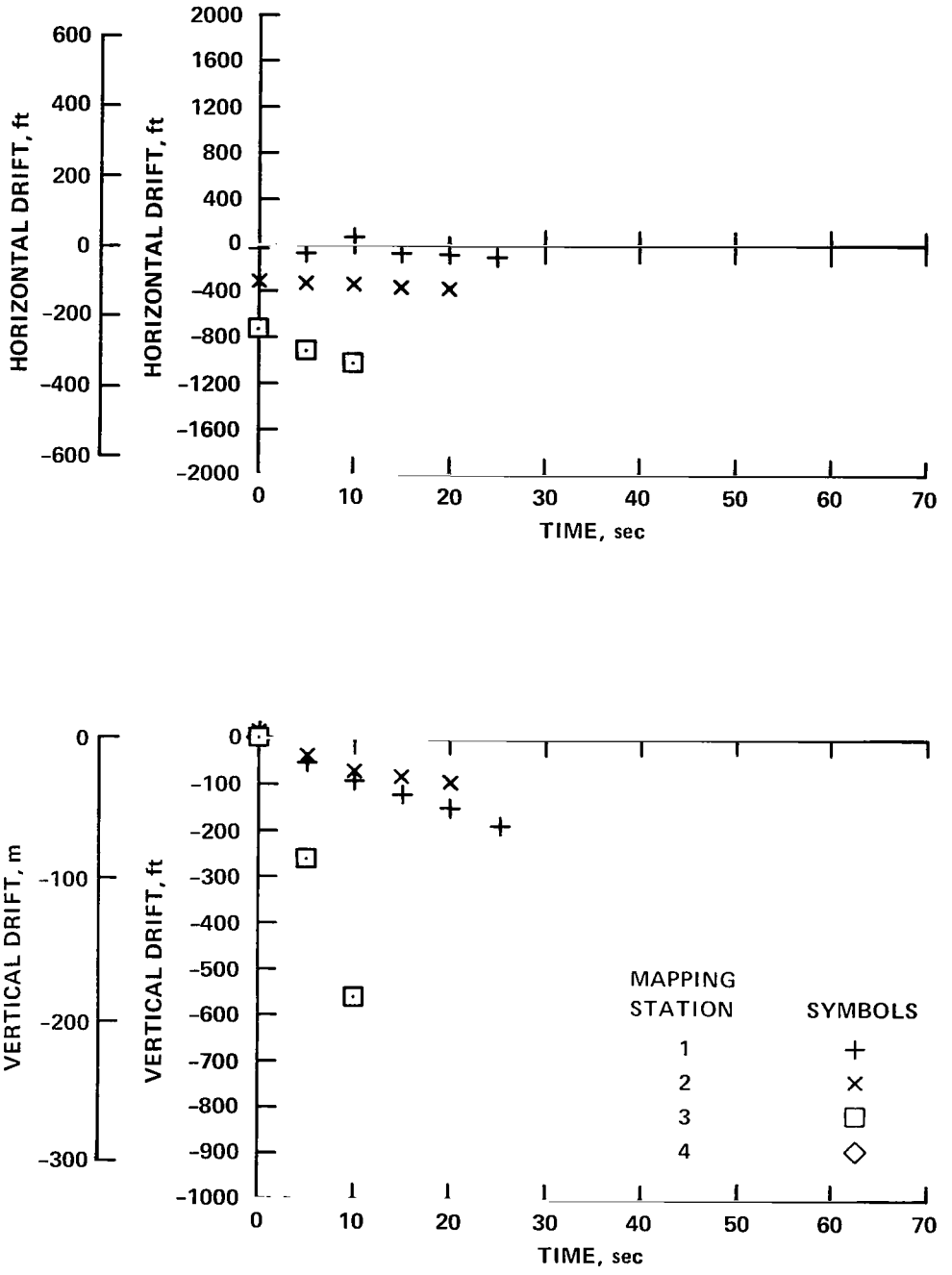

(n) Takeoff: flaps, 15°; airspeed, 200 knots; weight, 69,000 kg (155,000 lb); winds, 160° at 4 knots; turbulence, light.

Figure 27.– Concluded.

REFERENCES

1. Denery, D. G.; White, K. C.; and Drinkwater III, F. J.: A Resume of the Status and Benefits of the Two-Segment Approach and Its Applicability to the Jet Transport Fleet. AIAA 6th Aircraft Design, Flight Test, and Operations Meeting, Los Angeles, California, August 12–14, 1974.

2. Schwind, G. K.; Morrison, J. A.; Nylen, W. A., and Anderson, E. B.: Operational Flight Evaluation of the Two-Segment Approach for Use in Airline Service. United Air Lines, January 1974. NASA CR-2515.

3. Tombach, Ivar: Observations of Atmospheric Effects on Vortex Wake Behavior. Journal of Aircraft, vol. 10, no. 11, November 1973, pp. 641–647.

4. Andrews, William H.; Robinson, Glenn H.; Larson, Richard R.: Exploratory Investigation of Aircraft Response to the Wing Vortex Wake Generated by Jet Transport Aircraft. NASA TN D-6655, March 1972.

5. MacCready, Paul B., Jr.: Standardization of Gustiness Values from Aircraft. Journal of Applied Meteorology, vol. 3, no. 4, August 1964, pp. 439–449.

"The aeronautical and space activities of the United States shall be conducted so as to contribute . . . to the expansion of human knowledge of phenomena in the atmosphere and space. The Administration shall provide for the widest practicable and appropriate dissemination of information concerning its activities and the results thereof."

—NATIONAL AERONAUTICS AND SPACE ACT OF 1958

NASA SCIENTIFIC AND TECHNICAL PUBLICATIONS

TECHNICAL REPORTS: Scientific and technical information considered important, complete, and a lasting contribution to existing knowledge.

TECHNICAL NOTES: Information less broad in scope but nevertheless of importance as a contribution to existing knowledge.

TECHNICAL MEMORANDUMS: Information receiving limited distribution because of preliminary data, security classification, or other reasons. Also includes conference proceedings with either limited or unlimited distribution.

CONTRACTOR REPORTS: Scientific and technical information generated under a NASA contract or grant and considered an important contribution to existing knowledge.

TECHNICAL TRANSLATIONS: Information published in a foreign language considered to merit NASA distribution in English.

SPECIAL PUBLICATIONS: Information derived from or of value to NASA activities. Publications include final reports of major projects, monographs, data compilations, handbooks, sourcebooks, and special bibliographies.

TECHNOLOGY UTILIZATION PUBLICATIONS: Information on technology used by NASA that may be of particular interest in commercial and other non-aerospace applications. Publications include Tech Briefs, Technology Utilization Reports and Technology Surveys.

Details on the availability of these publications may be obtained from:

SCIENTIFIC AND TECHNICAL INFORMATION OFFICE

NATIONAL AERONAUTICS AND SPACE ADMINISTRATION

Washington, D.C. 20546